Neutron and x-ray spectroscopy

B. Keimer

Max-Planck-Institute for Solid State Research

outline

1. self-contained introduction
    - neutron scattering and spectroscopy
    - x-ray scattering and spectroscopy
2. application to correlated-electron materials
    - bulk
    - interfaces

Neutron and x-ray spectroscopy

outline

1. weak correlations: Pb, Nb
2. intermediate correlations: Sr_2RuO_4
3. strong correlations: $YBa_2Cu_3O_{6+x}$
4. orbital degeracy: $La_{1-x}Ca_xMnO_3$ (Y,La)TiO_3
5. oxide heterostructures

Neutron and x-ray spectroscopy

outline

1. weak correlations: Pb, Nb
2. intermediate correlations: Sr_2RuO_4
3. strong correlations: $YBa_2Cu_3O_{6+x}$
4. orbital degeracy: $La_{1-x}Ca_xMnO_3$ (Y,La)TiO_3
5. oxide heterostructures

Electron-phonon interaction

electron-phonon interaction in simple metals predicted by ab-initio LDA

example MgB_2

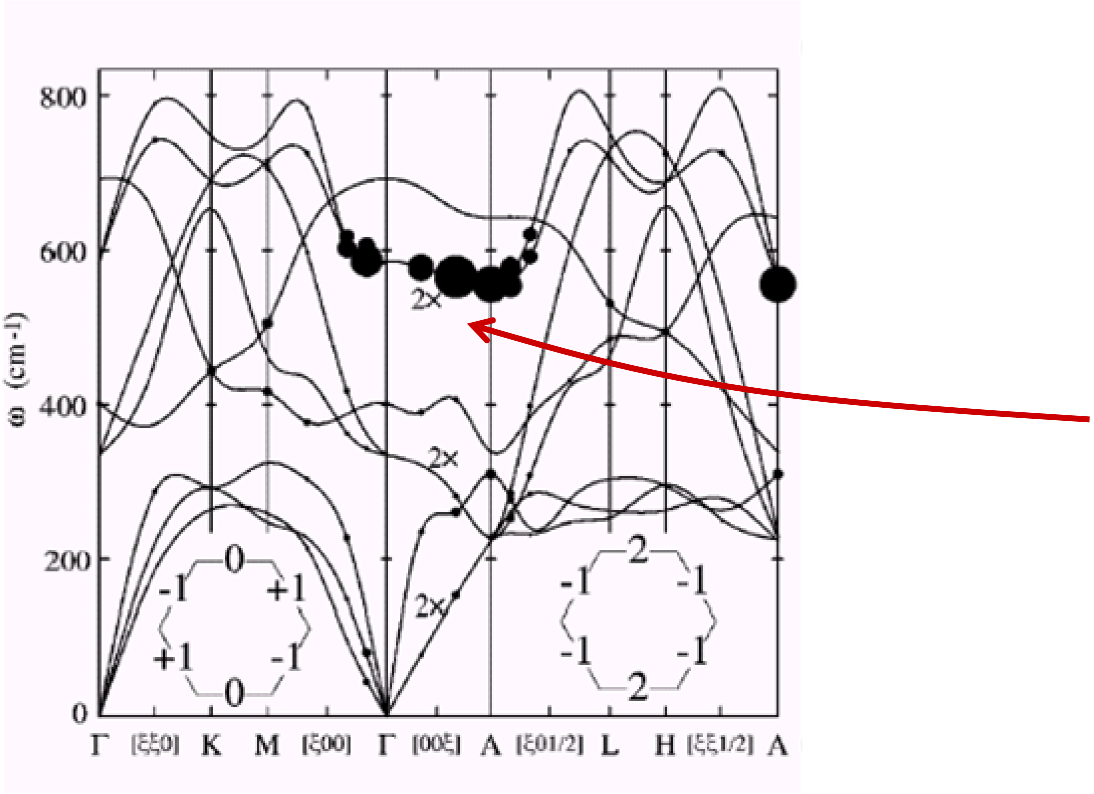

Kong et al., PRB 2001

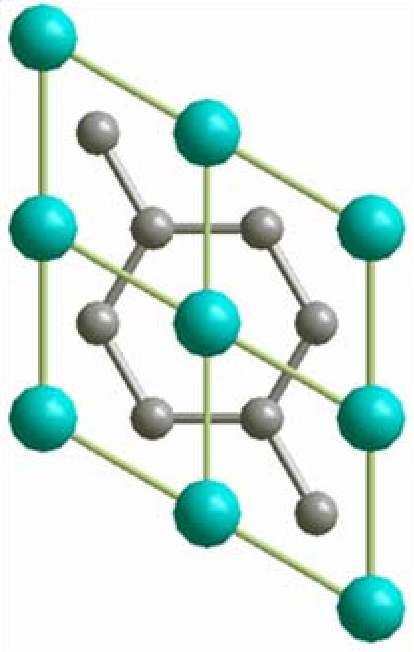

strong coupling

short phonon lifetime

typical phonon linewidth: 1-100 μeV

Inelastic nuclear neutron scattering

$$\frac{d^2\sigma}{d\Omega\,dE} = \frac{\sigma_{coh}}{4\pi}\frac{k_f}{k_i}\frac{(2\pi)^3}{v_0}\frac{1}{2M}e^{-2W}\sum_s\sum_\eta\frac{(\mathrm{Q}\cdot\mathrm{e}_s)^2}{\omega_s}\times$$

$$\{\langle n_s+1\rangle\,\delta(\omega-\omega_s)\,\delta(\mathrm{Q}-\mathrm{q}-\mathbf{K})+\langle n_s\rangle\,\delta(\omega+\omega_s)\,\delta(\mathrm{Q}+\mathrm{q}-\mathbf{K})\}$$

phonon creation
neutron energy loss

phonon annihilaion
neutron energy gain

Neutron spectroscopy

$$\hbar\omega = \frac{\hbar^2}{2m}(k_f{}^2 - k_i{}^2)$$

$$q = k_f - k_i$$

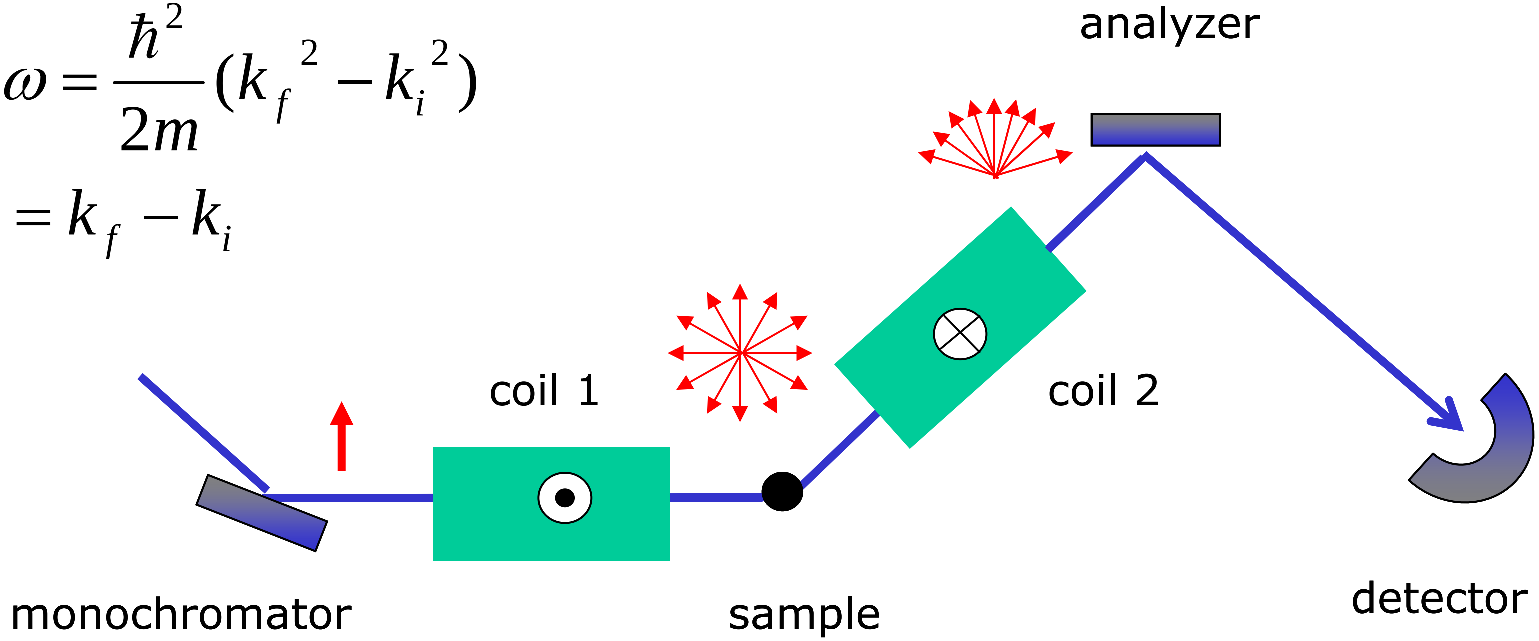

triple axis spectrometer: excitation energy ~ 1-100 meV
energy resolution ~ 0.1-10 meV

triple axis – spin echo spectrometer: excitation energy ~ 1-100 meV
energy resolution ~ 1 – 100 μeV

3 orders of magnitude gain in energy resolution
→ possible to resolve excitation lifetimes in solids

Max-Planck-Institut für Festkörperforschung

TRISP Spectrometer at FRM-II

Electron-phonon interaction in Pb

phonon dispersions

Brockhouse et al., PR 1963

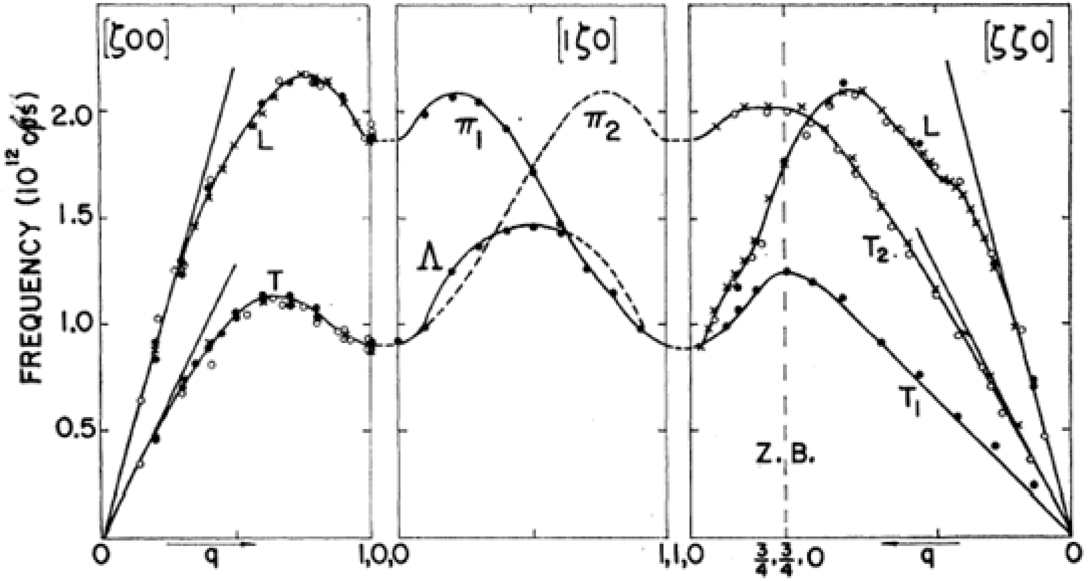

ab-initio lattice dynamics

L. Boeri, MPI-FKF

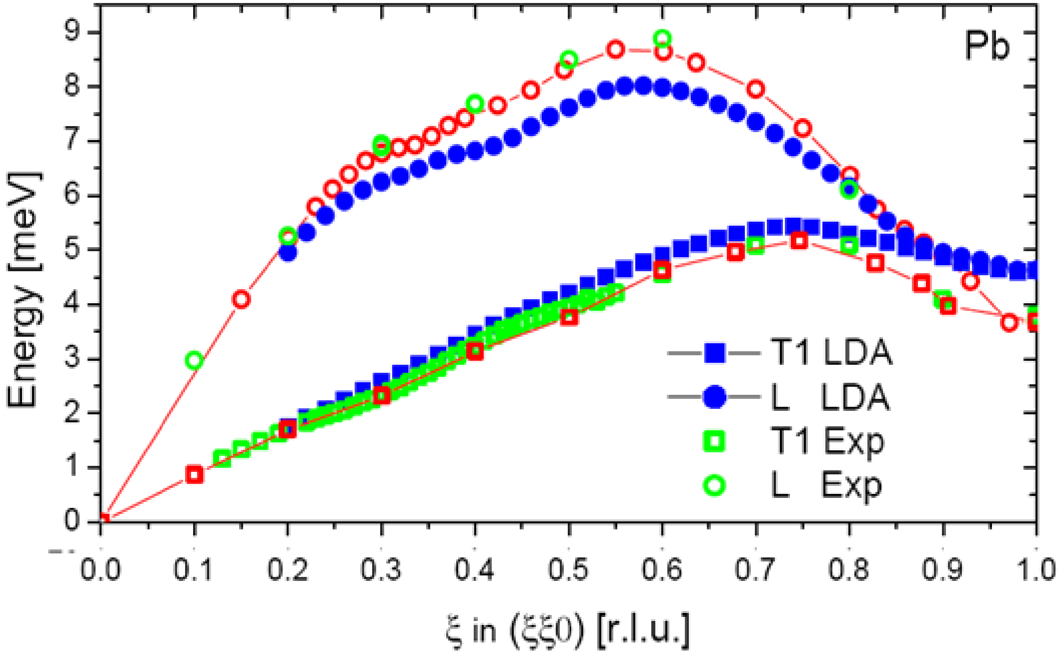

Electron-phonon interaction in Pb

lifetime renormalization below superconducting T_c = 7.2 K

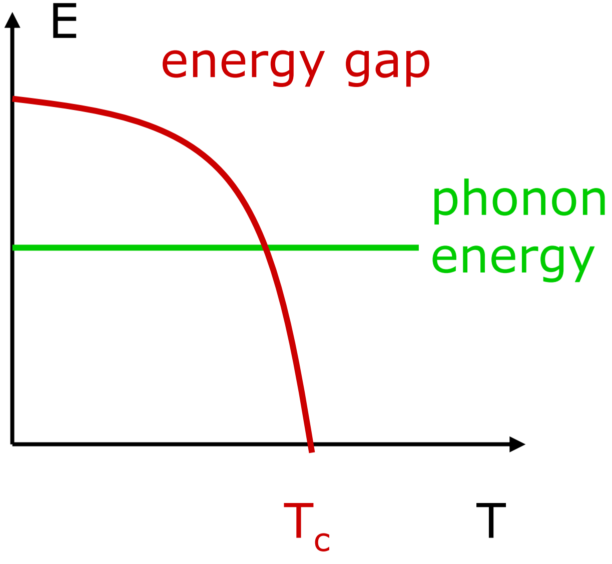

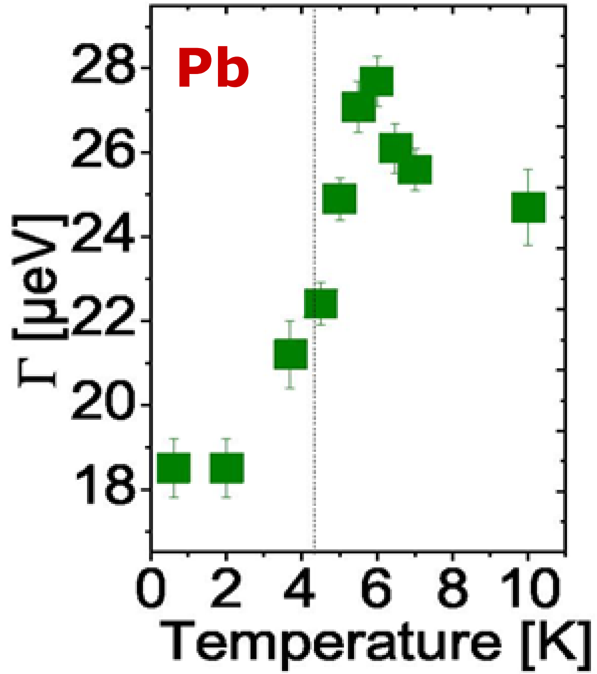

Keller et al., PRL 2006

Electron-phonon interaction in Pb

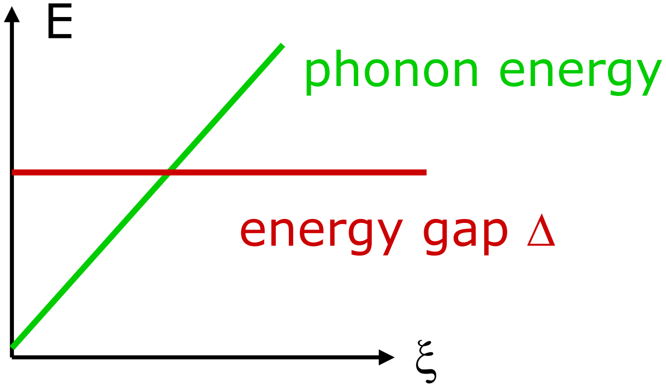

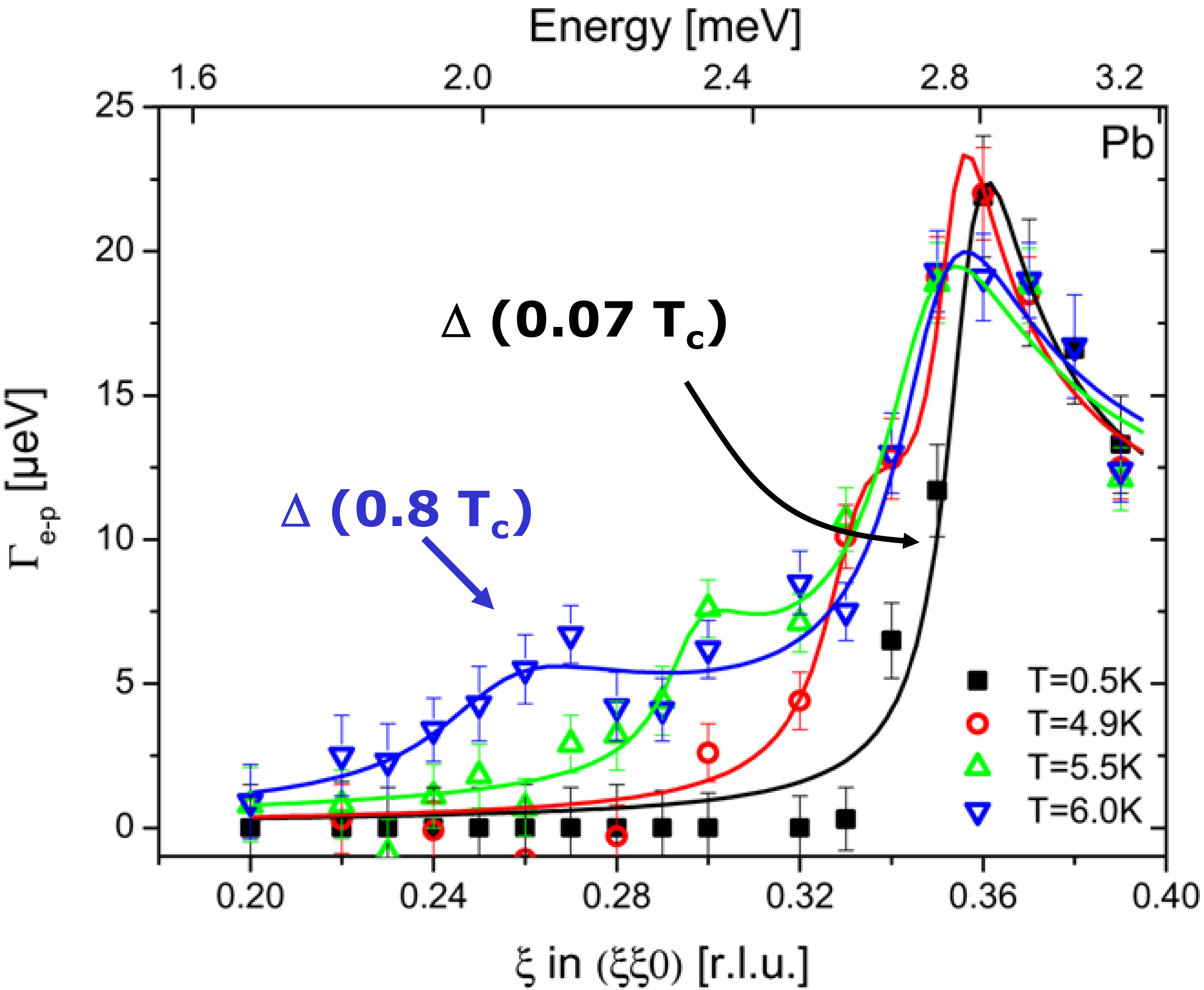

Δ (0.07 T_c)

Δ (0.8 T_c)

Aynajian et al.
Science 2008

Electron-phonon interaction in Pb

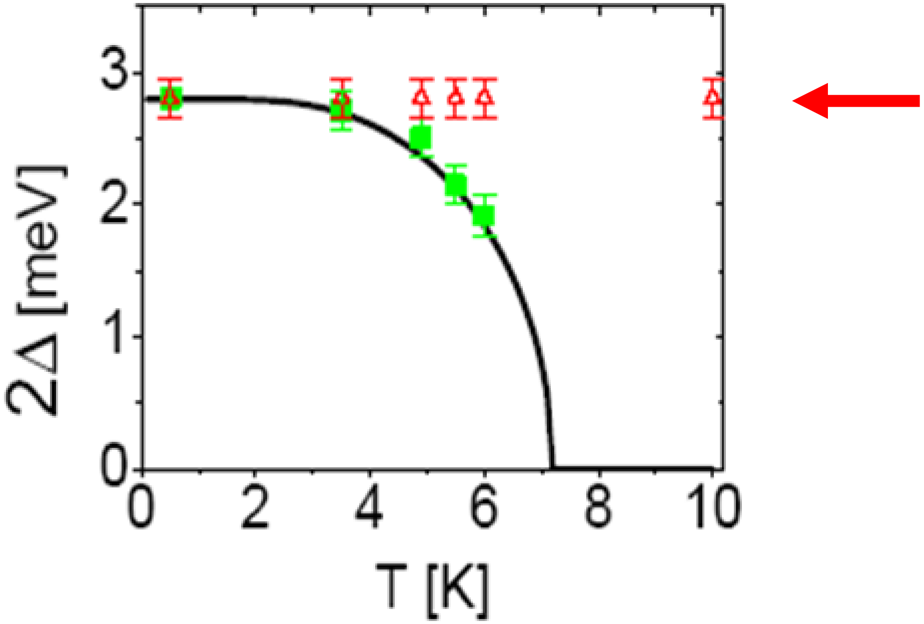

superconducting energy gap

merges with second linewidth maximum at low T

Electron-phonon interaction in Pb

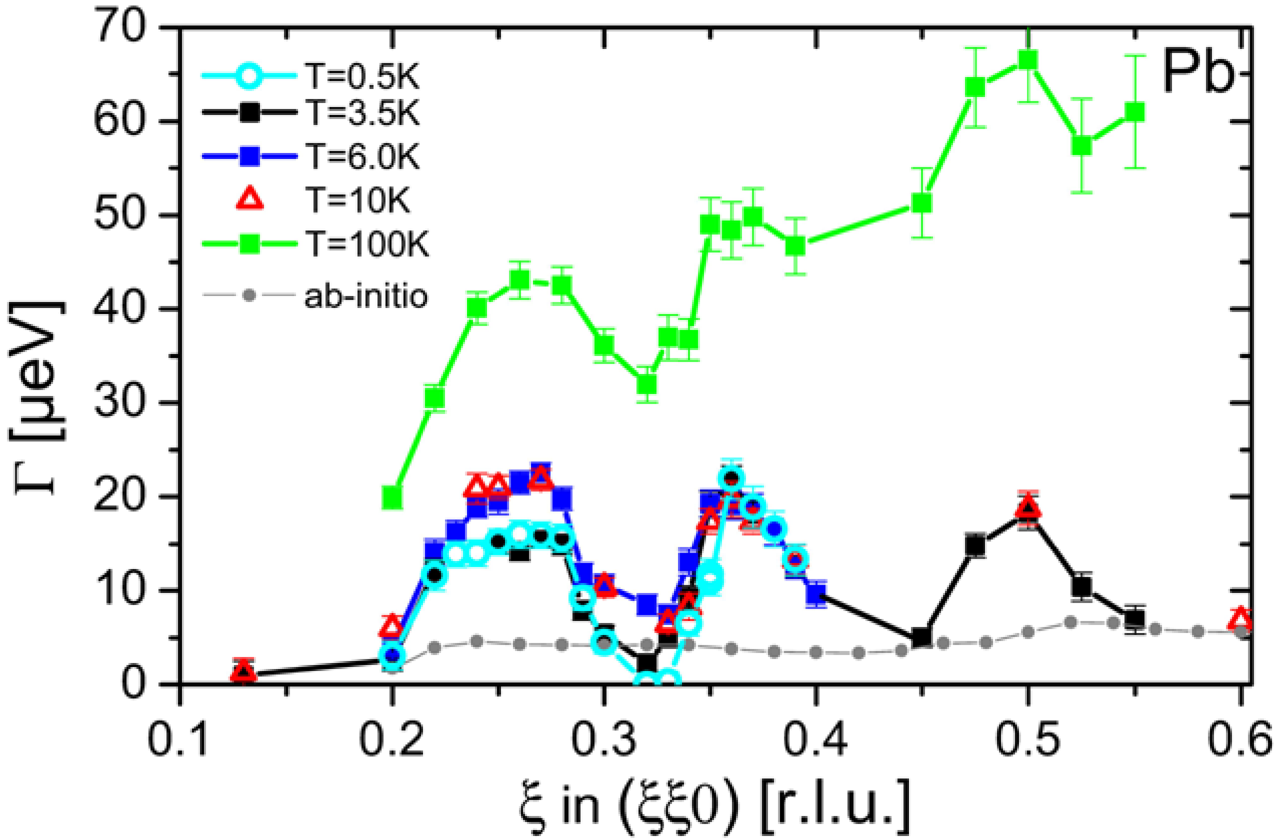

Aynajian et al.
Science 2008

series of linewidth maxima persists up to T >> T_c

most likely origin: Kohn anomalies

but not predicted in TA branch by ab-initio LDA calculations

Accident ?

niobium

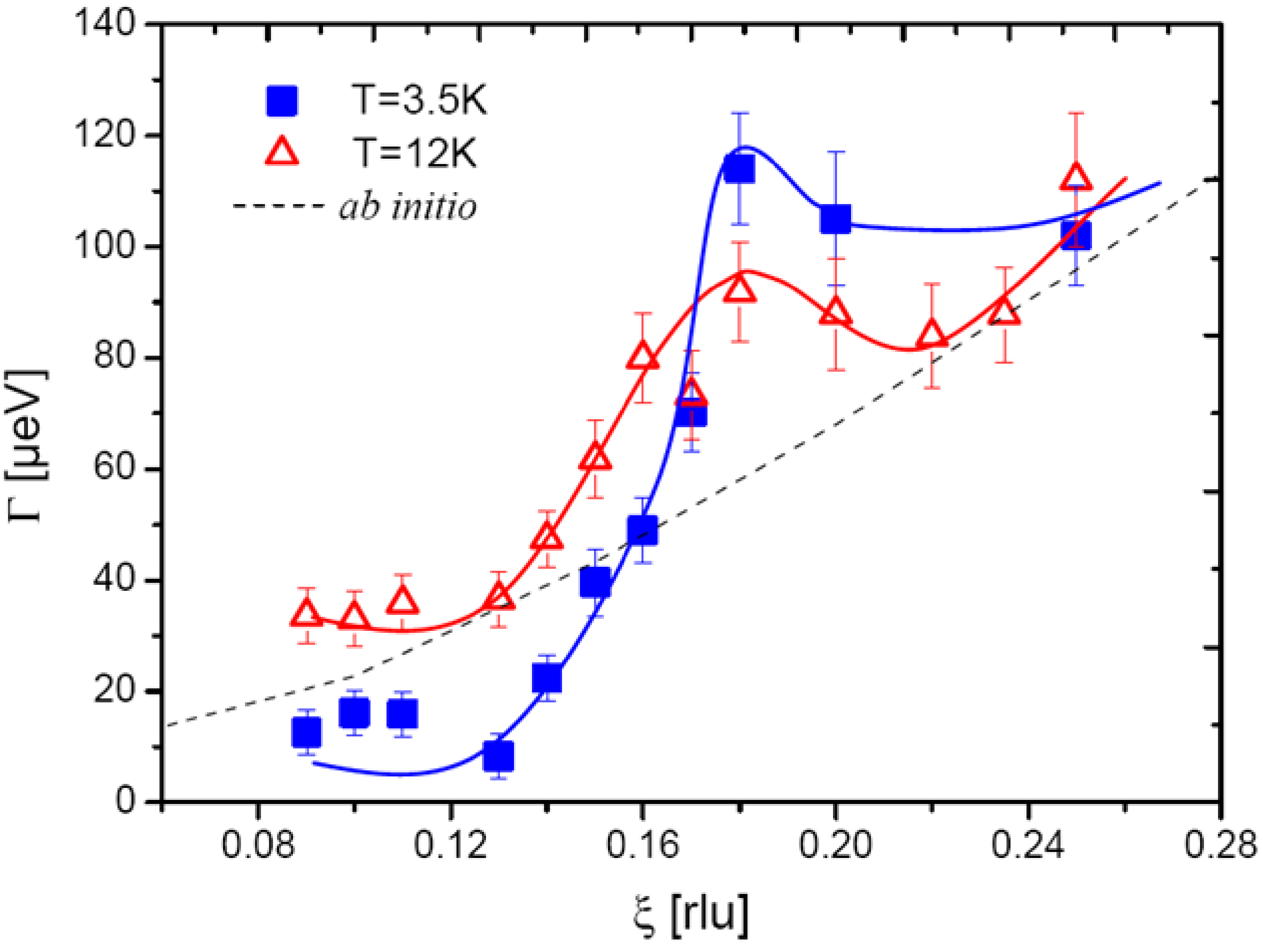

Aynajian et al.
Science 2008

no! same effect observed in Nb

also rules out spin-orbit coupling as origin

für Festkörperforschung

Origin: Kohn anomaly?

acoustic phonons in TaS_2

quasi-2D metal

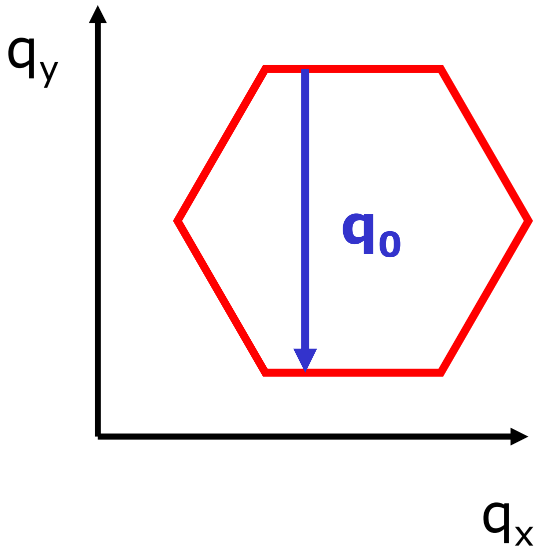

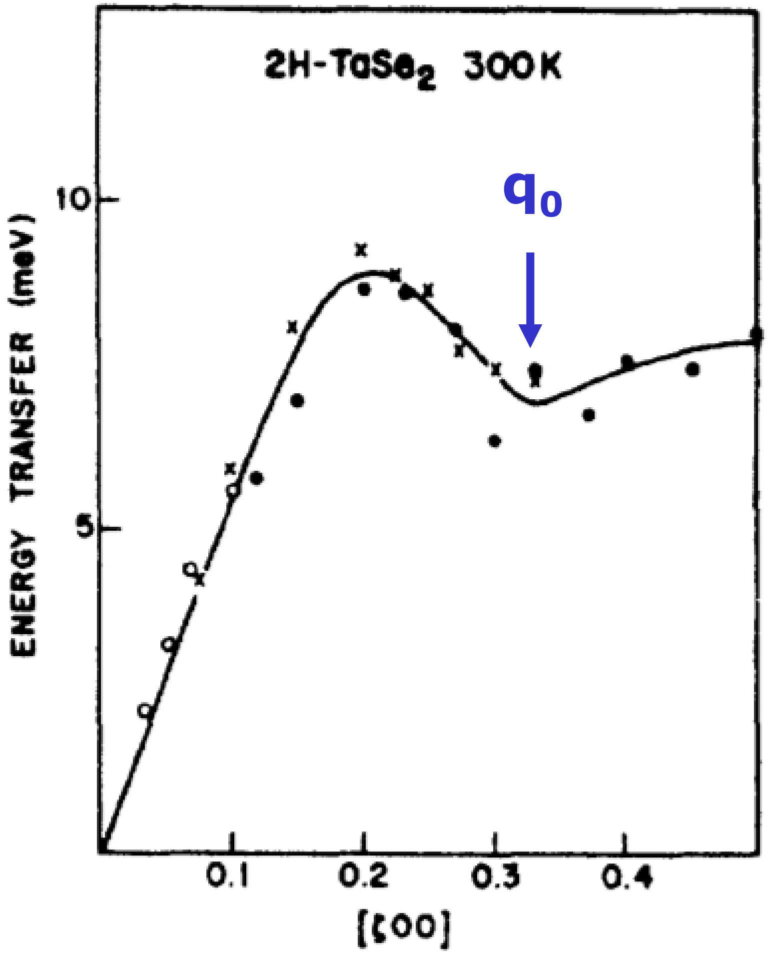

Kohn anomaliy precursor to

charge-density-wave formation

at T = 122 K

Moncton et al., PRB 1977

Electron-phonon interaction in Pb and Nb

scenario

- many-body effects beyond LDA:
  spin/charge density wave fluctuations

- dynamical nesting → Kohn anomalies

- interference between SDW/CDW and superconducting fluctuations limits growth of superconducting energy gap

- not anticipated by theory

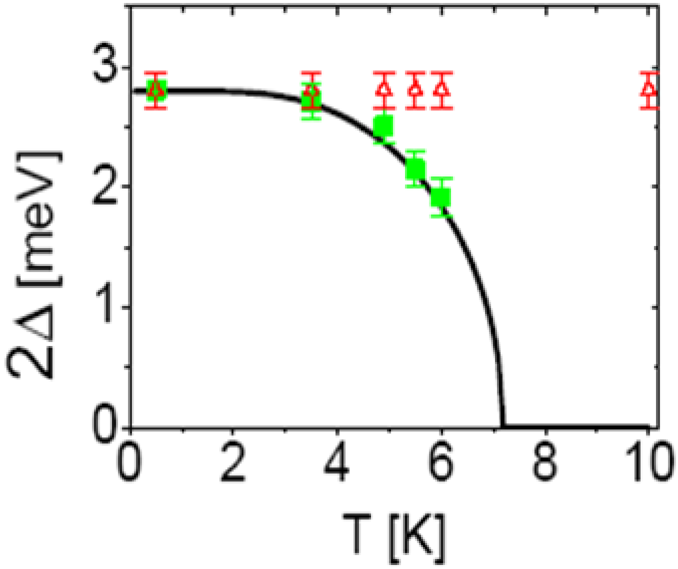

calculations needed !

Neutron and x-ray spectroscopy

outline

1. weak correlations: Pb, Nb
2. intermediate correlations: Sr_2RuO_4
3. strong correlations: $YBa_2Cu_3O_{6+x}$
4. orbital degeracy: $La_{1-x}Ca_xMnO_3$ (Y,La)TiO_3
5. oxide heterostructures

Max-Planck-Institut
für Festkörperforschung

Inelastic magnetic neutron scattering

$$\frac{d^2\sigma}{d\Omega\, dE} = (\gamma r_0)^2 \frac{k_f}{k_i} N \left|F(\mathrm{Q})\right|^2 e^{-2W} \sum_{\alpha\beta} (\delta_{\alpha\beta} - \hat{Q}_\alpha \hat{Q}_\beta) S^{\alpha\beta}(\mathrm{Q},\omega)$$

$$S^{\alpha\beta}(\mathrm{Q},\omega) = \frac{1}{2\pi\hbar} \int \sum_l e^{i\mathrm{Q}\mathrm{r}_l} \left\langle S_0^\alpha(0) S_l^\beta(t) \right\rangle e^{-i\omega t} dt$$

fluctuation-dissipation theorem

$$S^{\alpha\beta}(\mathrm{Q},\omega) = \frac{1}{\pi (g\mu_{\mathrm{B}})^2} \frac{1}{1 - e^{-\hbar\omega\beta}} \chi''_{\alpha\beta}(\mathrm{Q},\omega)$$

$$\chi''(\mathrm{Q},\omega) = \mathrm{Tr}\left[\chi''_{\alpha\beta}(\mathrm{Q},\omega)\right]/3$$

dynamical magnetic susceptibility
response to time- and position-dependent magnetic field

$$\frac{d^2\sigma}{d\Omega\, dE} = 2(\gamma r_0)^2 \frac{k_f}{k_i} N \left|F(\mathrm{Q})\right|^2 e^{-2W} \frac{1}{\pi (g\mu_{\mathrm{B}})^2} \frac{1}{1 - e^{-\hbar\omega\beta}} \chi''(\mathrm{Q},\omega)$$

Stoner model

susceptibility of electron band

$$\chi_0(q,\omega) = \sum_k \frac{f(E_{k+q\uparrow}) - f(E_{k\downarrow})}{\hbar\omega - (E_{k+q} - E_k - \Delta) + i\varepsilon}$$

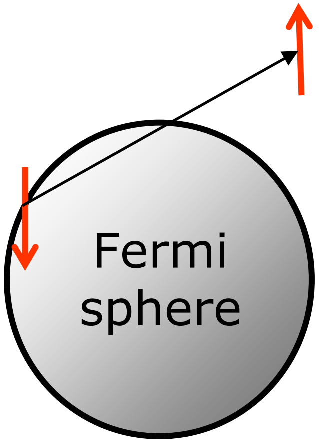

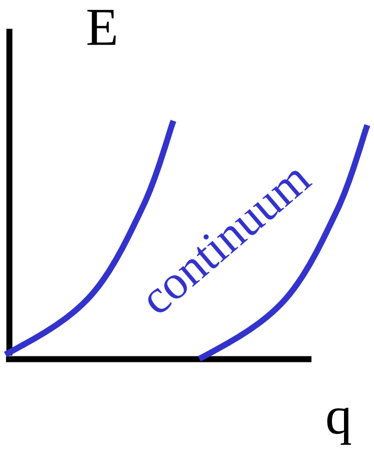

enhanced by electronic correlations (RPA)

$$\chi(q,\omega) = \frac{\chi_0(q,\omega)}{1 - J(q)\chi_0(q,\omega)}$$

J(q) peaked at q=0, sufficiently strong → ferromagnetism

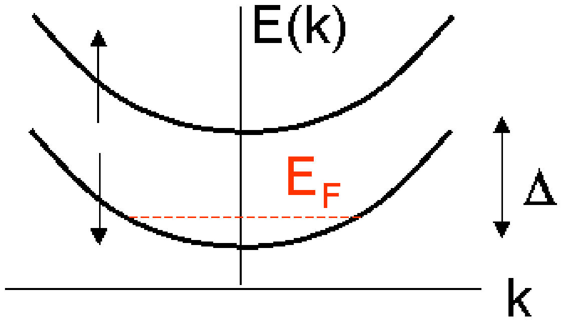

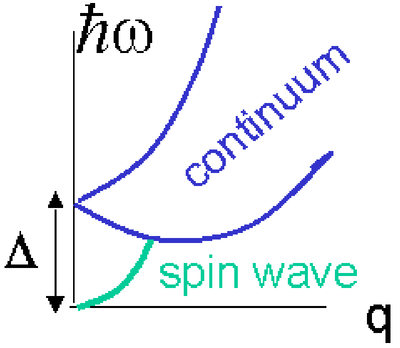

e.g. Fe, Ni

Sr_2RuO_4

layered structure

isostructural to layered cuprates

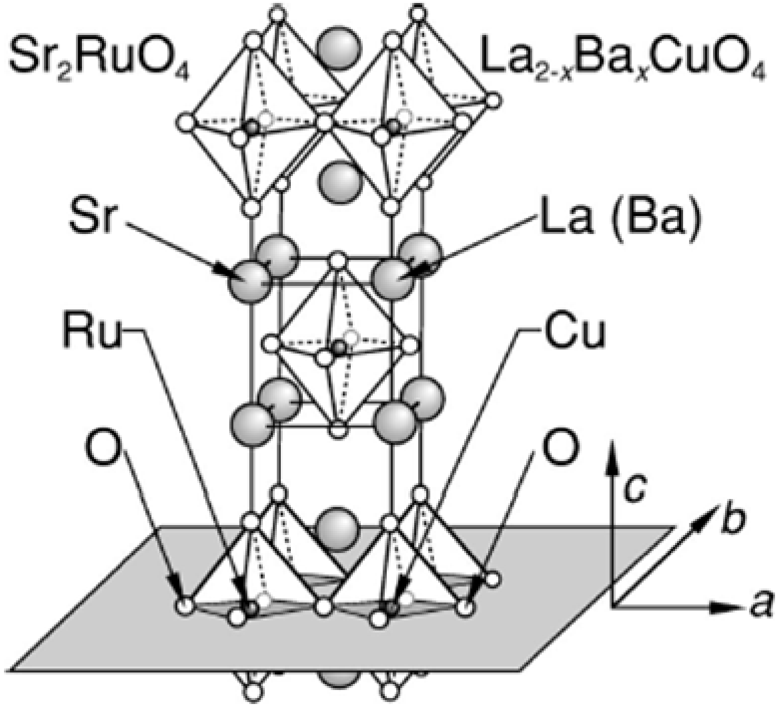

electron configuration $3d^4$

electrons in t_{2g} orbitals

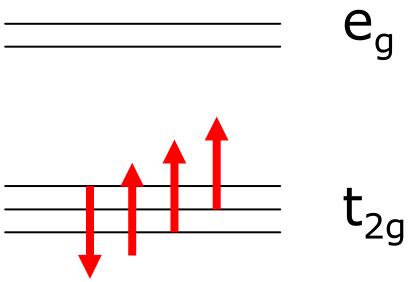

Sr_2RuO_4 spin excitations

ARPES Fermi surface
strongly nested

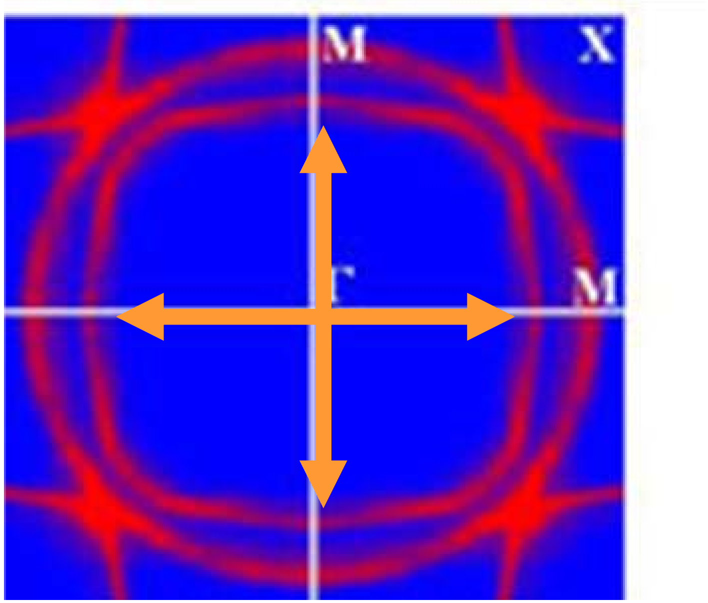

band susceptibility

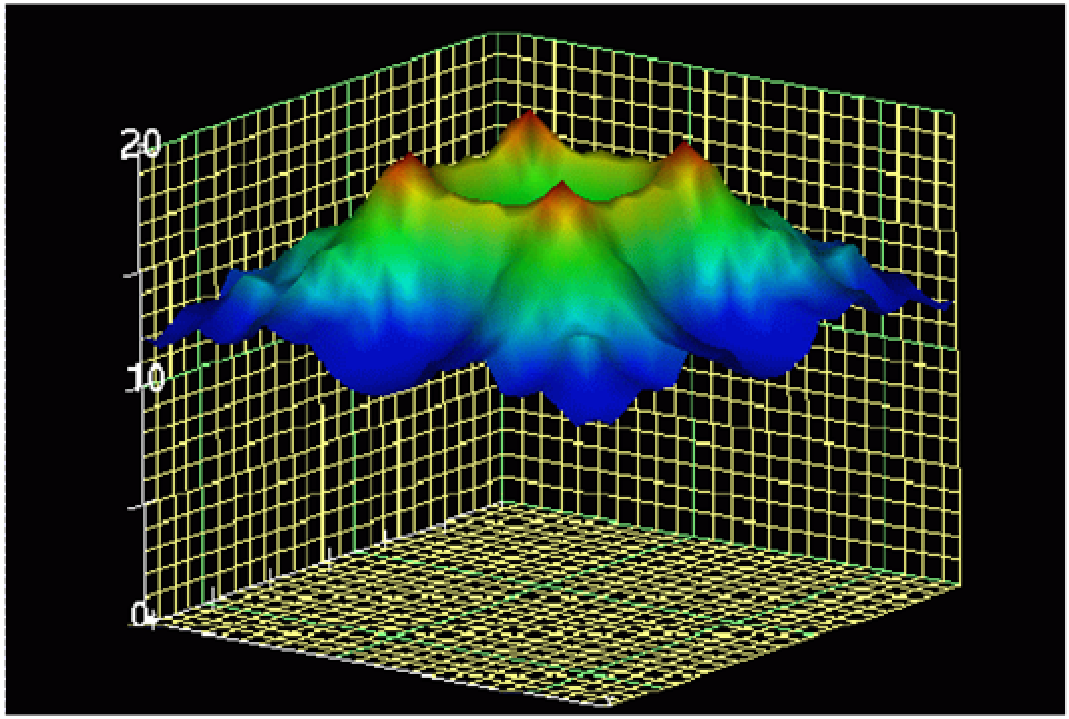

Mazin et al., PRL 1999

Sr_2RuO_4 spin excitations

inelastic magnetic neutron scattering

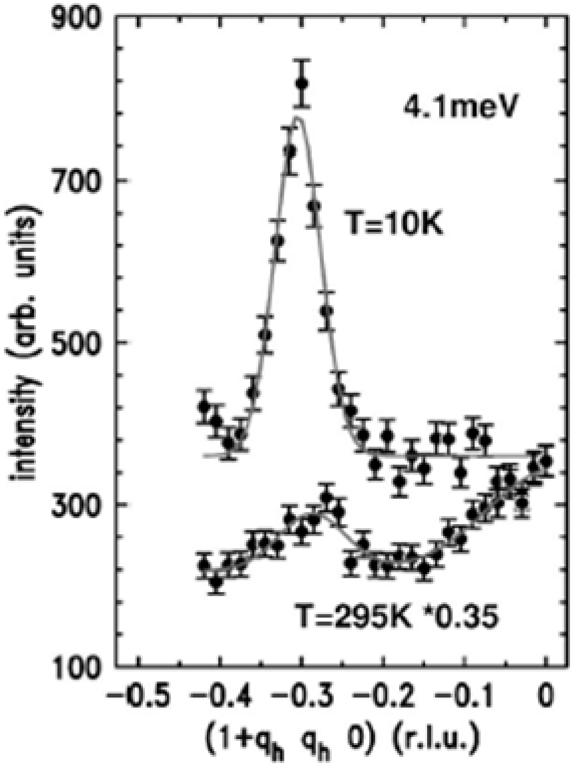

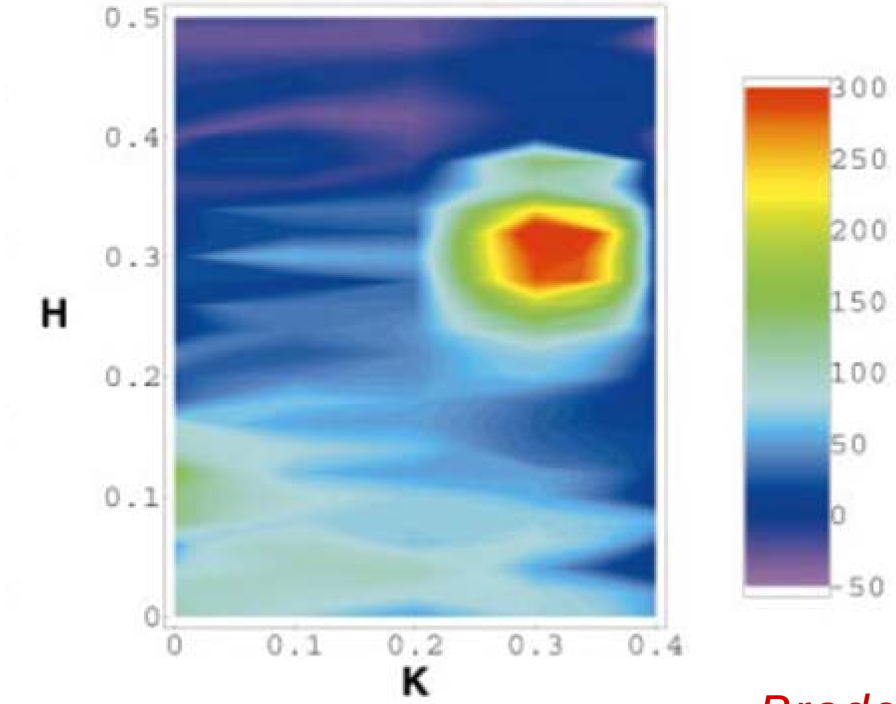

Braden et al., PRB 2002

signal explained by “bare” band susceptibility

no apparent role in driving p-wave superconductivity

Neutron and x-ray spectroscopy

outline

1. weak correlations: Pb, Nb
2. intermediate correlations: Sr_2RuO_4
3. strong correlations: $YBa_2Cu_3O_{6+x}$
4. orbital degeracy: $La_{1-x}Ca_xMnO_3$ $(Y,La)TiO_3$
5. oxide heterostructures

$YBa_2Cu_3O_{6+x}$

CuO_2 →

CuO_2 →

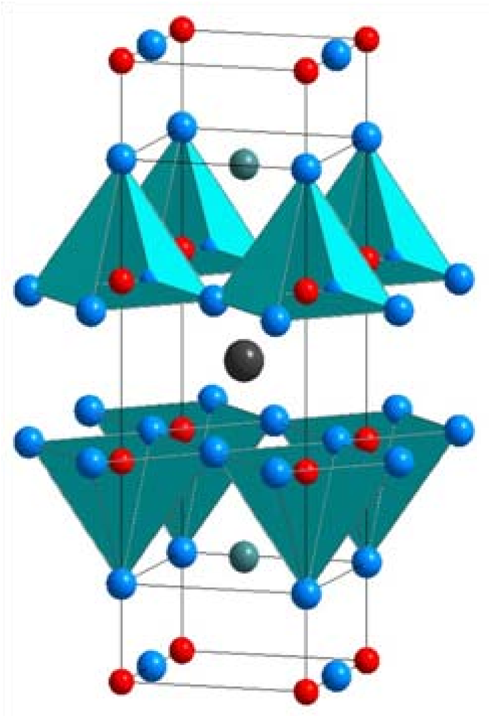

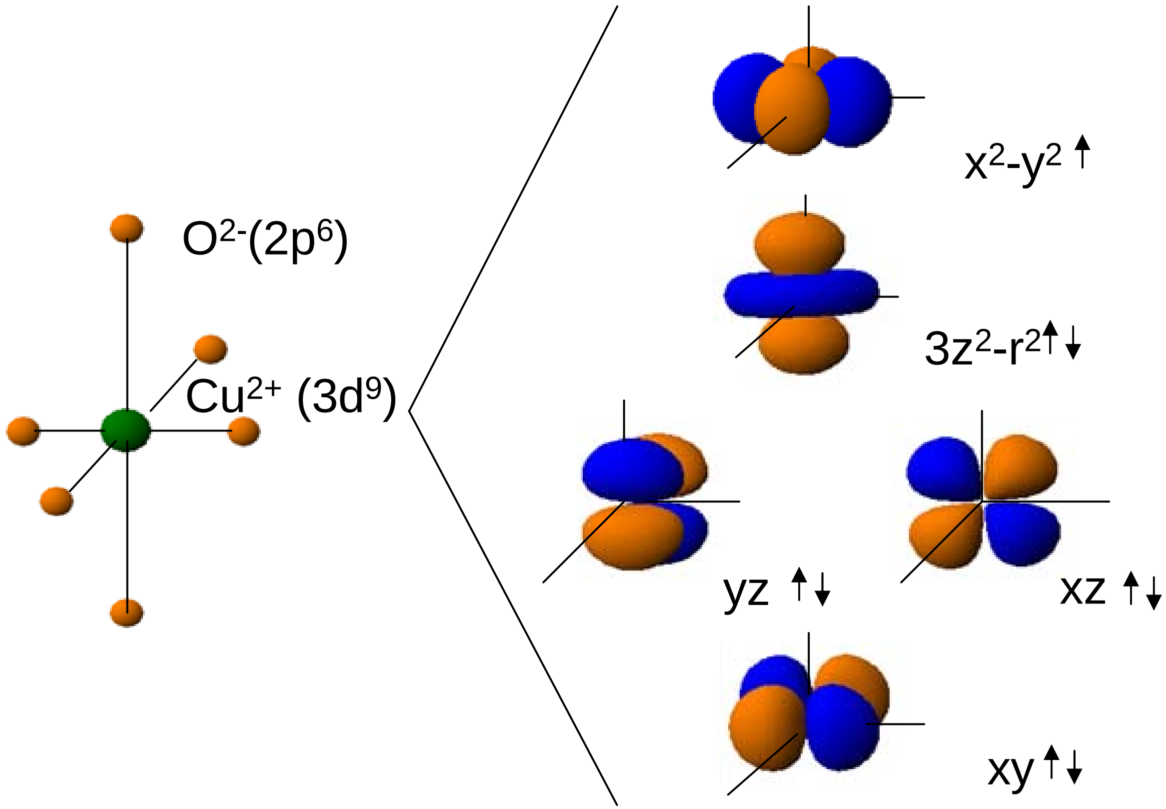

- **two-dimensional electronic structure**
- **no orbital degeneracy**

$YBa_2Cu_3O_{6+x}$ x-ray linear dichroism

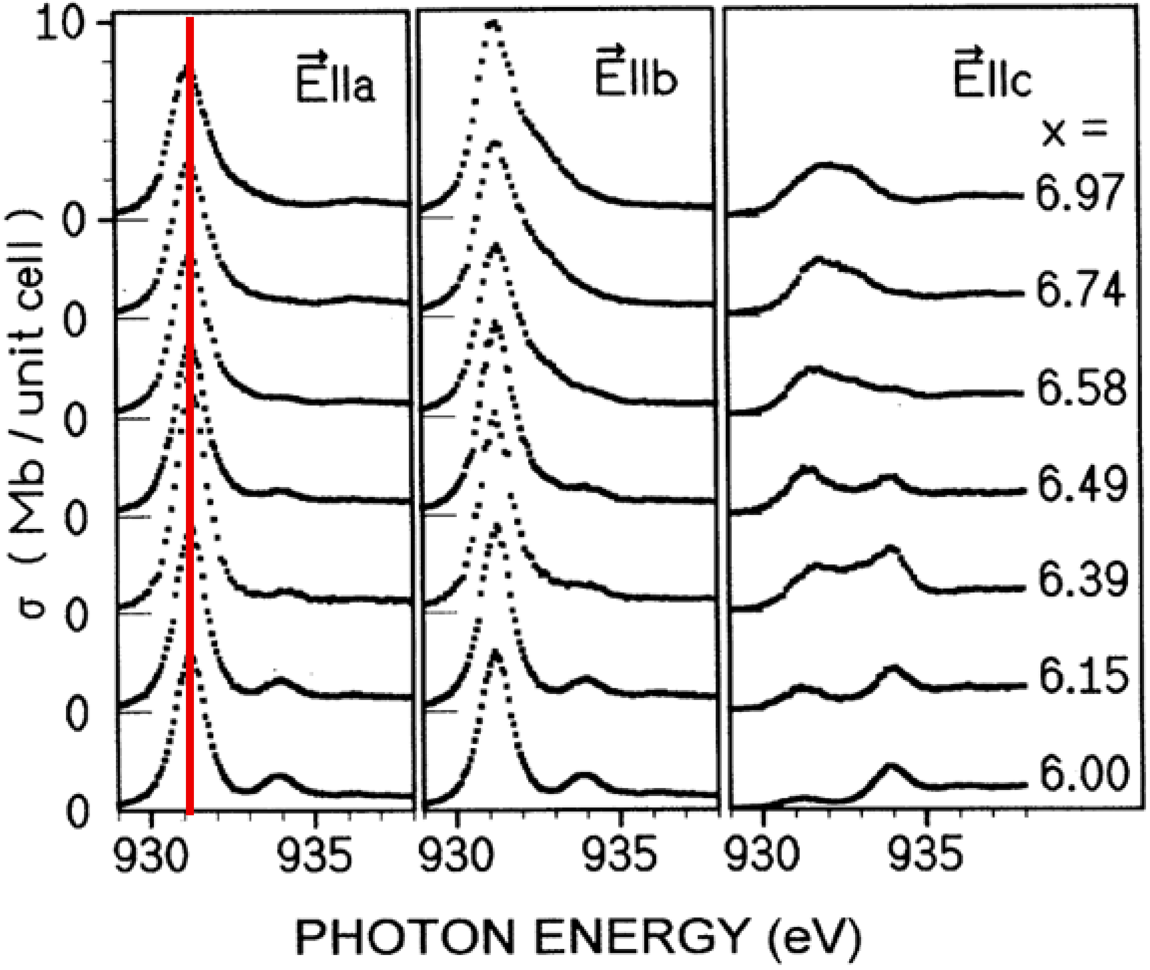

- absorption cross section much greater for E ∣∣ ab-plane → x^2-y^2 orbital partially occupied
- peak position independent of doping (Zhang-Rice singlet state)

Nücker et al., PRB 1995

$YBa_2Cu_3O_{6+x}$

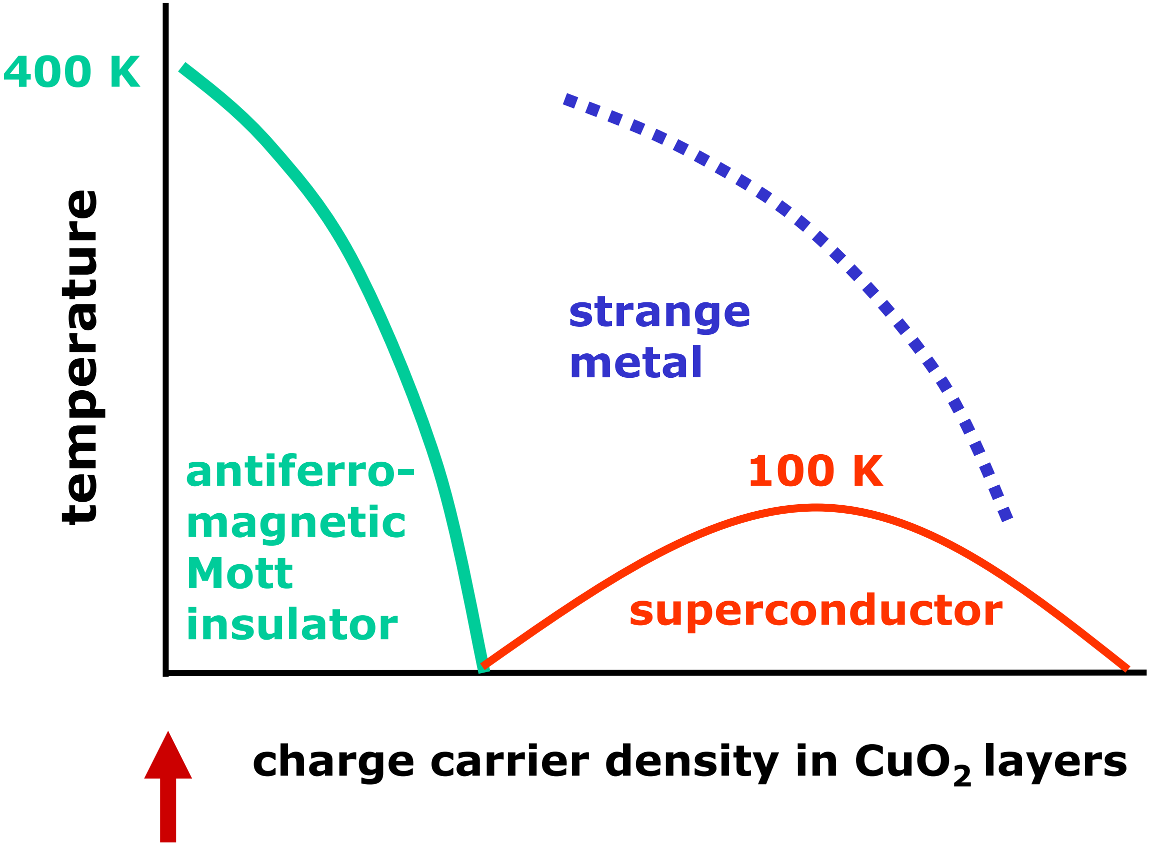
400 K
temperature
strange metal
antiferro-magnetic Mott insulator
100 K
superconductor
charge carrier density in CuO_2 layers

Inelastic magnetic neutron scattering

$$\frac{d^2\sigma}{d\Omega\, dE} = (\gamma r_0)^2 \frac{k_f}{k_i} N \left|F(\mathbf{Q})\right|^2 e^{-2W} \sum_{\alpha\beta} (\delta_{\alpha\beta} - \hat{Q}_\alpha \hat{Q}_\beta) S^{\alpha\beta}(\mathbf{Q},\omega)$$

polarization factor

$$S^{\alpha\beta}(\mathbf{Q},\omega) = \frac{1}{2\pi\hbar} \int \sum_l e^{i\mathbf{Q}\mathbf{r}_l} \left\langle S_0^\alpha(0) S_l^\beta(t) \right\rangle e^{-i\omega t} dt$$

spin-spin correlation function

Heisenberg antiferromagnet, magnon creation

$$\frac{d^2\sigma}{d\Omega\, dE} = (\gamma r_0)^2 \frac{k_f}{k_i} \left|F(\mathbf{Q})\right|^2 e^{-2W} \frac{(2\pi)^3}{4N v_0} \{1 + (\hat{Q}\hat{\eta})^2\} \times$$

$$\sum_{a=0,1} \sum_{q,K_m} \langle n_{q,a} + 1 \rangle\, \delta(\omega_{q,a} - \omega)\, \delta(\mathbf{Q} - \mathbf{q} - \mathbf{K_m})$$

$YBa_2Cu_3O_6$ magnons

$$H = \Sigma_{ij} (J_{\|}\, S_i^{(a,b)} \bullet S_j^{(a,b)}) + \Sigma_i (J_{\perp 1}\, S_i^{(a)} \bullet S_i^{(b)} + J_{\perp 2}\, S_i^{(b)} \bullet S_i^{(a)})$$

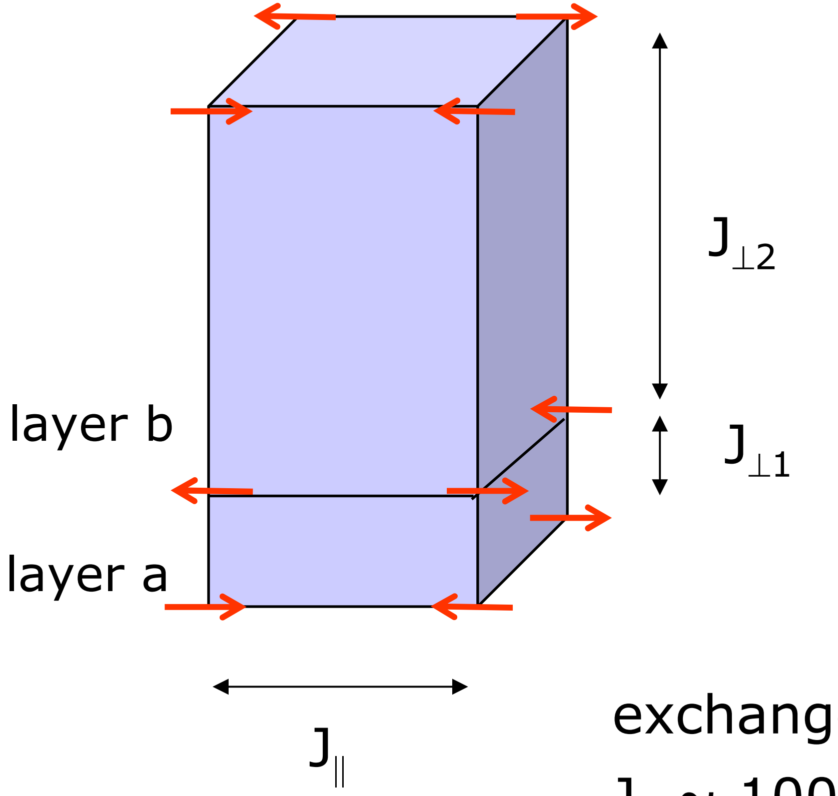

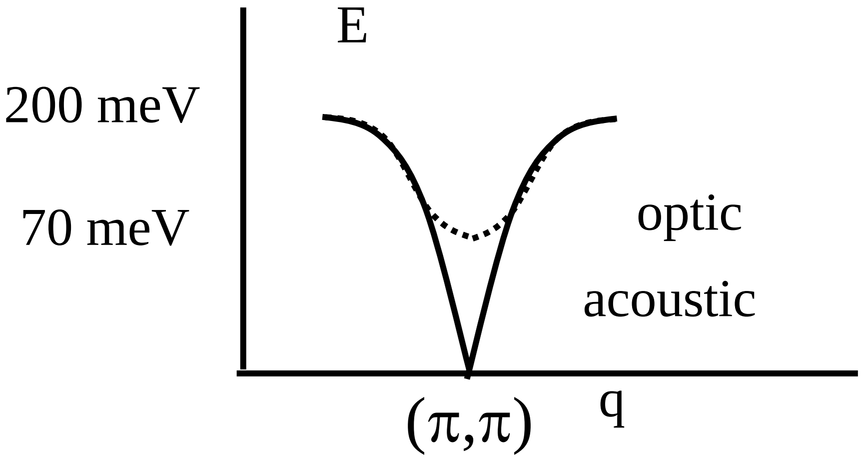

exchange parameters from magnon dispersions

$J_{\|} \sim 100$ meV

$J_{\perp 1} \sim 10$ meV

$J_{\perp 2} \sim 0.01$ meV

Tranquada et al., PRB 1989
Reznik et al., PRB 1996

$YBa_2Cu_3O_{6+x}$

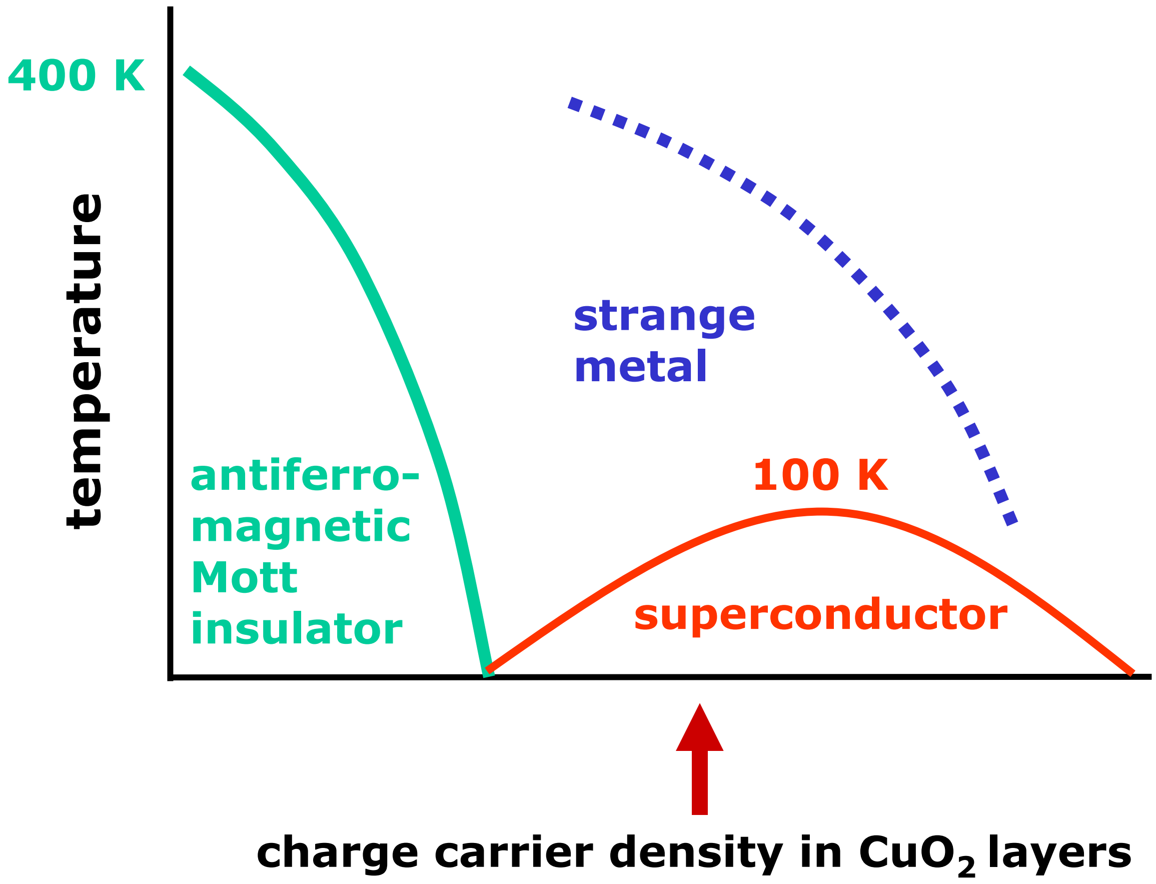

Max-Planck-Institut für Festkörperforschung

$YBCO_{6.6}$ spin dynamics

untwinned $YBCO_{6.6}$ (T_c = 61K)

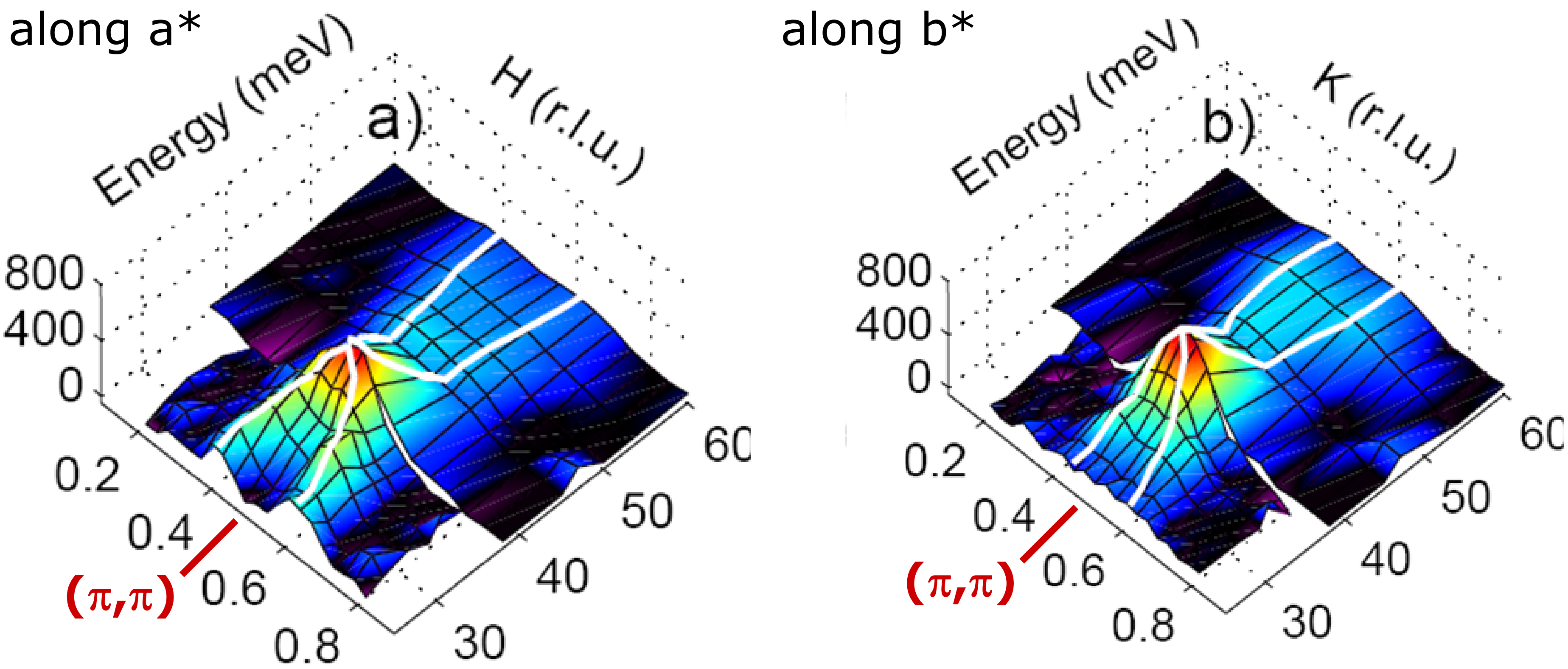

two-dimensional "hour glass" dispersion

also seen in $YBCO_7$ and other high-T_c cuprates

Hinkov et al.
Nature 2004
Nature Phys. 2007

$YBCO_{6.6}$ spin dynamics

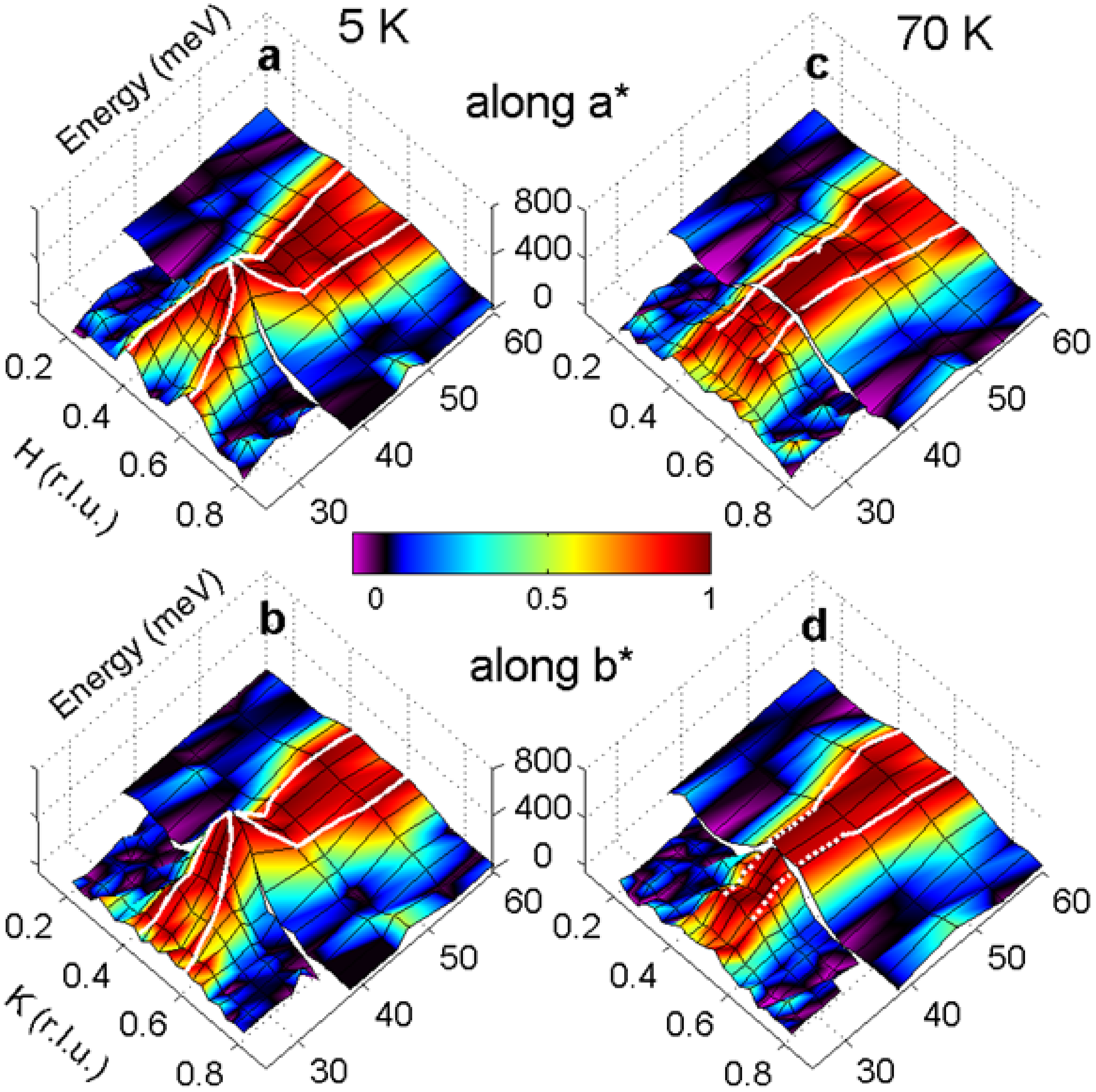

$T < T_c$

"hour glass" dispersion

$T > T_c$

"hour glass" replaced by
"vertical" dispersion

very large in-plane anisotropy

Hinkov et al.,
Nature Phys. 2007

Band susceptibility in superconducting state

coherence factor Fermi factor

$$\chi_0(q,\omega) = \Sigma_k \{ \tfrac{1}{2} (1 + \frac{\varepsilon_k \varepsilon_{k+q} + \Delta_k \Delta_{k+q}}{E_k E_{k+q}}) \frac{f(E_{k+q}) - f(E_k)}{\omega - (E_{k+q} - E_k) + i\delta}$$

scattering of
thermally excited pairs

$$+ \tfrac{1}{4} (1 - \frac{\varepsilon_k \varepsilon_{k+q} + \Delta_k \Delta_{k+q}}{E_k E_{k+q}}) \frac{1 - f(E_{k+q}) - f(E_k)}{\omega + (E_{k+q} + E_k) + i\delta}$$

pair annihilation

$$+ \tfrac{1}{4} (1 - \frac{\varepsilon_k \varepsilon_{k+q} + \Delta_k \Delta_{k+q}}{E_k E_{k+q}}) \frac{f(E_{k+q}) + f(E_k) - 1}{\omega - (E_{k+q} + E_k) + i\delta} \}$$

pair creation

ε_k band dispersion, measured from E_F

$$E_k = \sqrt{\varepsilon_k^2 + \Delta_k^2}$$

yields only broad features, inconsistent with experiment

Spin exciton model

simplest formalism: RPA

$$\chi(\mathrm{q},\omega) = \frac{\chi_0(\mathrm{q},\omega)}{1 - \mathrm{J}(\mathrm{q})\ \chi_0(\mathrm{q},\omega)}$$

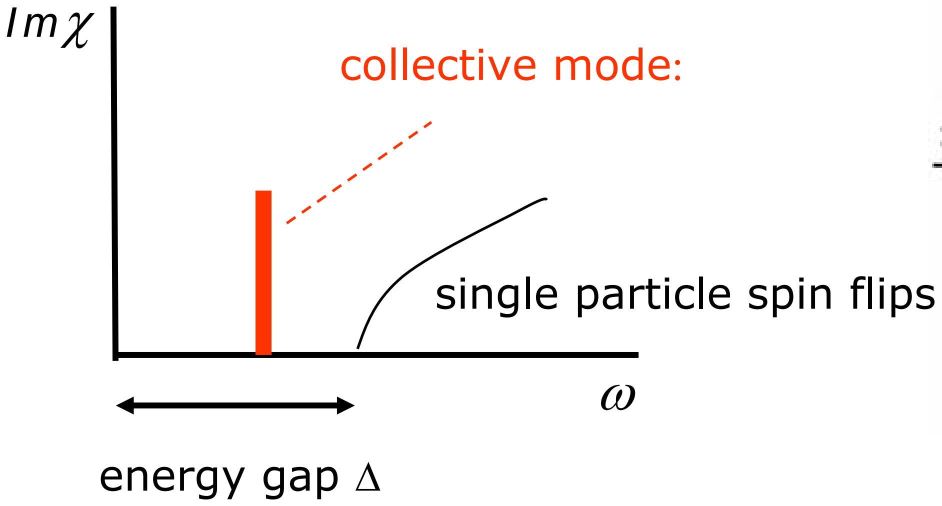

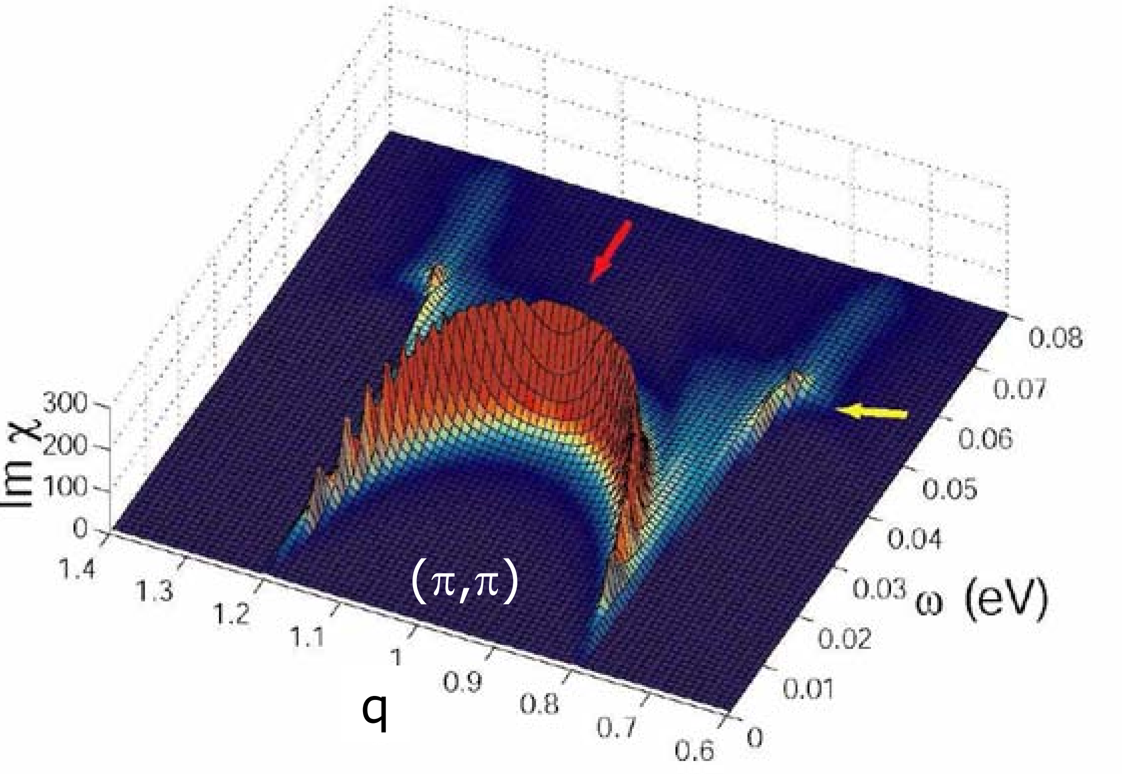

- "hour glass" reproduced
- upper cutoff of neutron spectrum
  direct measure of **bulk** Δ(q)
- agrees well with other probes of Δ(q)

Eremin et al., PRL 2005
see also: many other RPA calculations

Spin exciton model

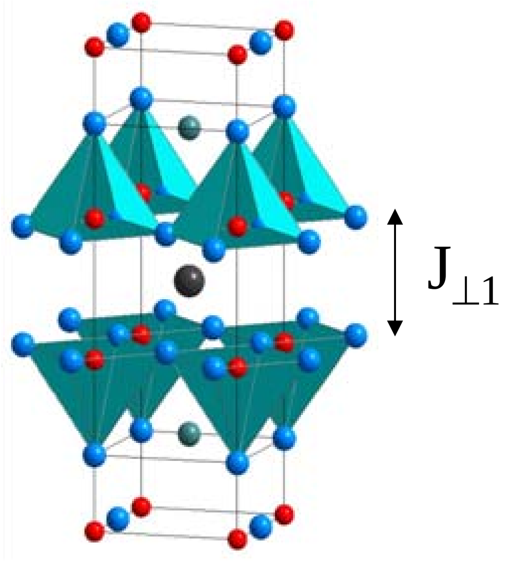

interlayer exchange interaction

Pailhes et al., PRL 2003, PRL 2006

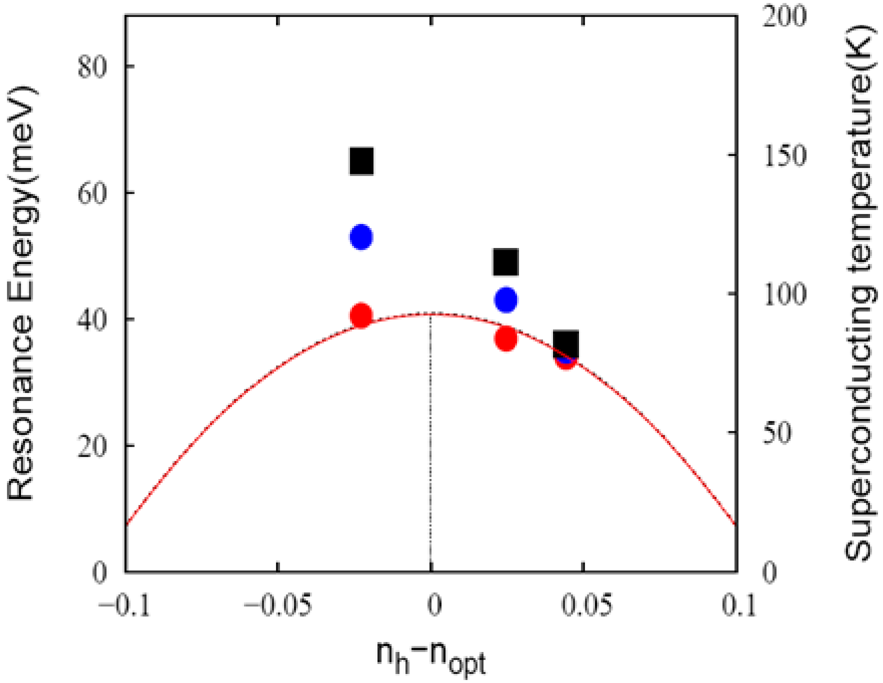

- ● odd
- ● even
- ■ gap estimated based on RPA

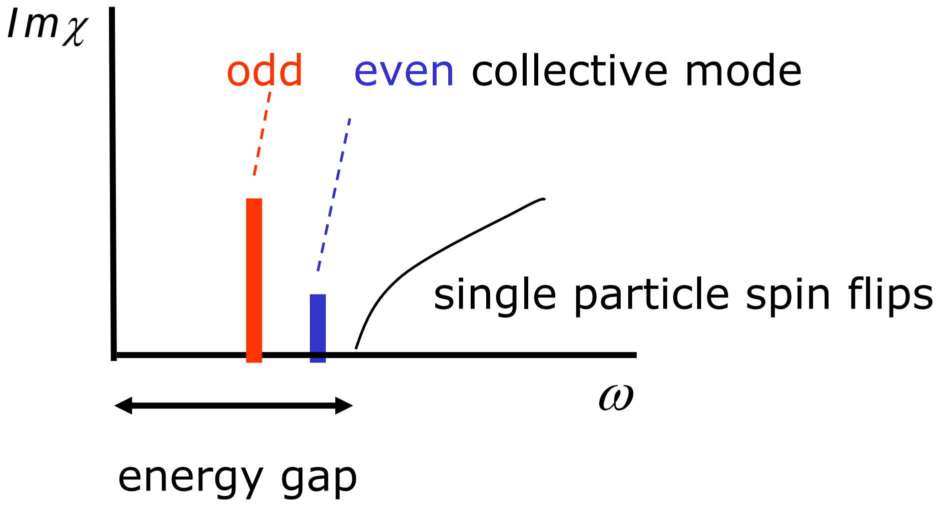

$$\frac{\omega_c - E_r^{odd}}{\omega_c - E_r^{even}} = \frac{W_{odd}(q_{AF})}{W_{even}(q_{AF})}$$

$$W_{e,o} = \int \chi''(q_{AF}, \omega) d\omega$$

Max-Planck-Institut für Festkörperforschung

Spin dynamics in superconducting state

neutron intensity maps

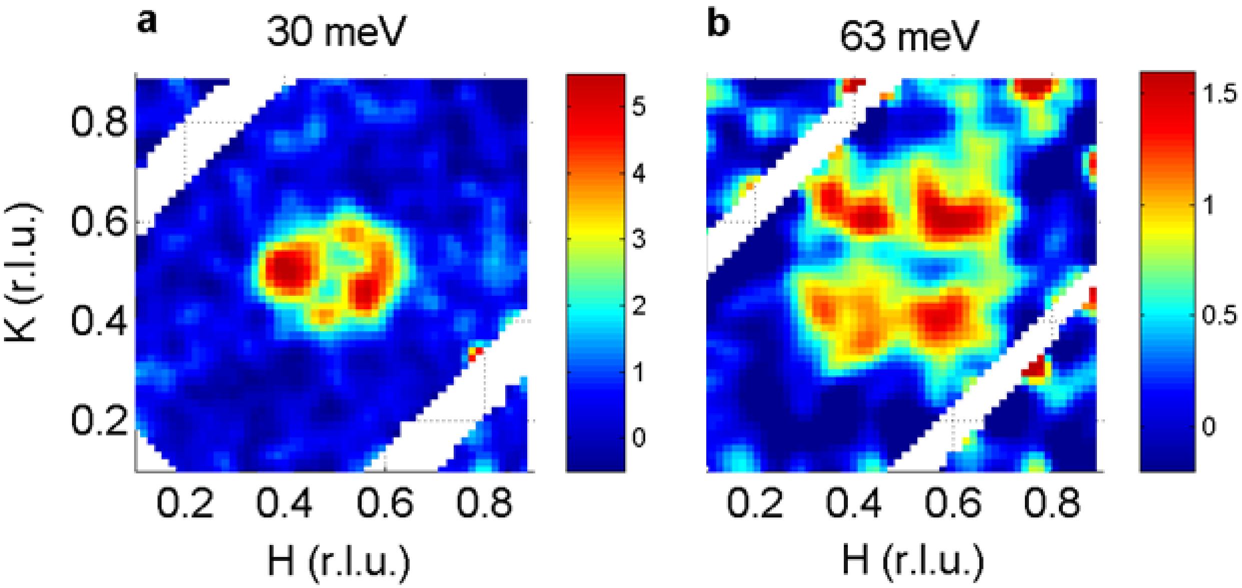

square at high energies
ellipse at low energies

Hinkov et al., Nature Phys. 2007
see also: Mook et al., Nature 2000
Hayden et al., Nature 2004

RPA calculation

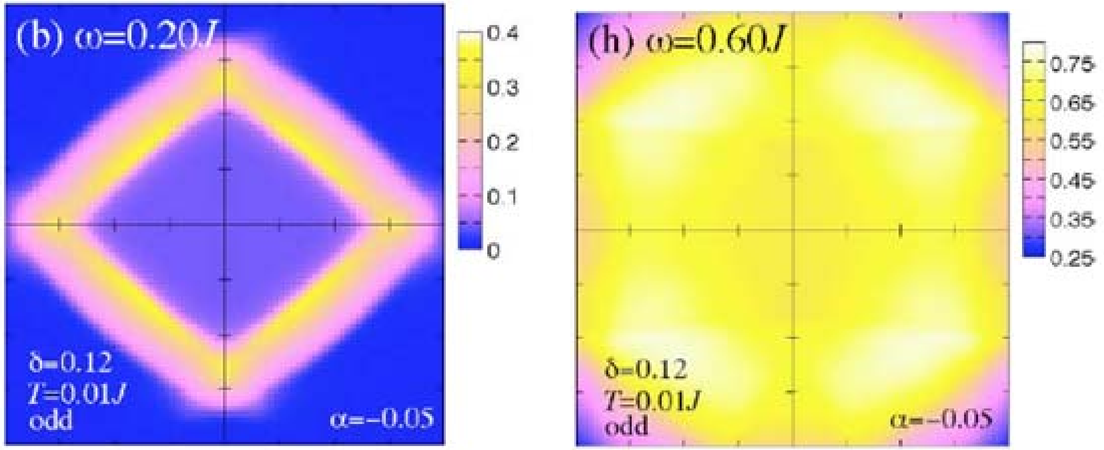

parameters from ARPES & LDA

overall behavior
consistent with experiment

but: hard to reproduce spectral weight anisotropy at low E

Yamase & Metzner, PRB 2006

Static stripes ?

generic magnetic dispersion

low energies: quasi-1D

high energies: 1D

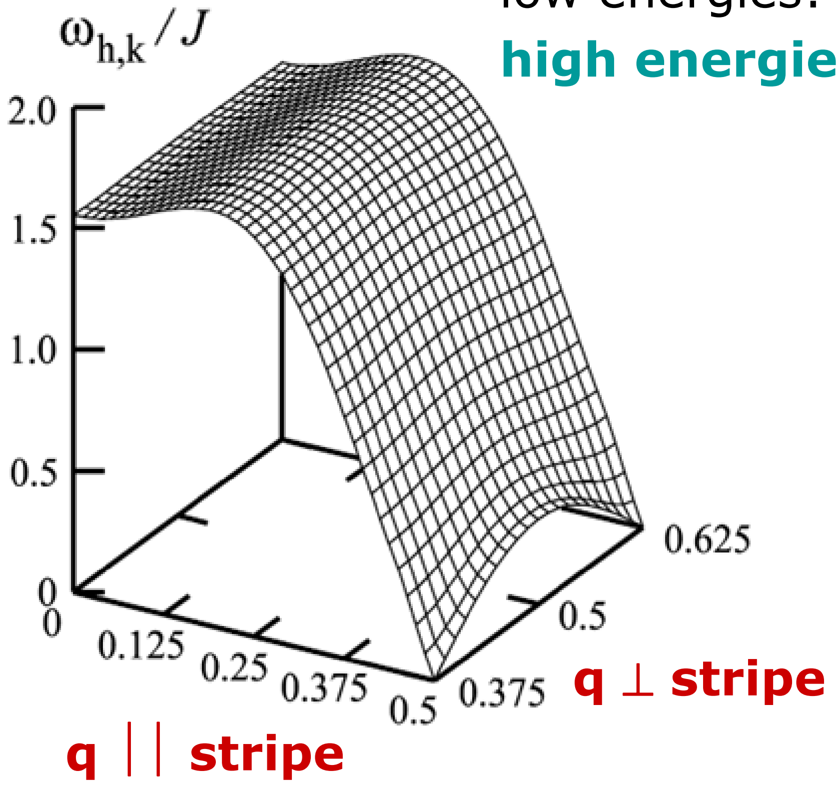

predicted intensity maps at high energies

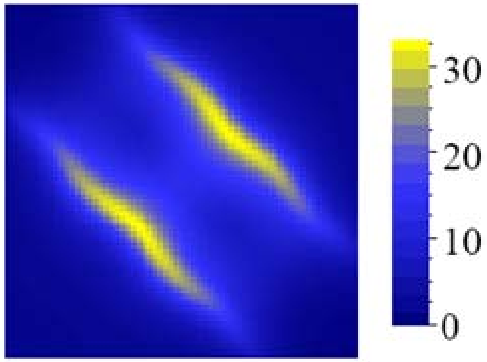

Vojta & Ulbricht, PRL 2004

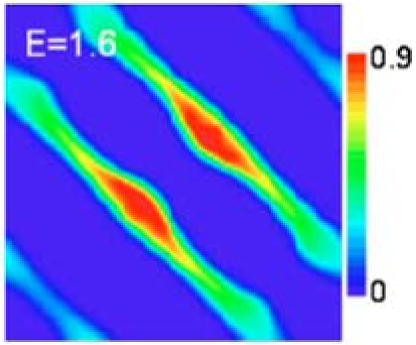

Yao et al., PRB 2006 ... etc.

streaks at high energy predicted for untwinned samples

inconsistent with square pattern observed in $YBCO_{6.6}$

Fluctuating stripes ?

calculations incorporating directional stripe fluctuations

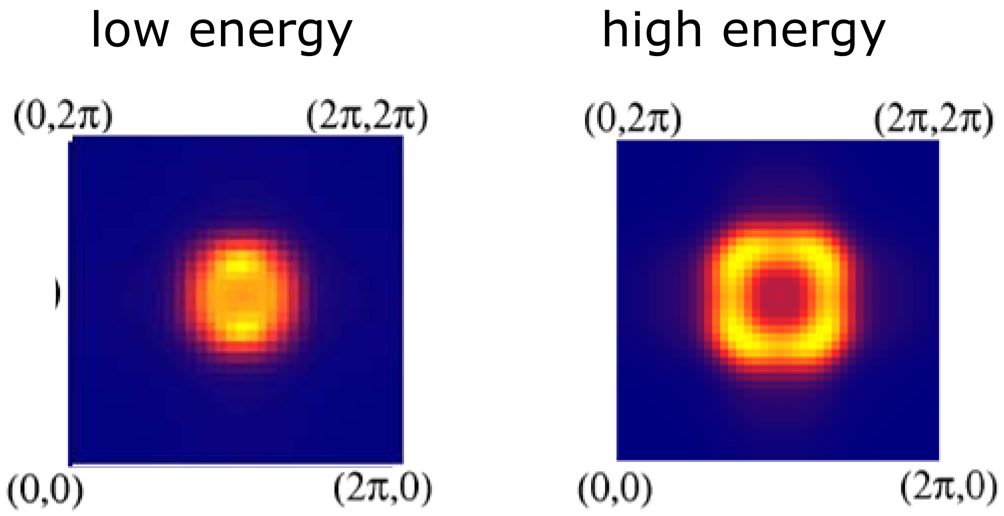

Vojta et al., PRL 2006

can reproduce large anisotropy at low energies, square at high energies

but: too many free parameters

effect of superconductivity not described

$YBCO_{6+x}$ transport properties

in-plane resistivity anisotropy

$YBCO_{6.45}$ $YBCO_{6.6}$

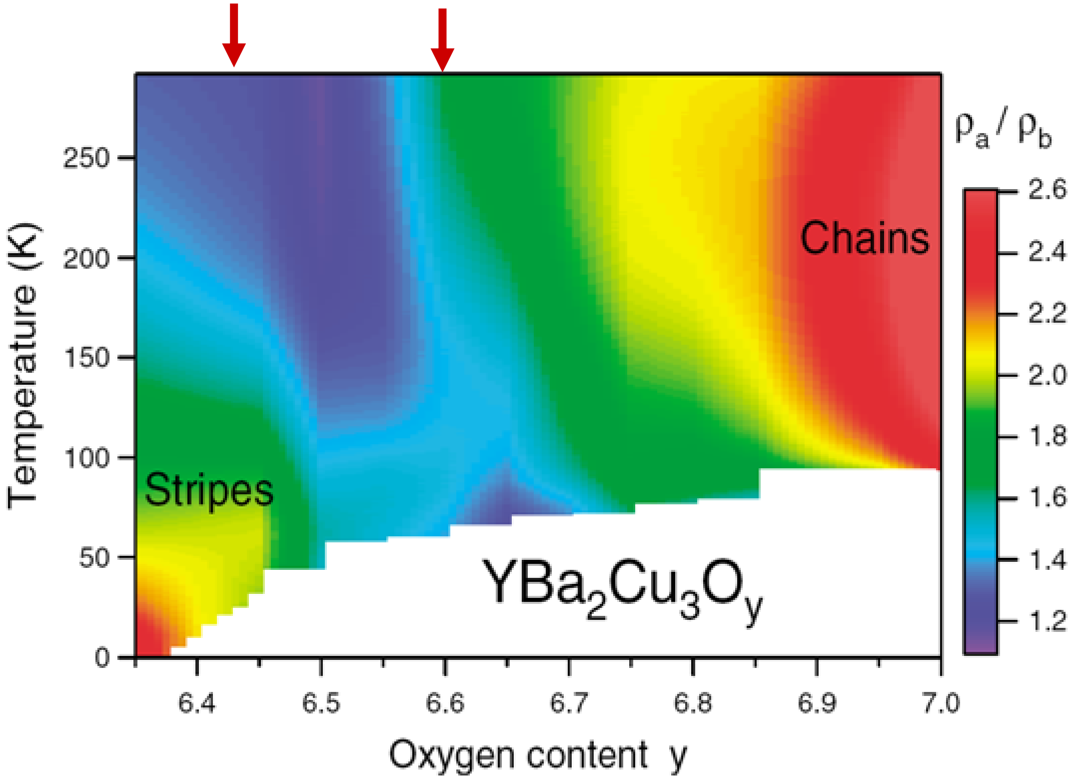

Ando et al., PRL 2002

high-field phase diagram

$YBCO_{6.45}$ $YBCO_{6.6}$

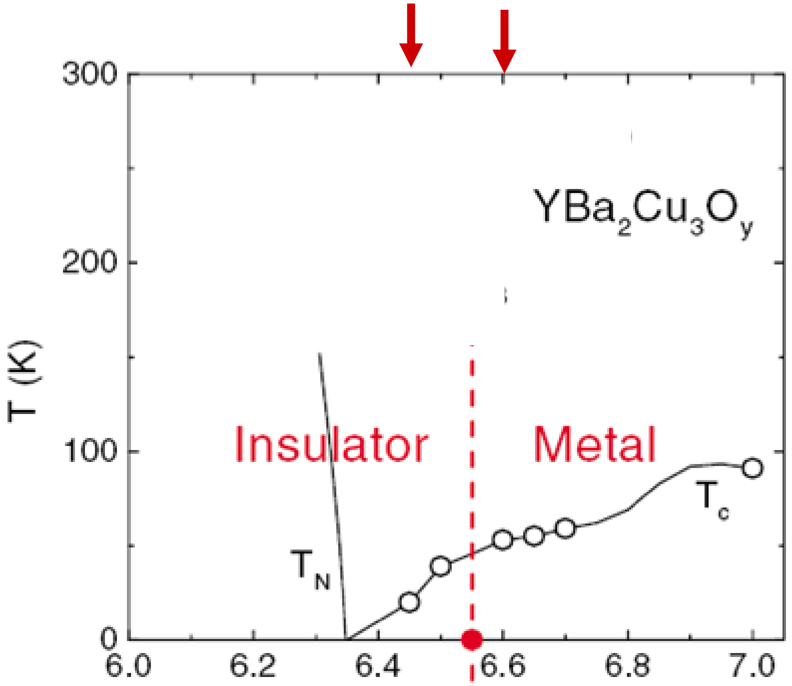

Sun et al., PRL 2005

Comparison: YBCO$_{6.45}$ and YBCO$_{6.6}$

YBa$_2$Cu$_3$O$_{6.6}$ (T$_c$ = 61 K)

- large spin gap
- qualitative difference between superconducting and normal states

YBa$_2$Cu$_3$O$_{6.45}$ (T$_c$ = 35 K)

- small or absent spin gap
- spectrum evolves smoothly through T$_c$

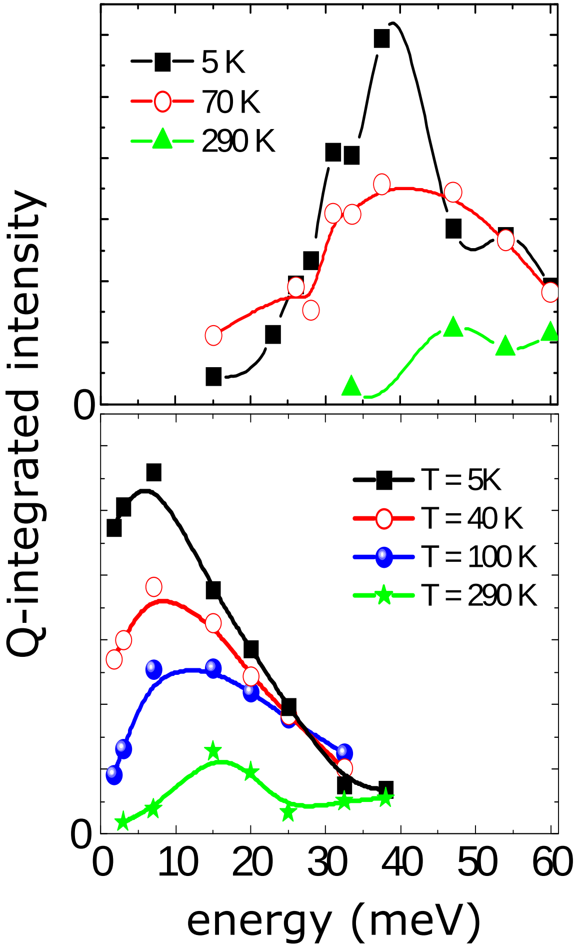

YBCO$_{6.45}$ constant-energy cuts

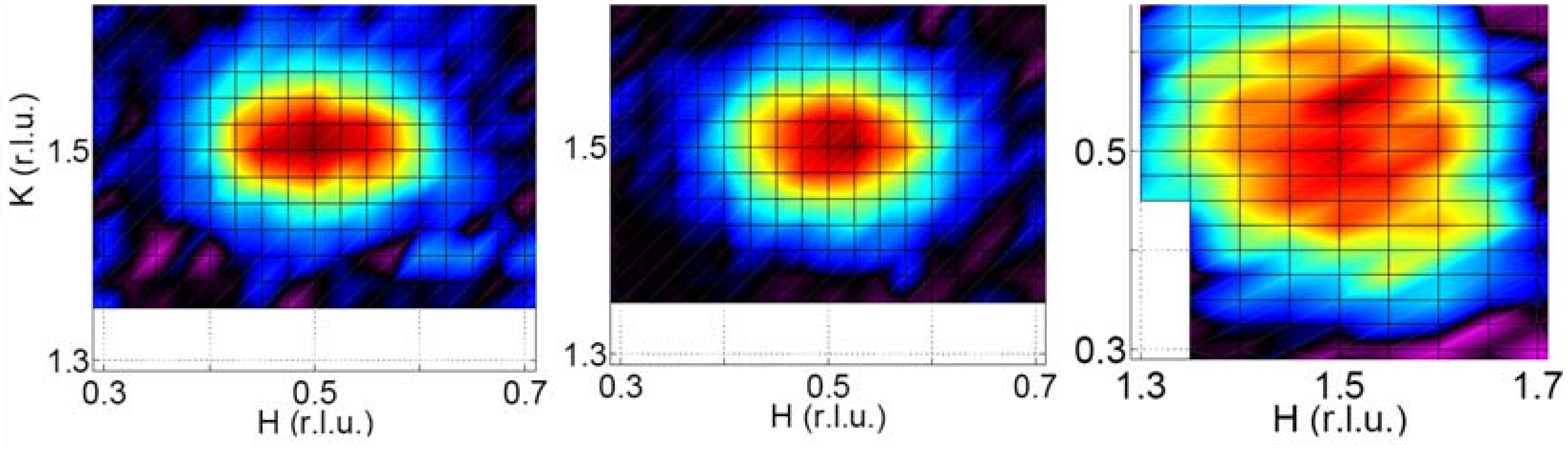
3 meV **7 meV** **50 meV**

E = 3 meV, T = 5 K

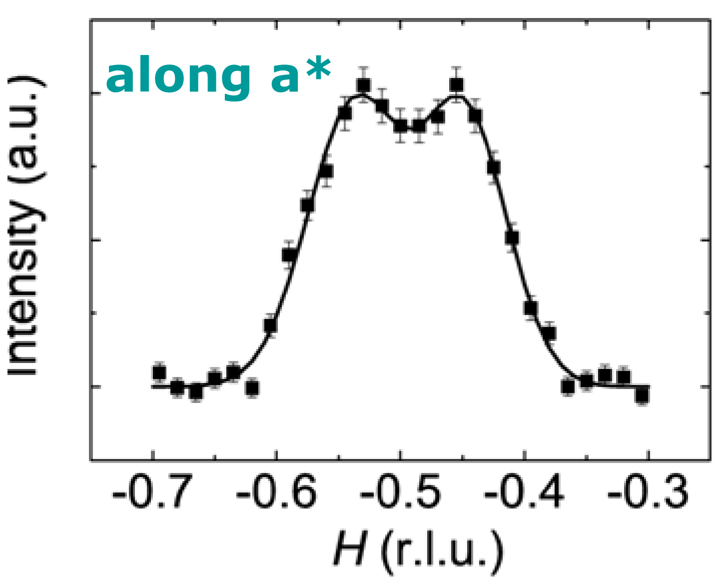

E > 15 meV isotropic

E < 15 meV large anisotropy

incommensurate along a*

commensurate along b*

→ **one-dimensional geometry**

Hinkov et al., Science 2008

Phase transition

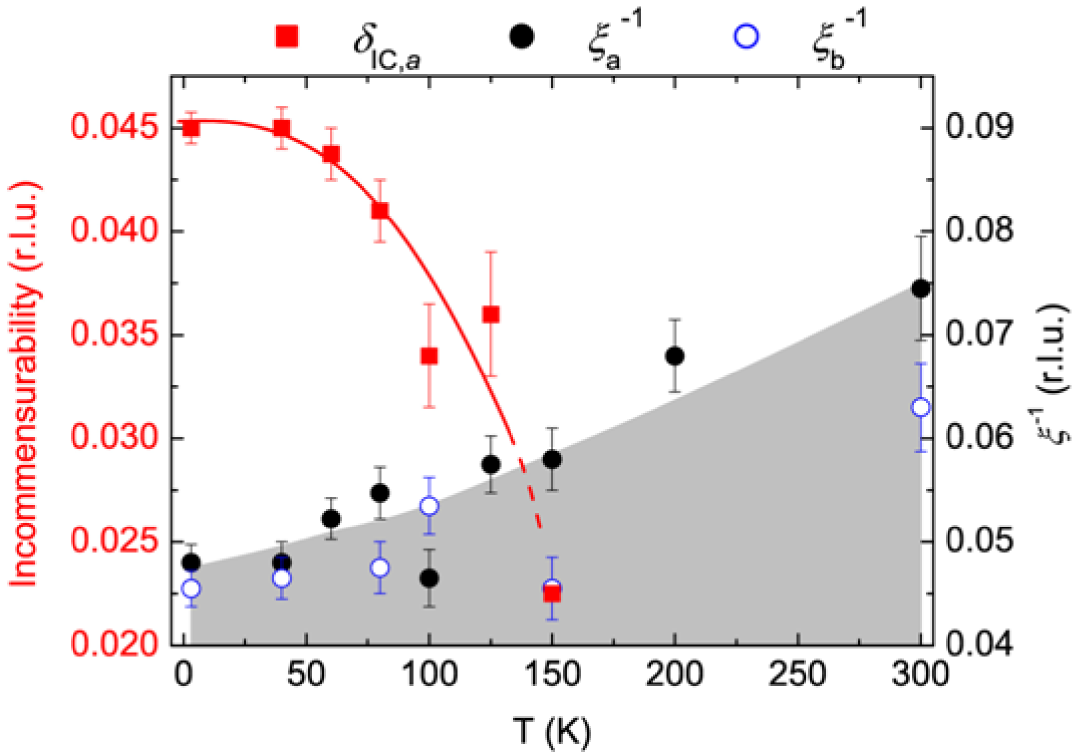

Hinkov et al.
Science 2008

phase transition at ~ 150 K

spin system spontaneously develops 1D incommensurate modulation

weak structural in-plane anisotropy selects unique incommensurate domain

Magnetic order ?

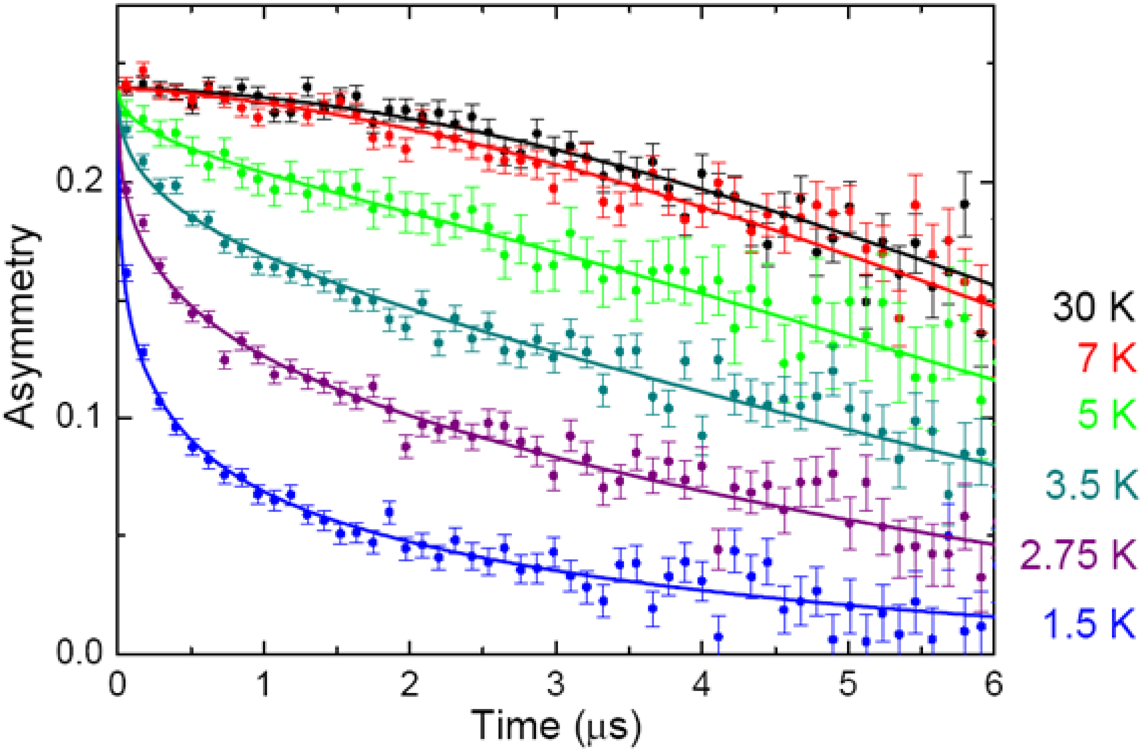

muon spin relaxation

E ~ 1 μeV

slow electronic spin relaxation for T ≤ 10 K

static magnetic order **for T ≤ 2 K**

Nematic order ?

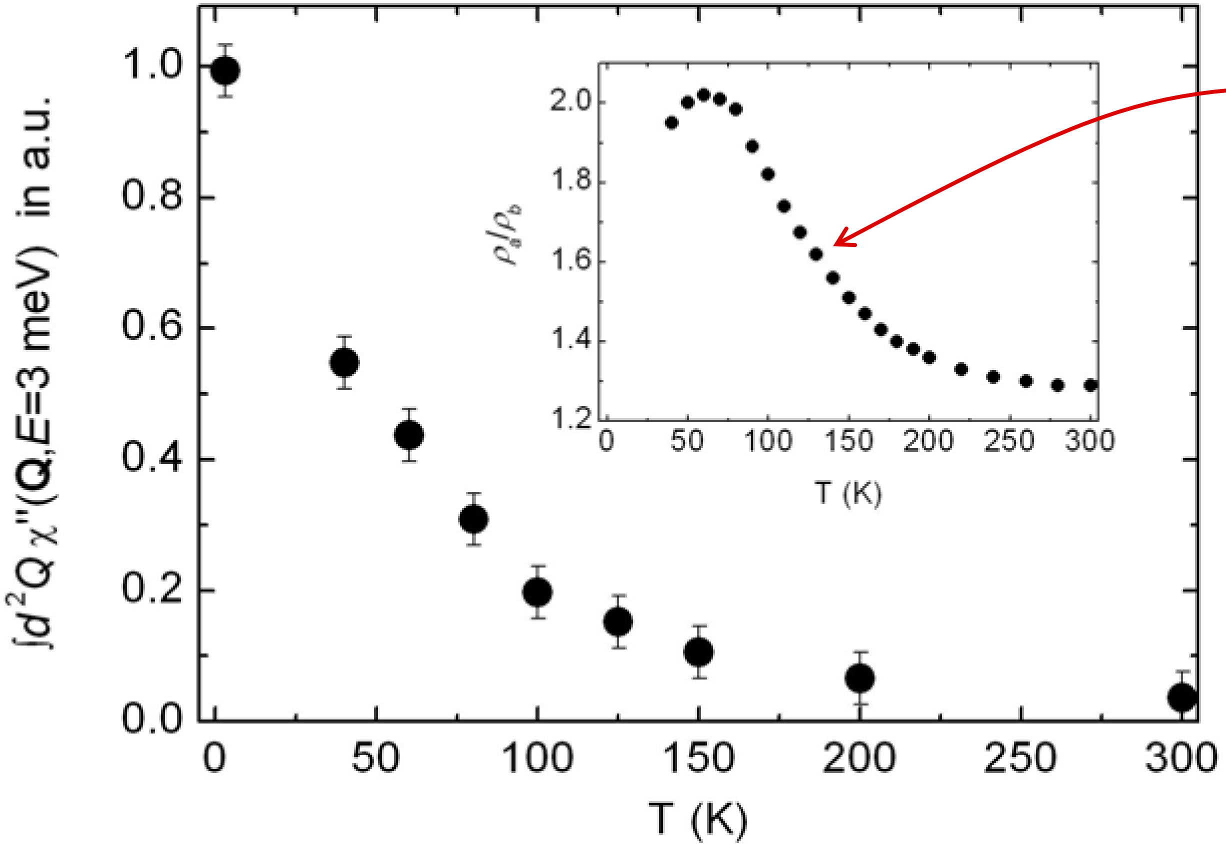

data from
Ando et al., PRL 2002

Hinkov et al.
Science 2008

T ≤ 150 K: pronounced increase of

- intensity of low-energy, 1D incommensurate spin fluctuations
- resistivity anisotropy → **isotropic-nematic transition**

broadened by disorder, finite energy, finite field

nematic transition **two orders-of-magnitude** higher than onset of magnetic order

Analogies

1. **nematic liquid-crystal** in weak electric field

2. **"electronic nematic phase"** in $Sr_3Ru_2O_7$

in-plane component of H aligns nematic director

Borzi et al., Science 2007

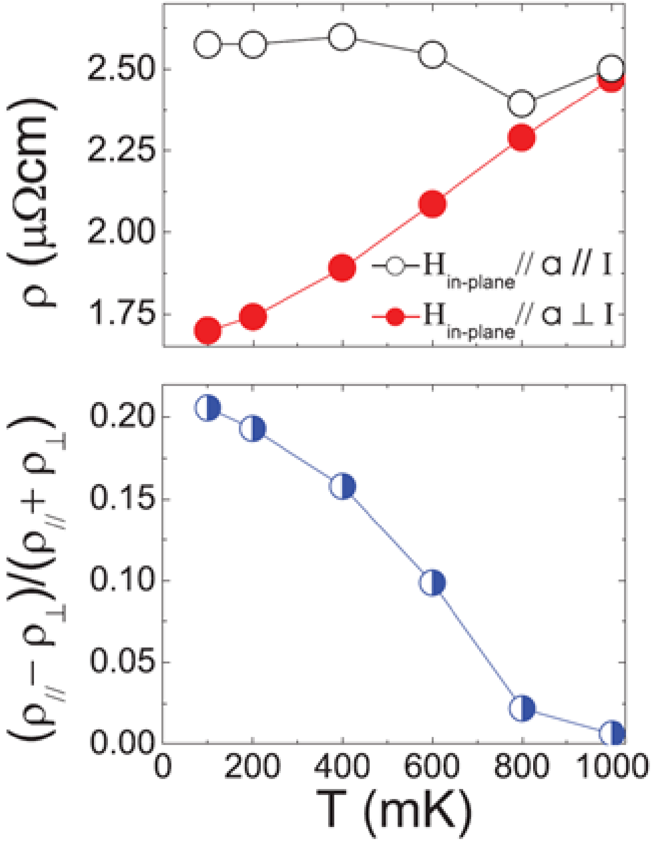

Dynamical scaling

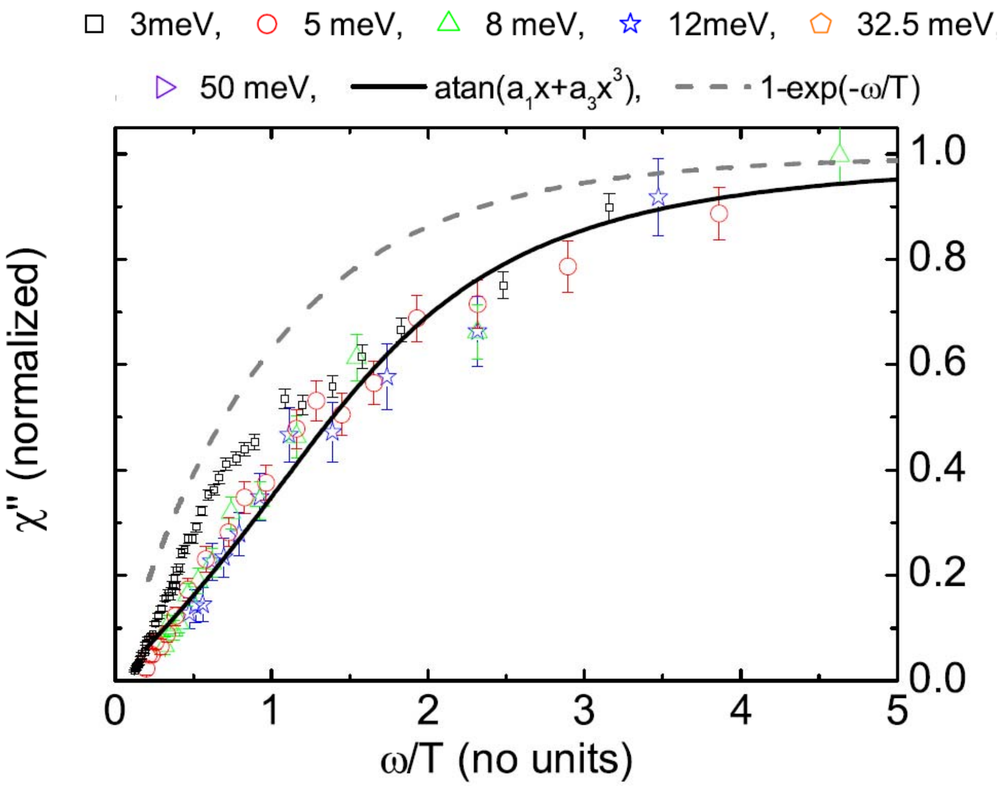

$YBCO_{6.45}$

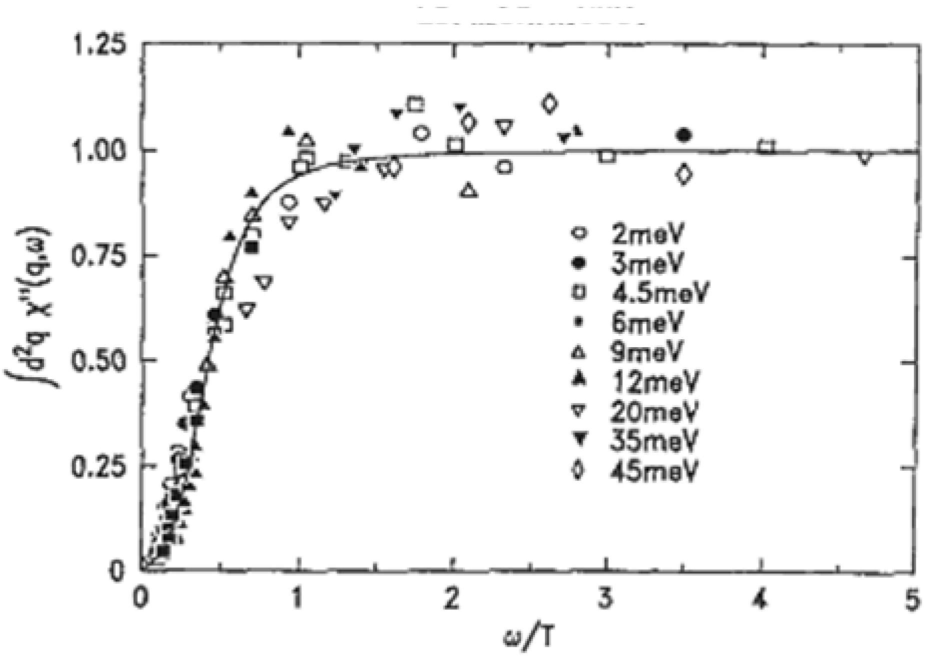

$La_{1.96}Sr_{0.04}CuO_4$

Keimer et al.
PRB 1992

signature of proximity to quantum phase transition

$$\chi(q,\omega) \propto T^{-(2-\eta)/z} F\left(\frac{q-Q_{AF}}{T^{1/z}}, \frac{\hbar\omega}{k_B T}\right)$$

$YBa_2Cu_3O_{6+x}$

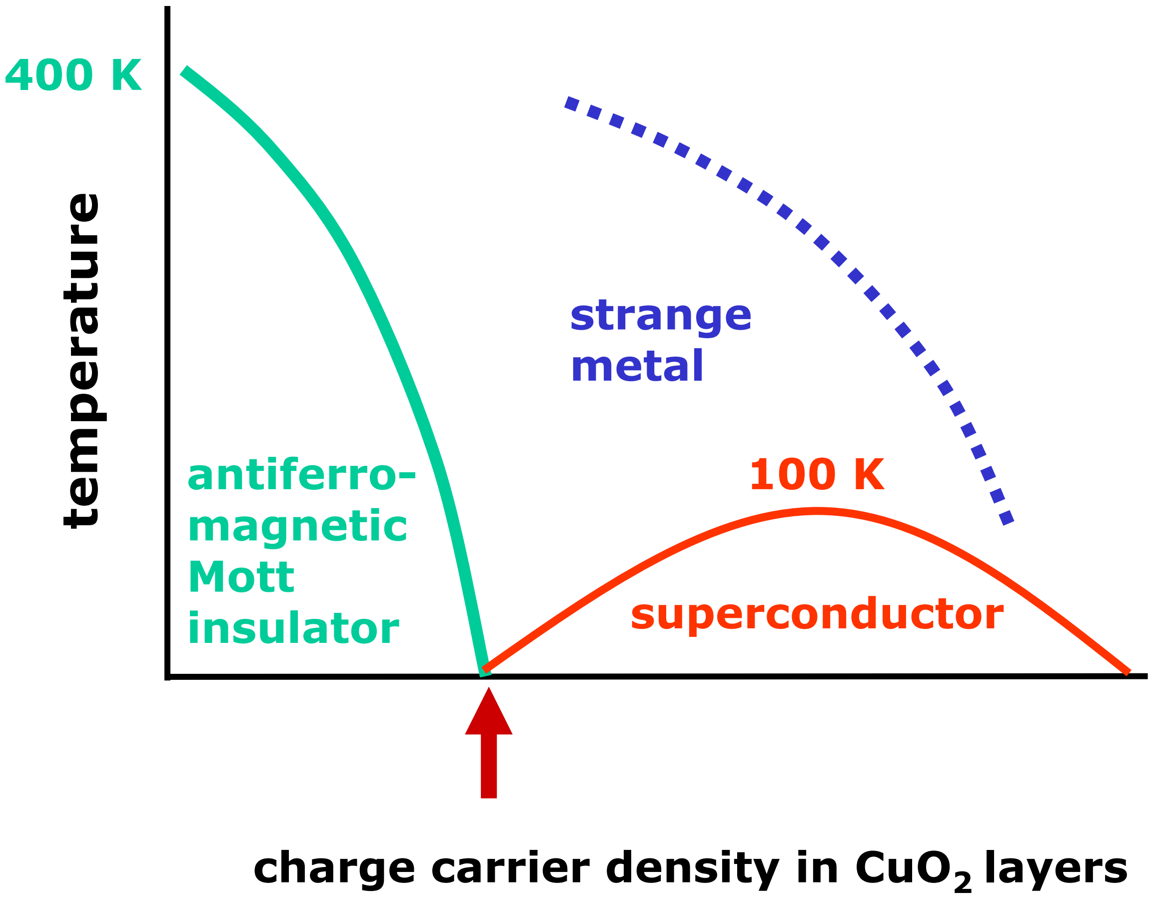

additional ordered phases near Mott insulator

Electronic liquid crystals

electronic nematic phase

- fourfold rotational symmetry spontaneously broken
- translational symmetry unbroken

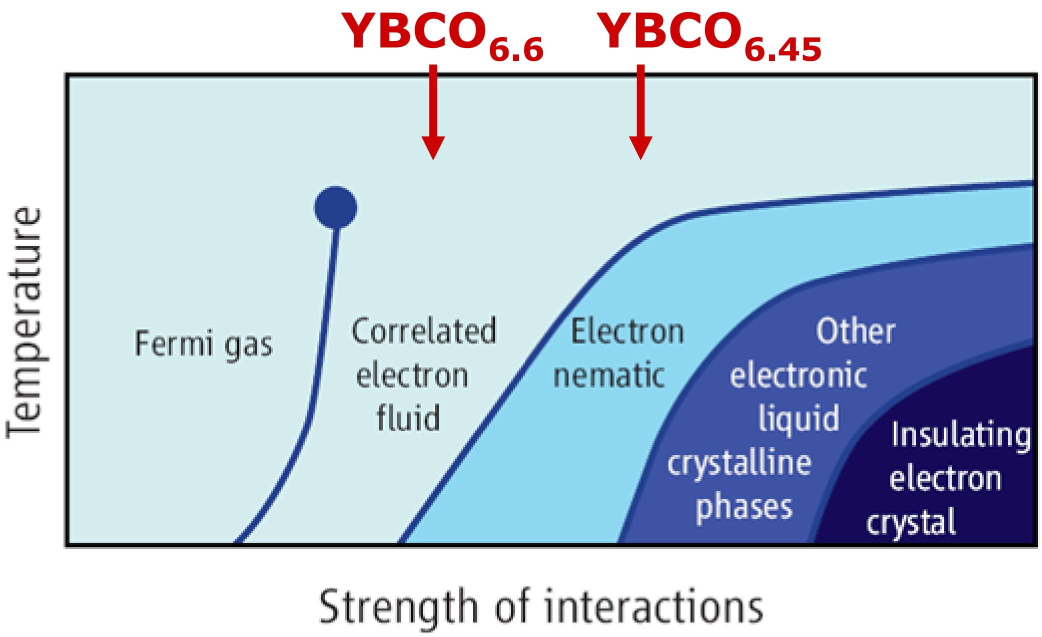

Kivelson et al., Nature 1998

Pomeranchuk instability

renormalization group calculations
→ spontaneous formation of open Fermi surface

Halboth & Metzner, PRL 2000
Yamase & Kohno, JPSJ 2000

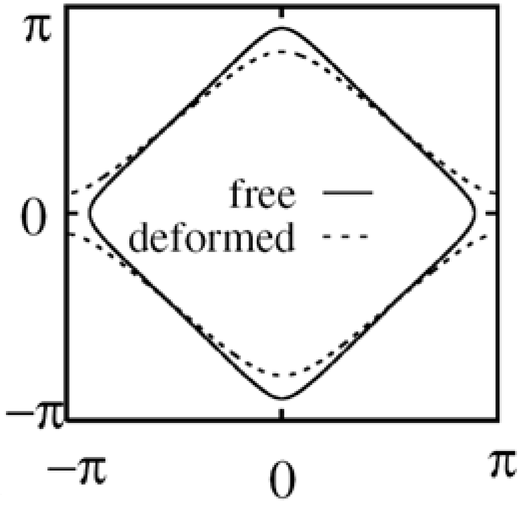

Neutron and x-ray spectroscopy

outline

1. weak correlations: Pb, Nb
2. intermediate correlations: Sr_2RuO_4
3. strong correlations: $YBa_2Cu_3O_{6+x}$
4. orbital degeracy: $La_{1-x}Ca_xMnO_3$ $(Y,La)TiO_3$
5. oxide heterostructures

Example: manganates

phase diagram

$LaMnO_3$
antiferromagnetic
Mott insulator

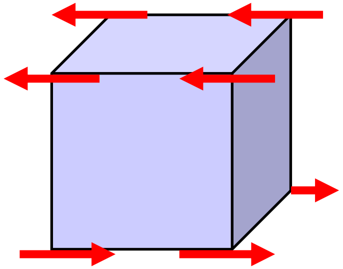

Phase Diagram of $La_{1-x}Ca_xMnO_3$

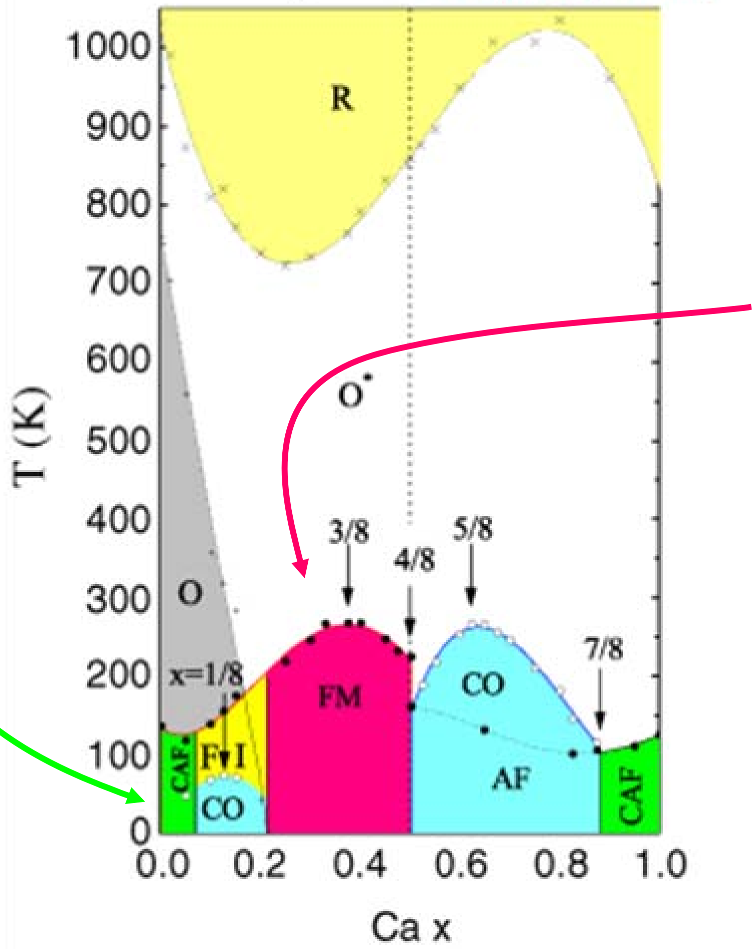

$La_{0.7}Ca_{0.3}MnO_3$
ferromagnetic metal

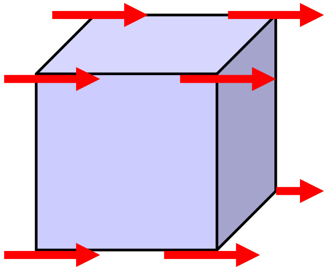

Elastic neutron scattering from $LaMnO_3$

PHYSICAL REVIEW VOLUME 100, NUMBER 2 OCTOBER 15, 1955

Neutron Diffraction Study of the Magnetic Properties of the Series of Perovskite-Type Compounds $[(1-x)La, xCa]MnO_3$†

E. O. Wollan and W. C. Koehler
Oak Ridge National Laboratory, Oak Ridge, Tennessee

(Received May 9, 1955)

nuclear Bragg reflections
extract lattice structure
& lattice parameters

magnetic Bragg reflections for $T < T_N$
extract magnetic structure

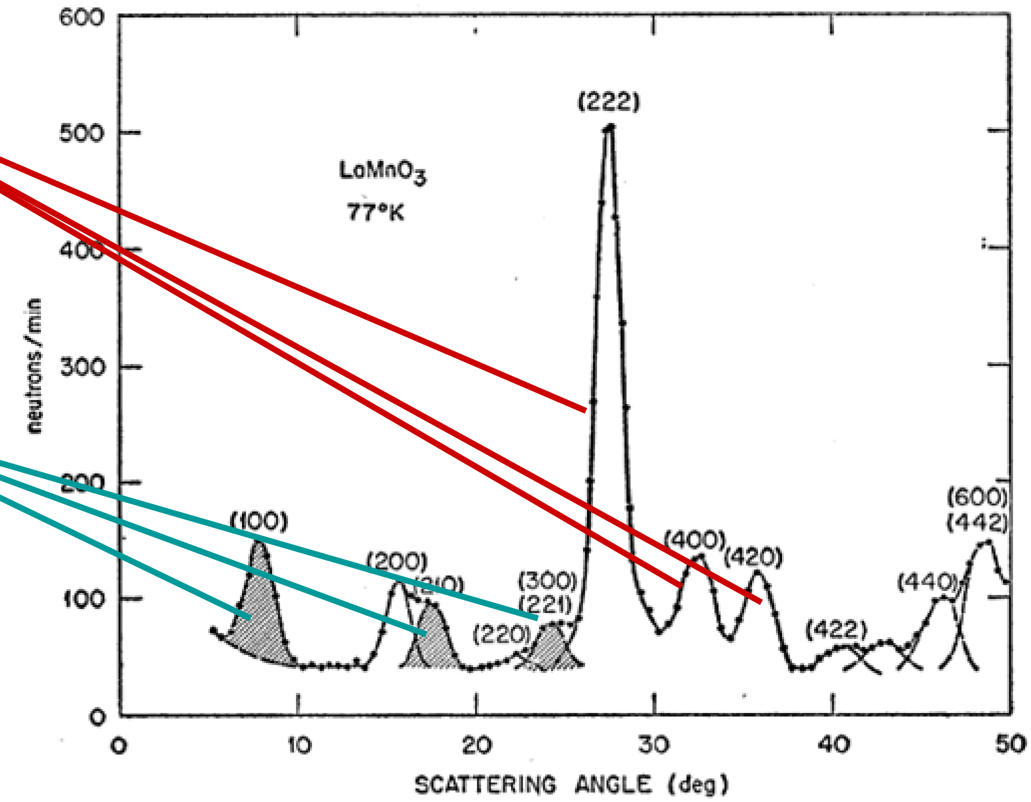

FIG. 2. Diffraction pattern for $LaMnO_3$ No. 1 at 77°K.

$LaMnO_3$ lattice structure

from neutron/x-ray diffraction

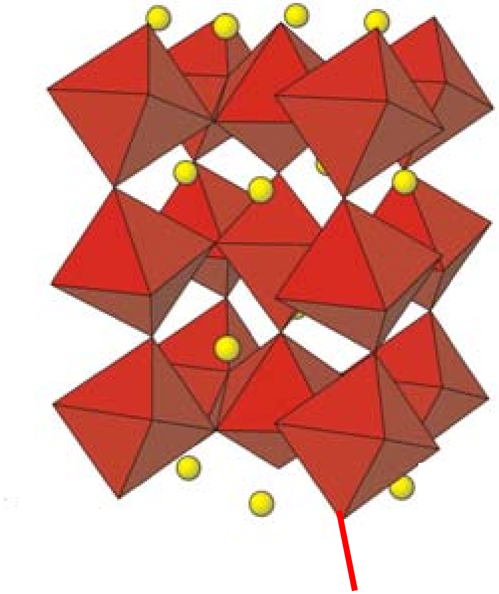

MnO_6 octahedra

octahedra distorted below ~ 800K

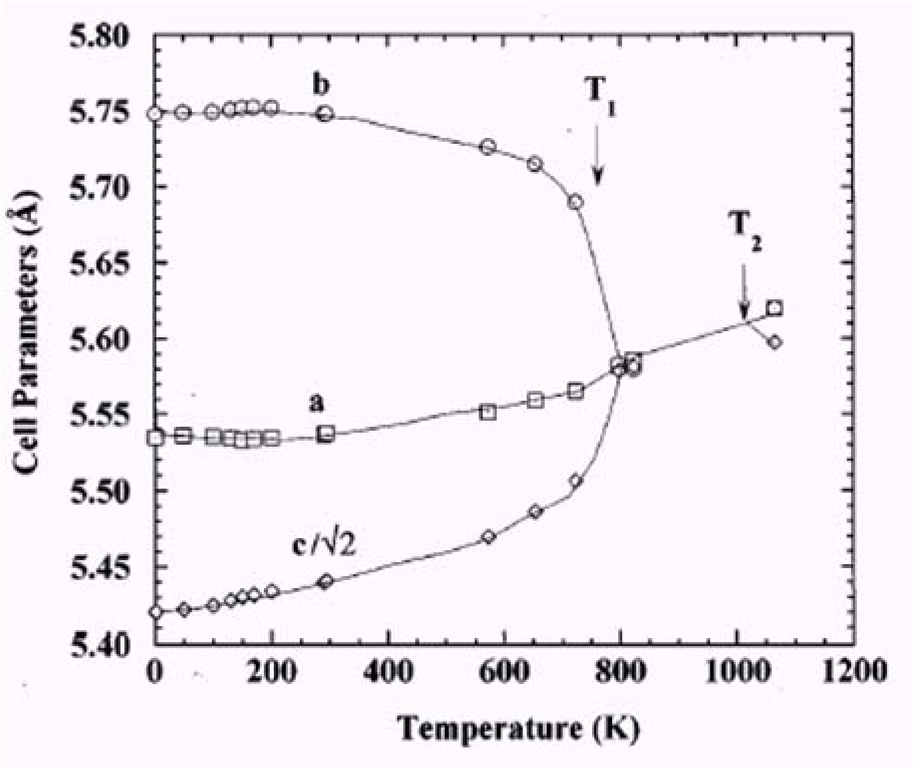

Rodriguez-Carvajal et al.,
PRB 1998

$LaMnO_3$ lattice structure

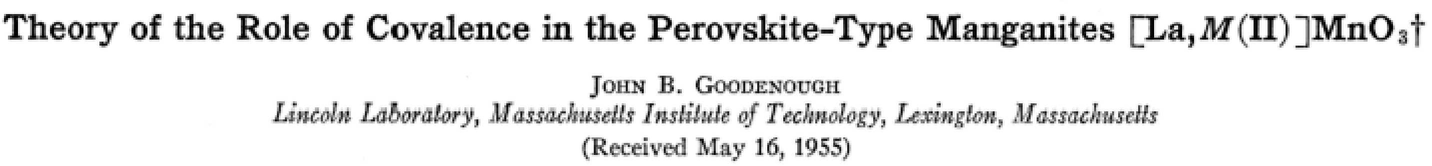

Theory of the Role of Covalence in the Perovskite-Type Manganites [La, *M*(II)]MnO_3†

John B. Goodenough

Lincoln Laboratory, Massachusetts Institute of Technology, Lexington, Massachusetts

(Received May 16, 1955)

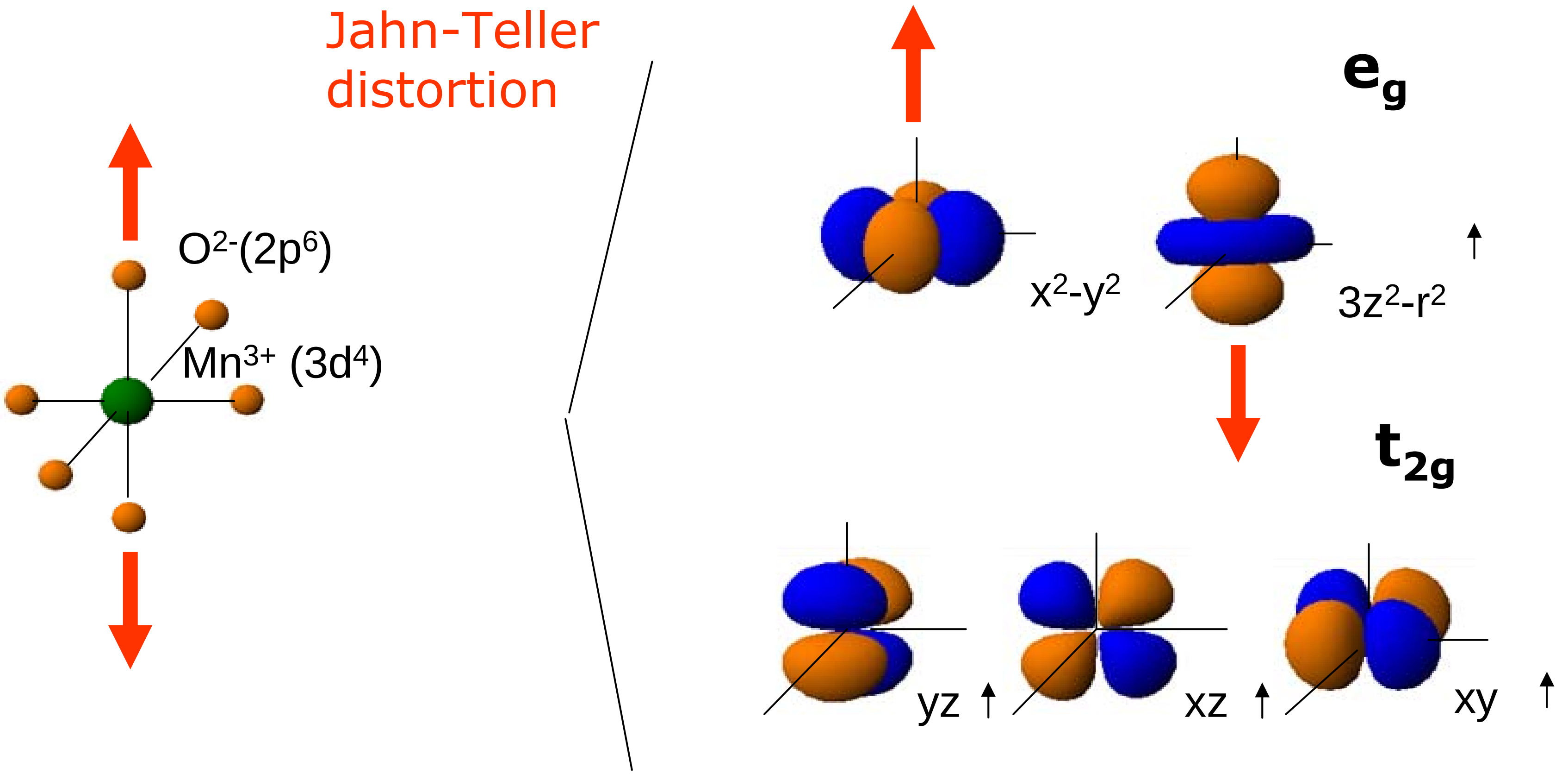

Jahn-Teller distortion

$O^{2-}(2p^6)$

Mn^{3+} $(3d^4)$

e_g

x^2-y^2

$3z^2$-r^2 ↑

t_{2g}

yz ↑

xz ↑

xy ↑

$LaMnO_3$ x-ray linear dichroism

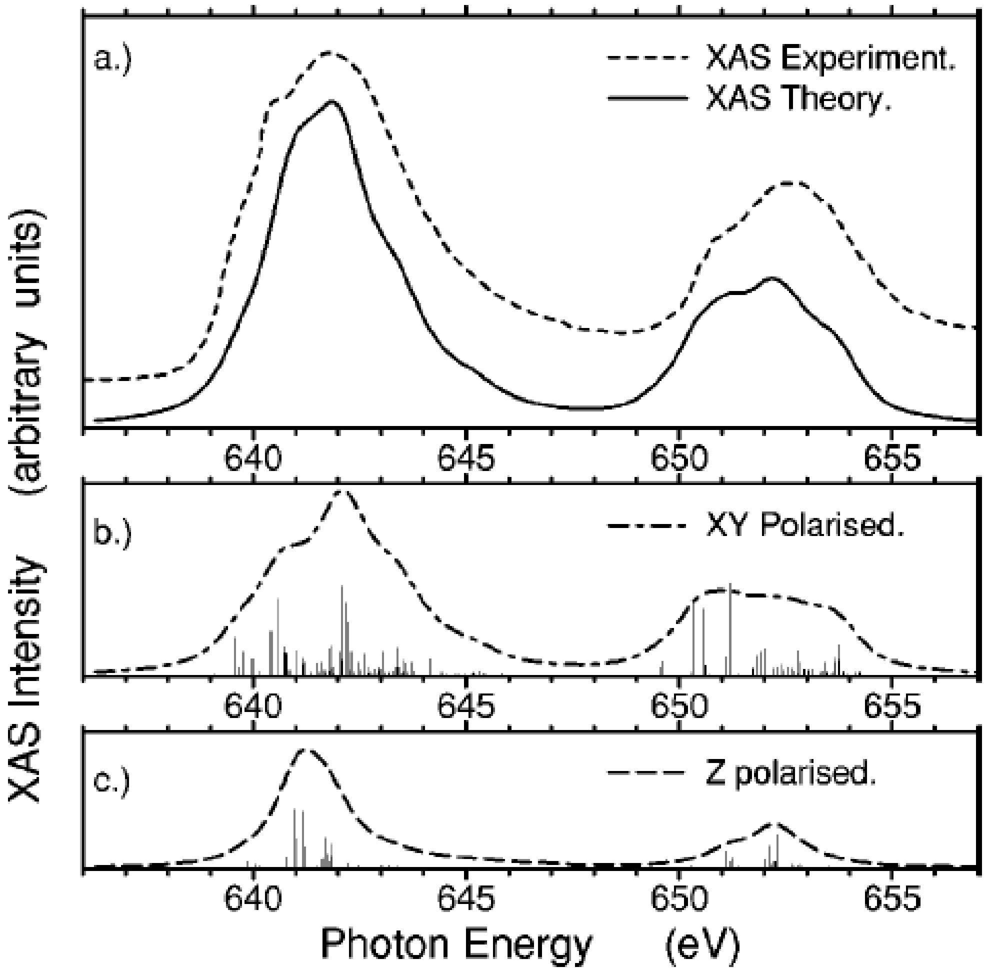

Castleton & Altarelli, PRB 2002

$LaMnO_3$ orbital & spin order

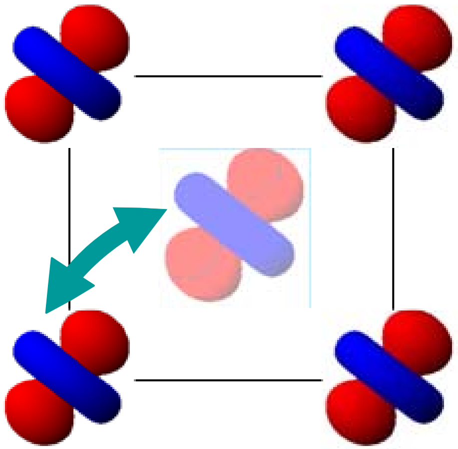

T < T_O: **orbital order**

locks in exchange interactions

superexchange rules

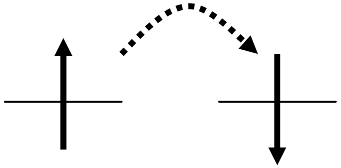

identical orbitals:
strong, antiferromagnetic

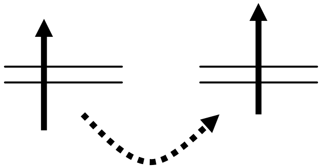

orthogonal orbitals:
weak, ferromagnetic

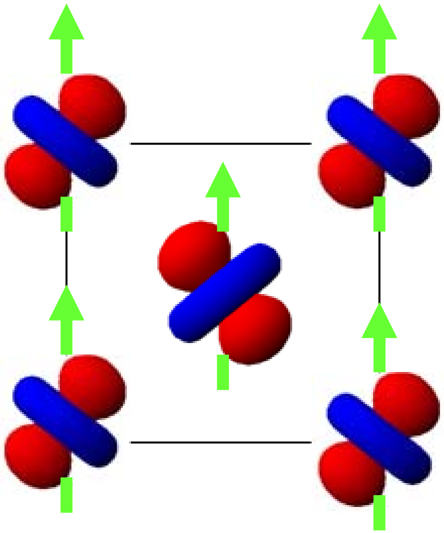

T < T_N << T_O:

spin order

für Festkörperforschung

$LaMnO_3$ orbital & spin order

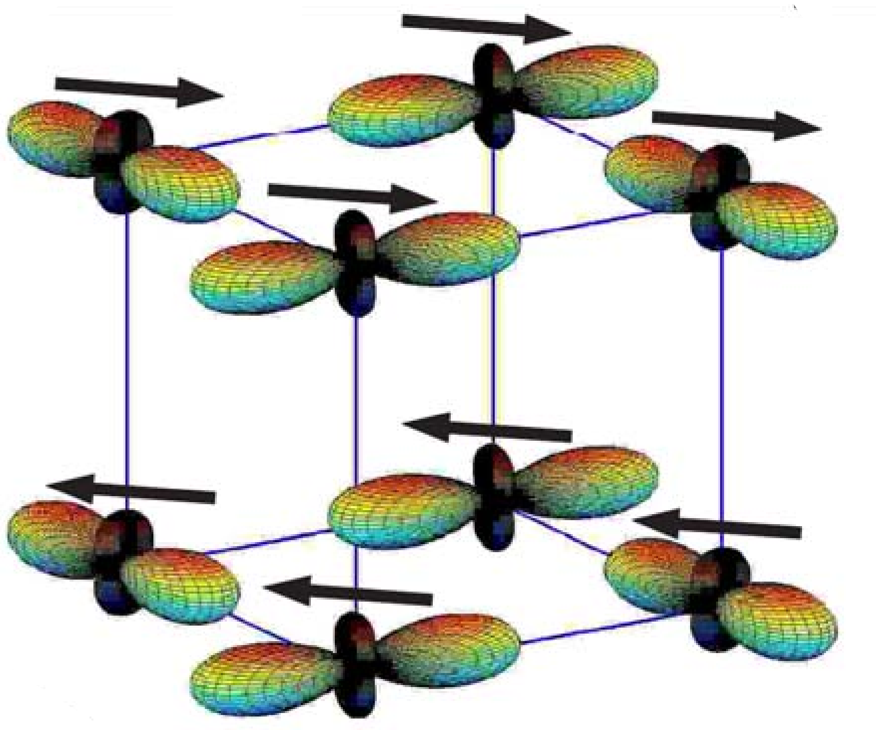

(La,Y)TiO$_3$ structure

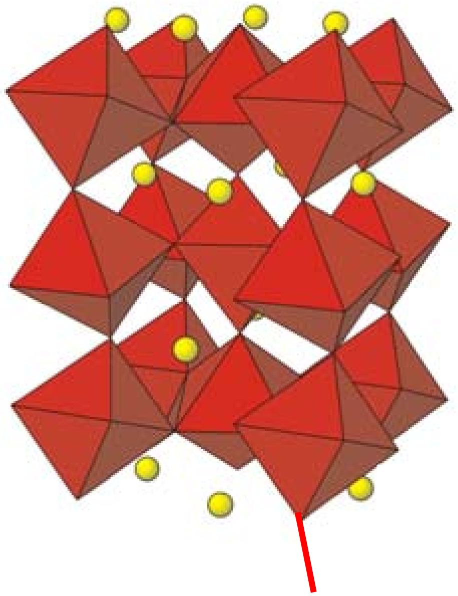

TiO$_6$ octahedra

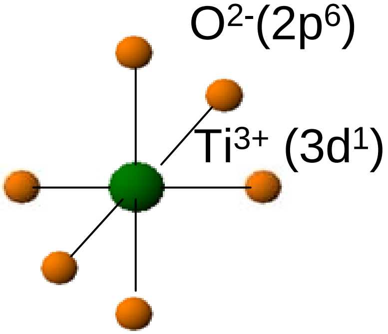

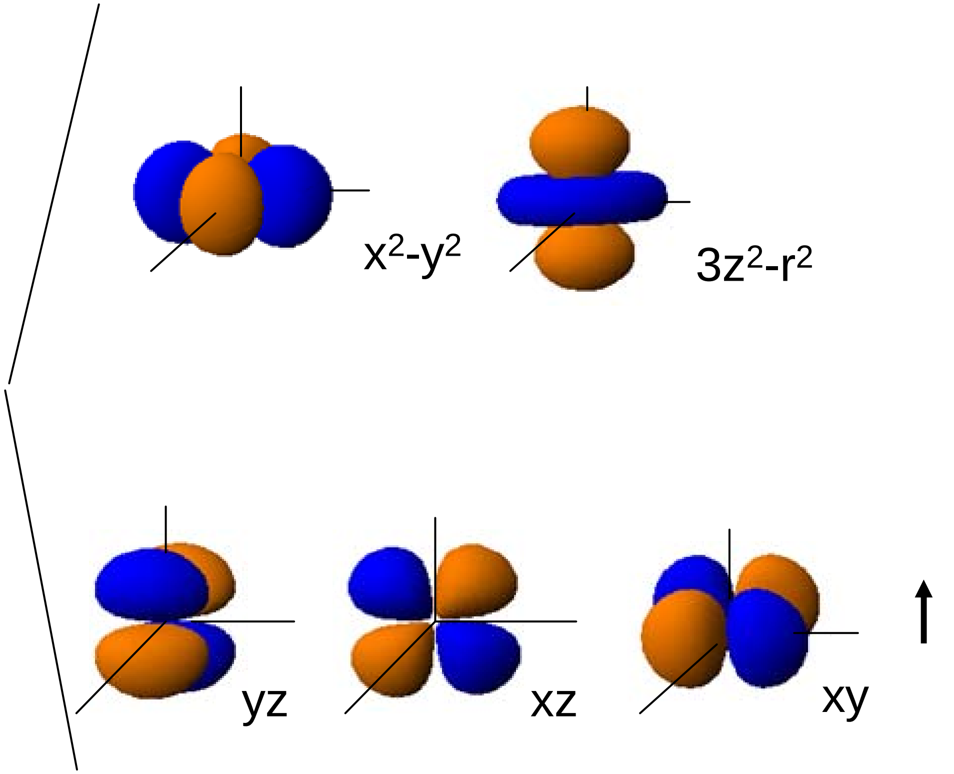

one electron in t$_{2g}$ orbitals

- larger orbital degeneracy
- weaker lattice coupling

than in e$_g$ systems

(La,Y)TiO_3 spin & orbital order

LaTiO_3

G-type antiferromagnet

YTiO_3

ferromagnet

orbital order according to electronic structure calculations:

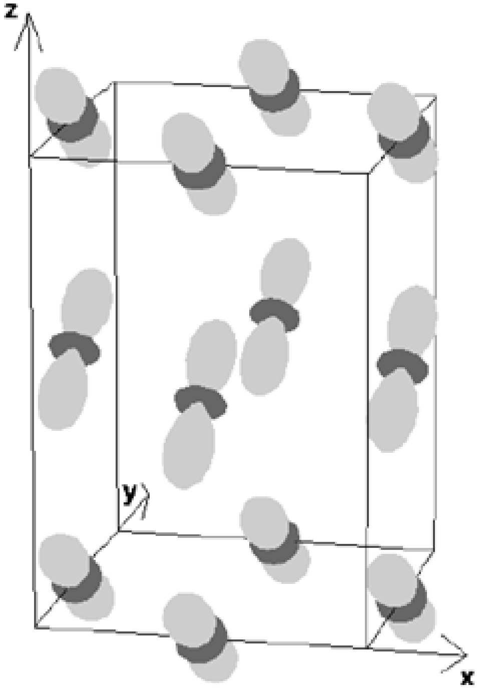

dumbell
orbitals

planar
orbitals

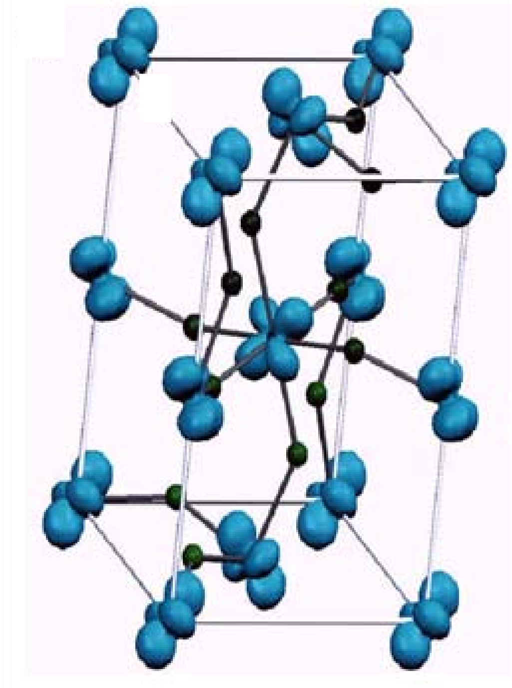

no orbital ordering transitions observed up to at least 700 K

→ orbital degeneracy lifted by lattice distortions?

→ orbital fluctuations?

Orbital excitations

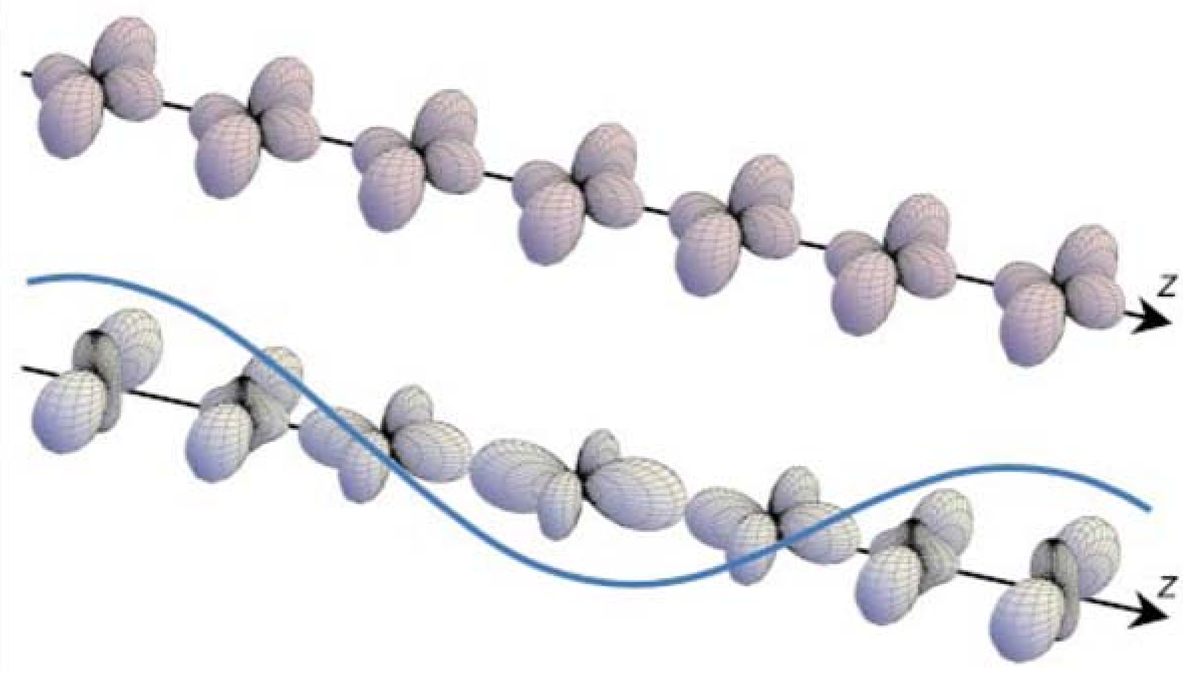

ground state

orbiton excitation

Raman scattering

photon energy tuned to intersite transitions

excitation in final state:
- phonon
- magnon
- orbiton?

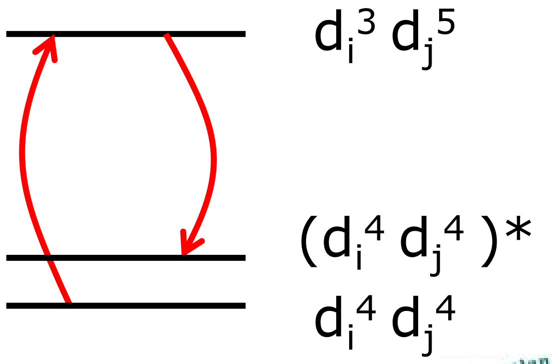

Raman scattering from orbitons

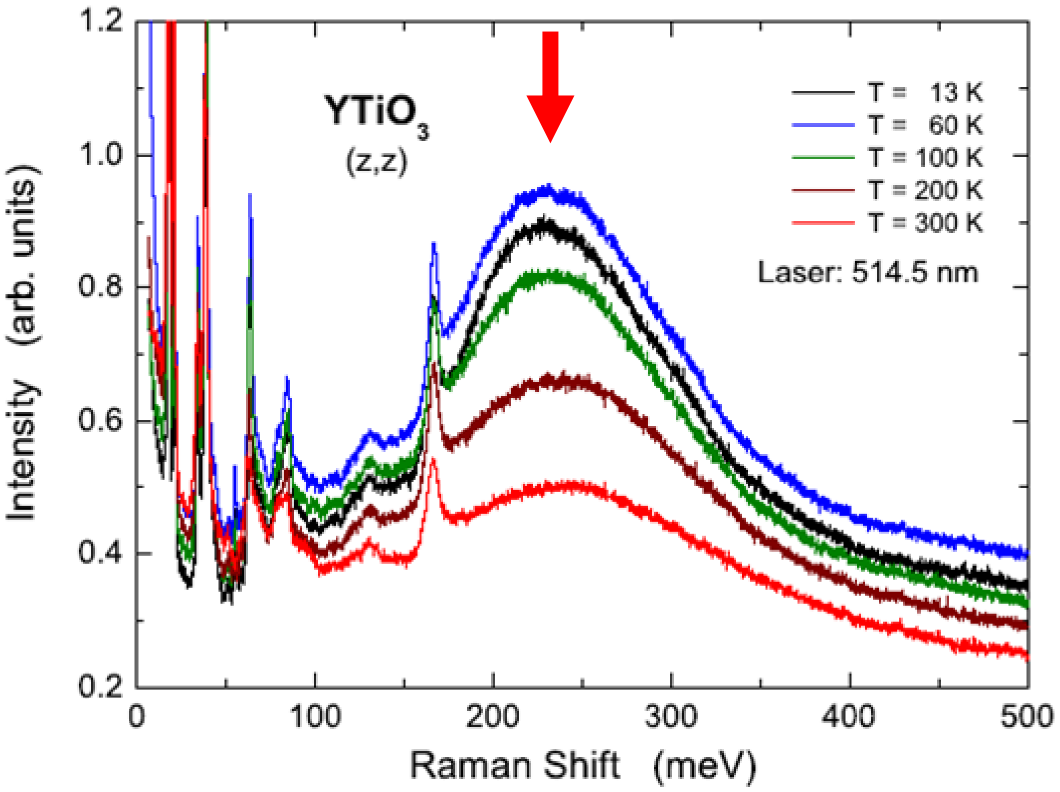

Ulrich et al.
PRL 2006

- peak above 2-magnon, 2-phonon ranges
- below charge excitations known from IR spectra

→ **orbital excitation**

Resonant inelastic x-ray scattering

photon energy tuned to
intra-atomic absorption edge

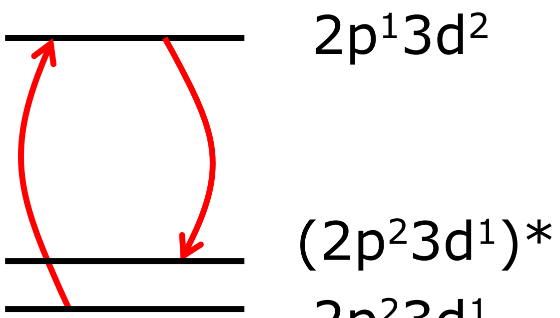

larger photon momentum than Raman

→ **dispersion of orbital excitations**

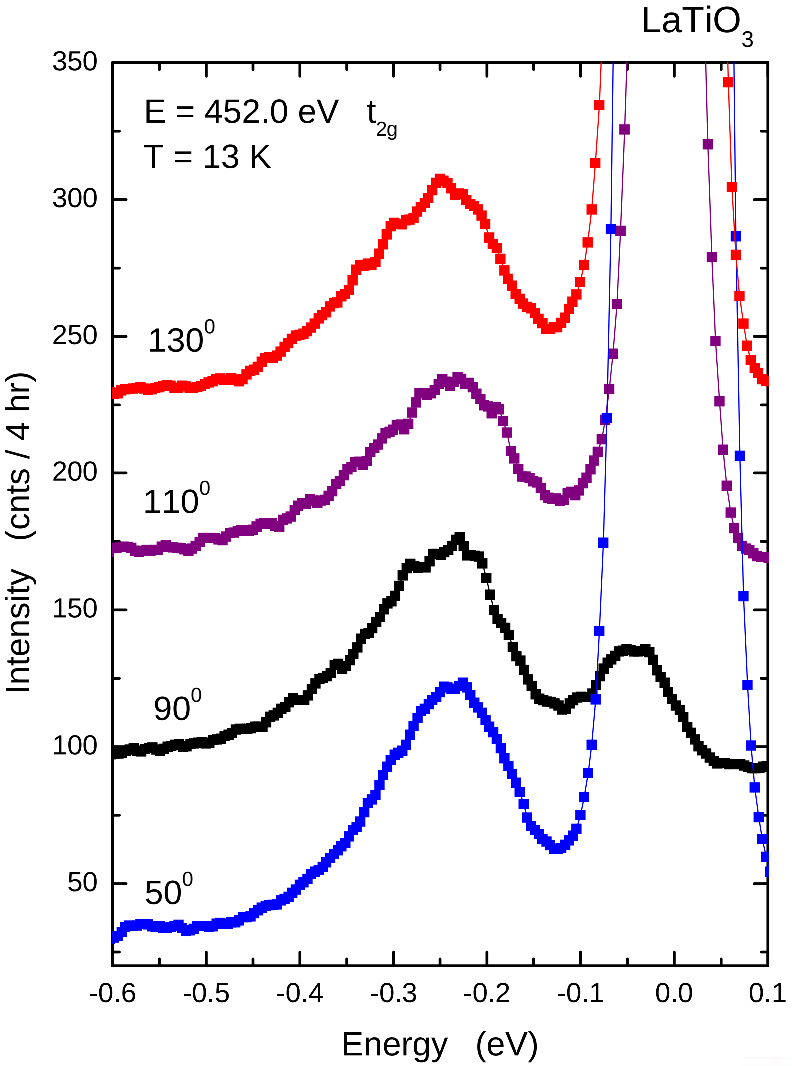

Ulrich et al., PRB 2008
and unpublished

Neutron and x-ray spectroscopy

outline

1. weak correlations: Pb, Nb
2. intermediate correlations: Sr_2RuO_4
3. strong correlations: $YBa_2Cu_3O_{6+x}$
4. orbital degeracy: $La_{1-x}Ca_xMnO_3$ (Y,La)TiO_3
5. oxide heterostructures

New physics at interfaces

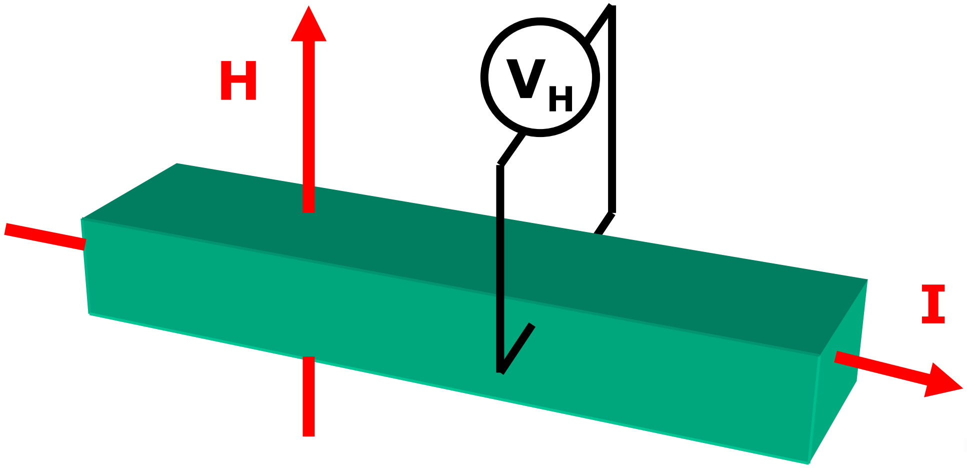

doped semiconductor

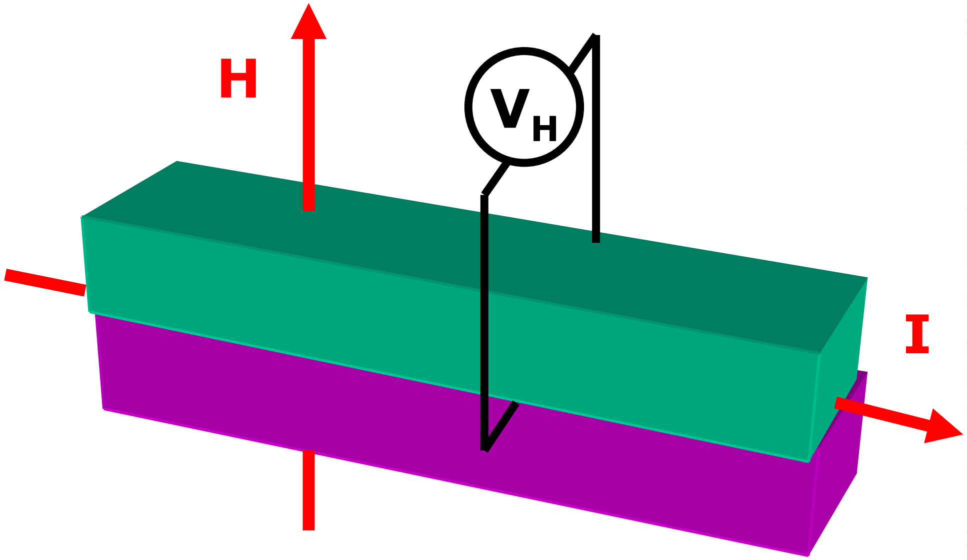

semiconductor heterostructure

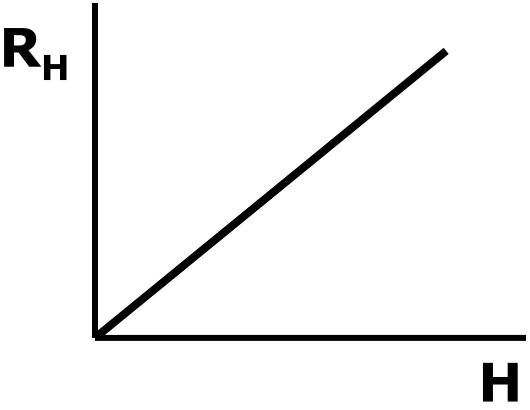

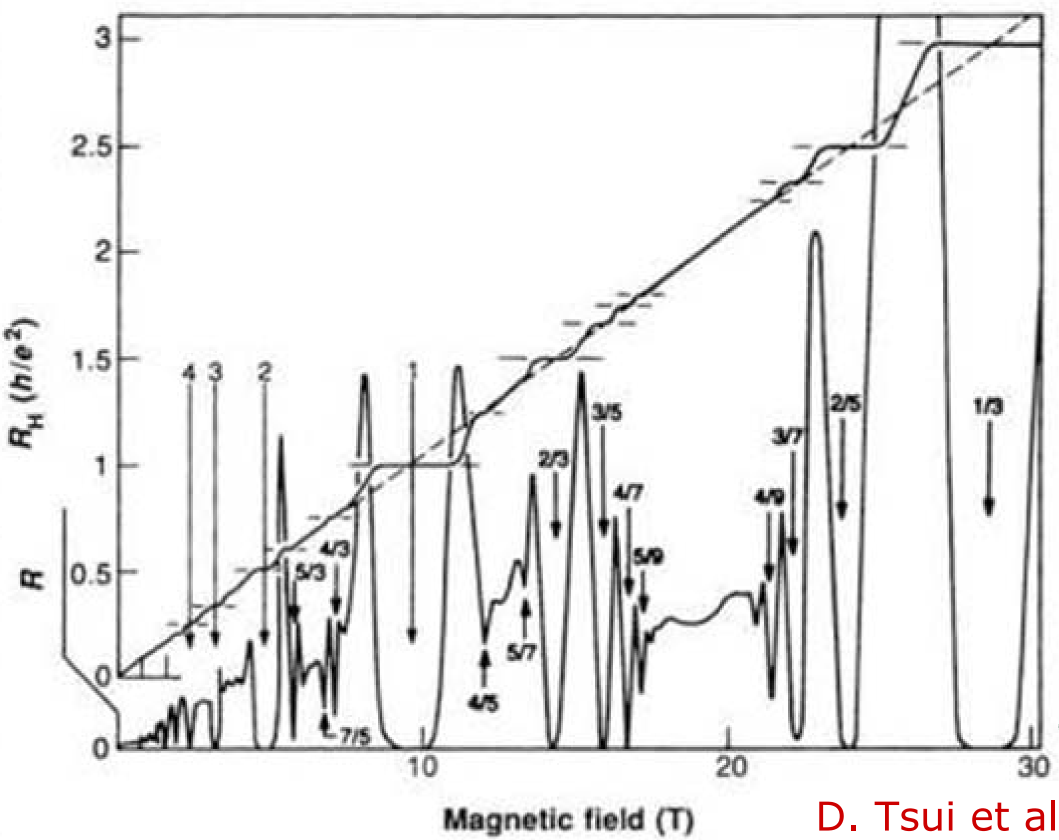

D. Tsui et al.

YBCO-LCMO interface

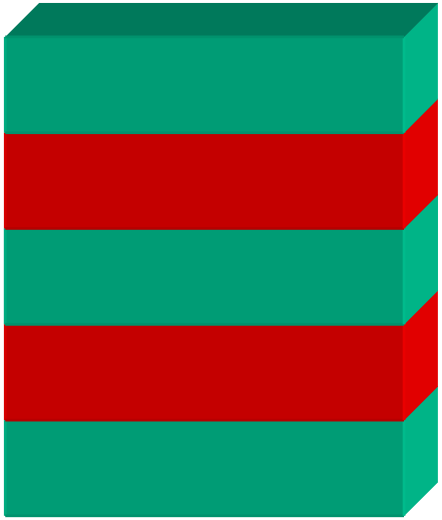

$YBa_2Cu_3O_7$ (YBCO): high-T_c superconducor

$La_{0.7}Ca_{0.3}MnO_3$ (LCMO): metallic ferromagnet

antagonistic order parameters at interface

YBCO-LCMO interface

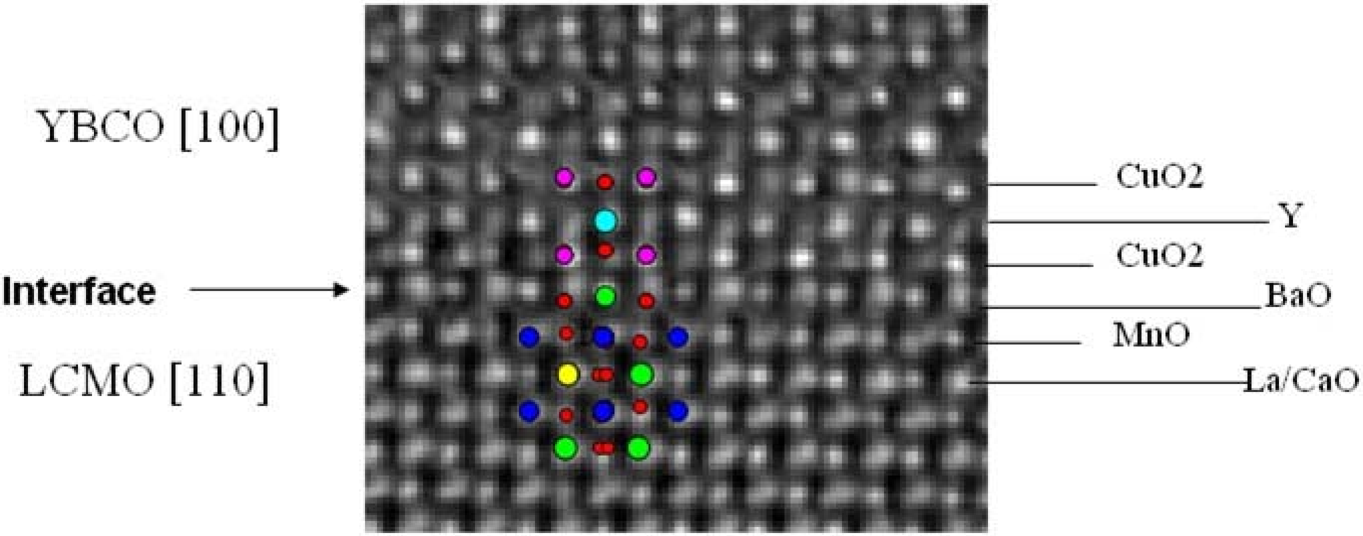

Z. Zhang, U. Kaiser

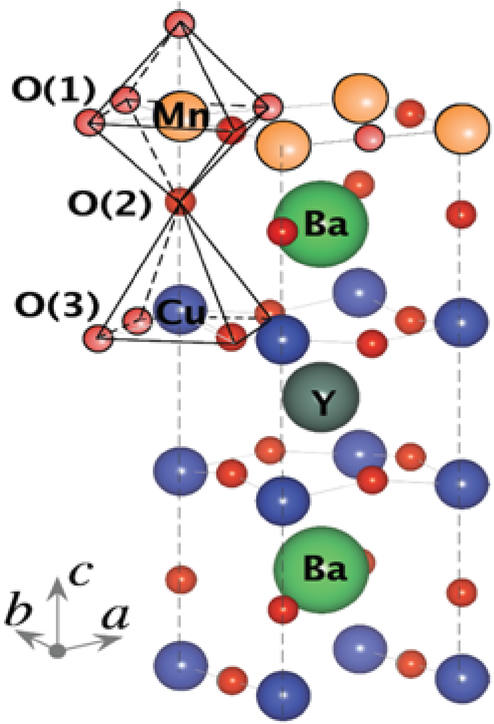

- different magnetic environment
- different valence state
- different crystal field
- different covalent bonding
- different stoichiometry (oxygen vacancies/interstitials) …

can superconductivity be modified/created at interfaces?

YBCO-LCMO superlattices

neutron reflectivity

→ Bragg reflections due to structural and magnetic periodicity

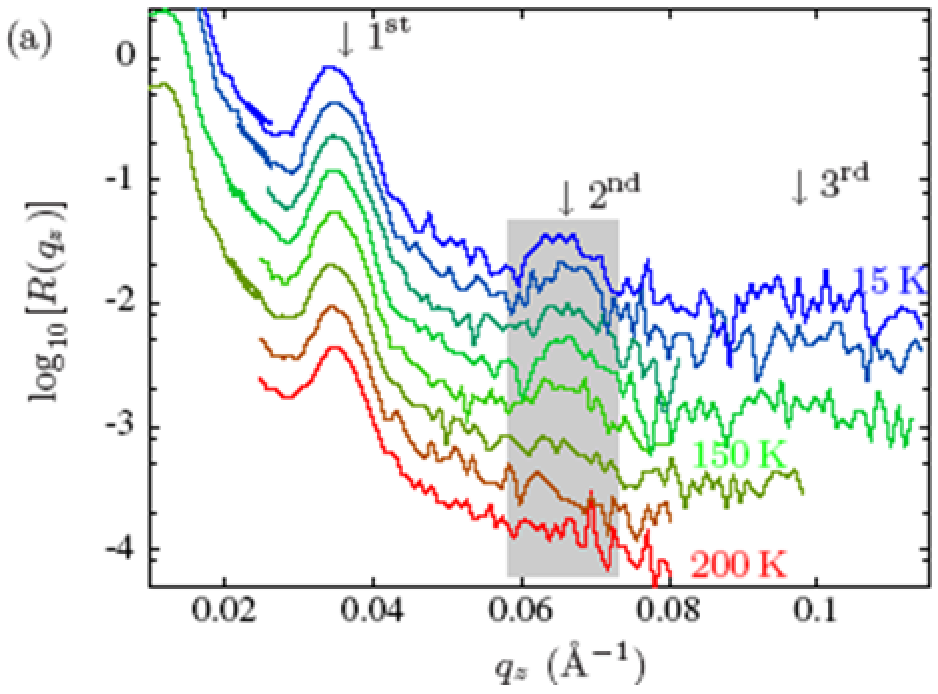

Stahn et al., PRB 2005

magnetic circular dichroism

at L- absorption edges

→ element-specific magnetization

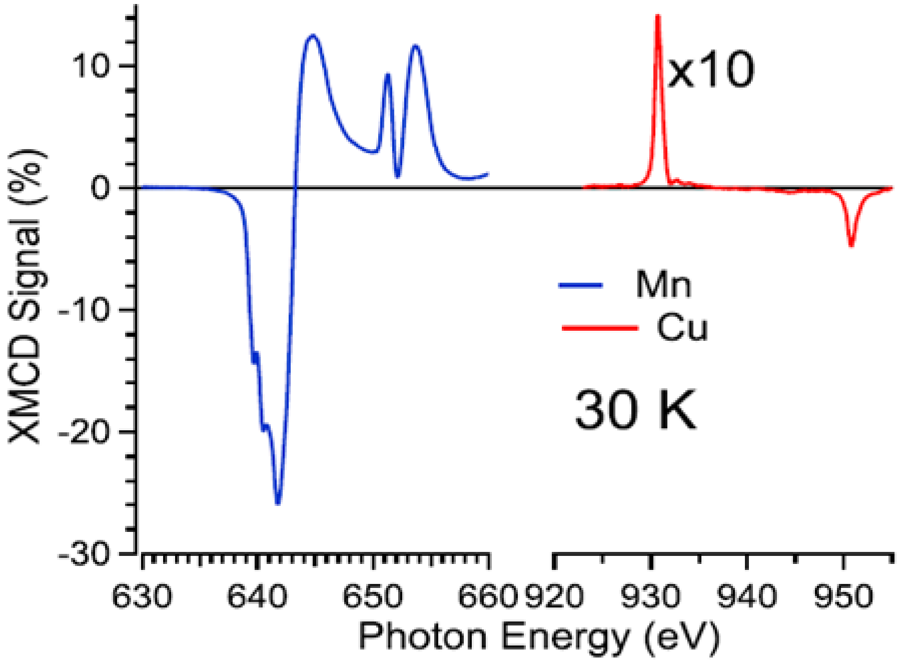

- ferromagnetic polarization of Cu in YBCO
- direction antiparallel to Mn

Spin polarization at interface

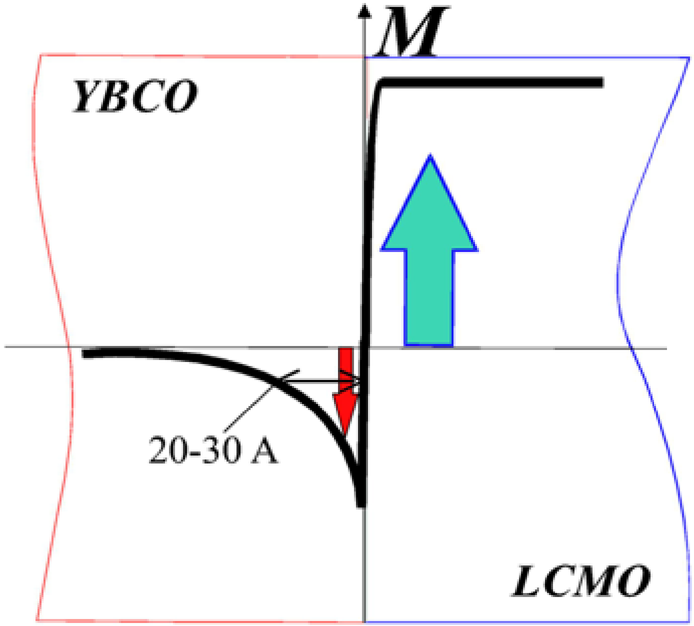

magnetization profile

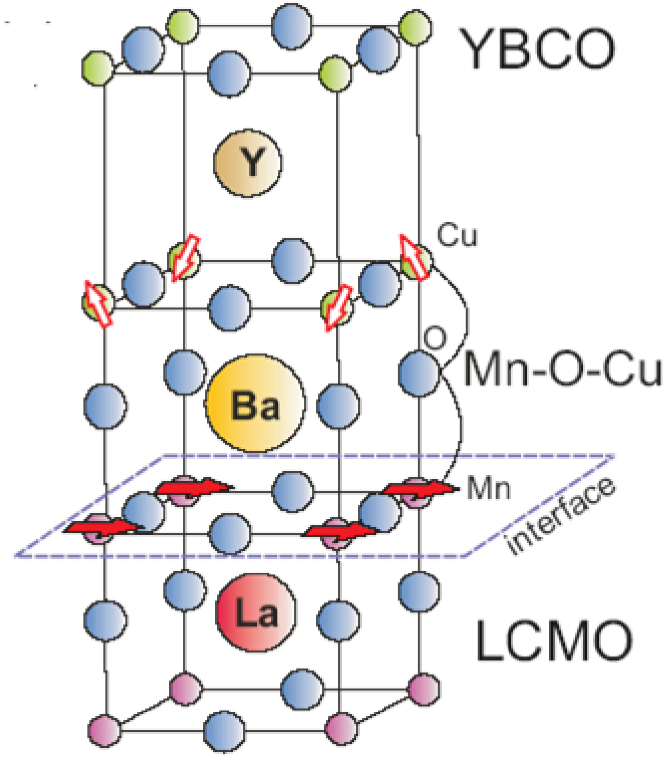

superexchange across interface

Chakhalian et al., Nature Phys. 2006

Temperature dependence of spin polarization

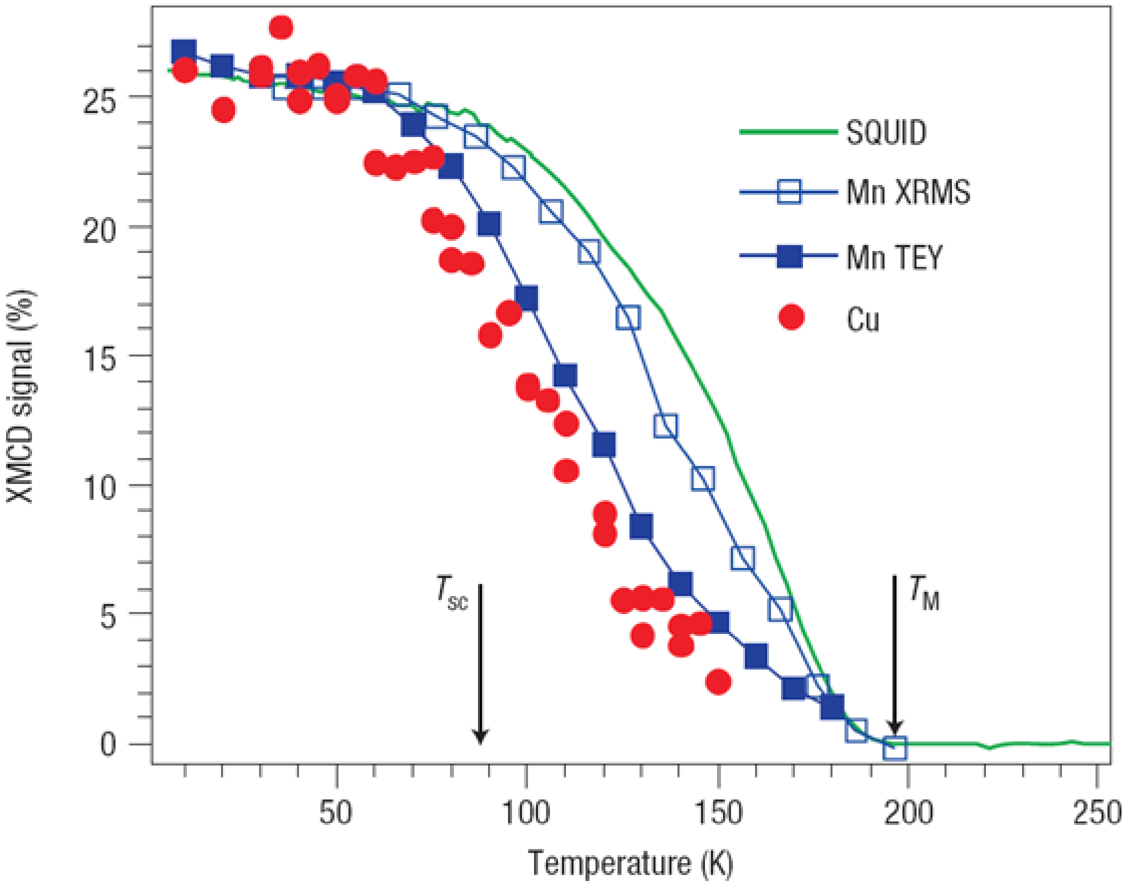

Cu magnetization closely follows Mn moment

→ **large antiferromagnetic Cu-Mn exchange interaction**

Exchange coupling across interface

assume bulk orbital occupancy is maintained at interface

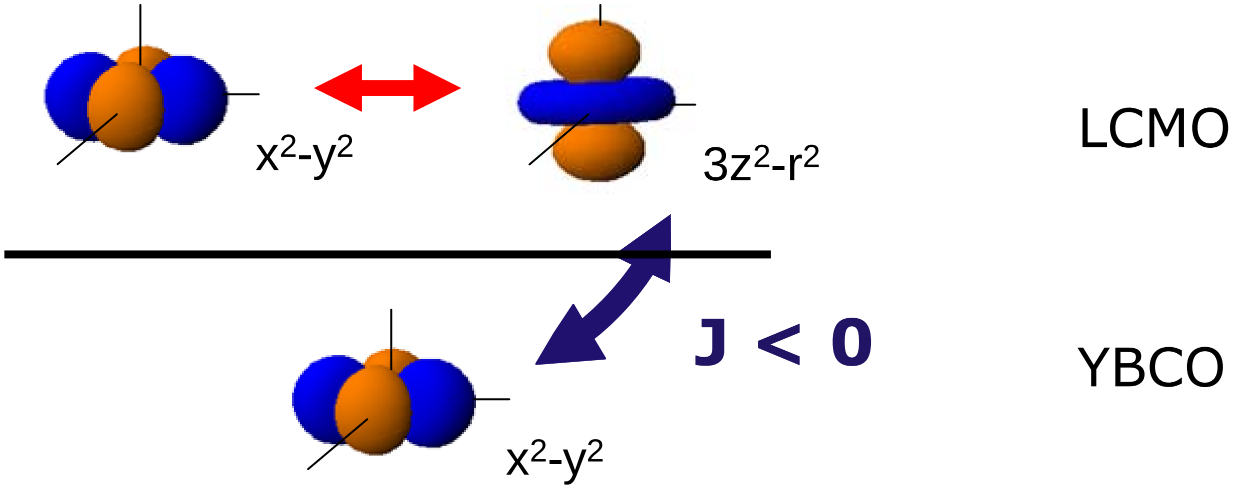

→ **weak ferromagnetic exchange** across interface expected from superexchange rules

inconsistent with experiment → **orbital reconstruction ?**

X-ray linear dichroism

interface sensitivity through “cap layers”

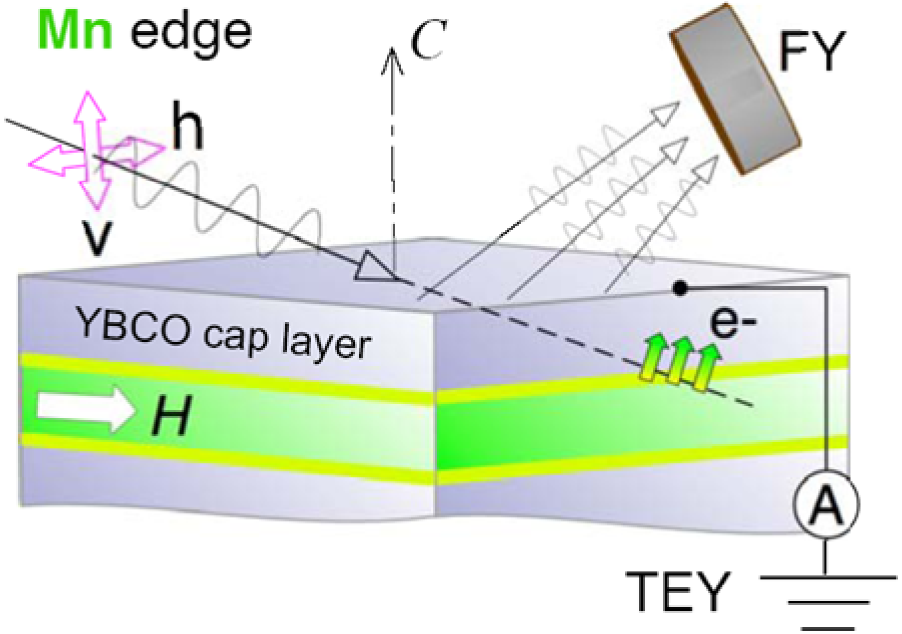

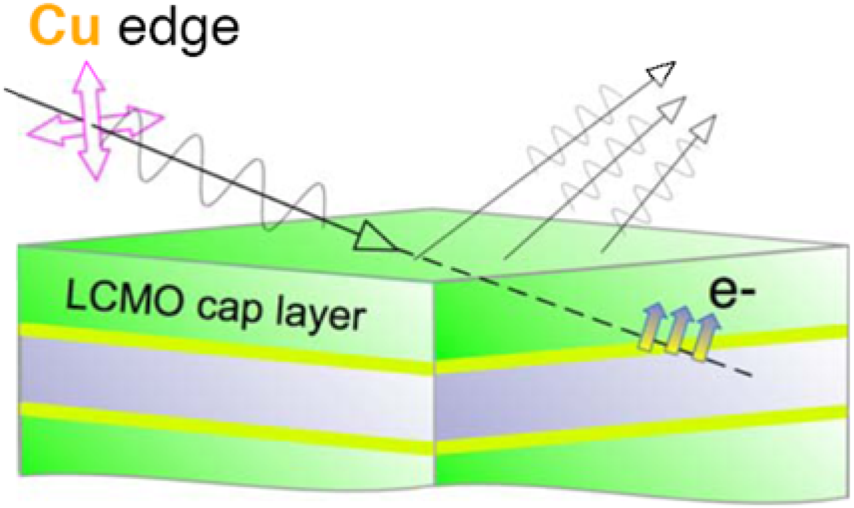

FY	bulk sensitive
TEY	low electron escape depth → probes first interface

Orbitals at interface

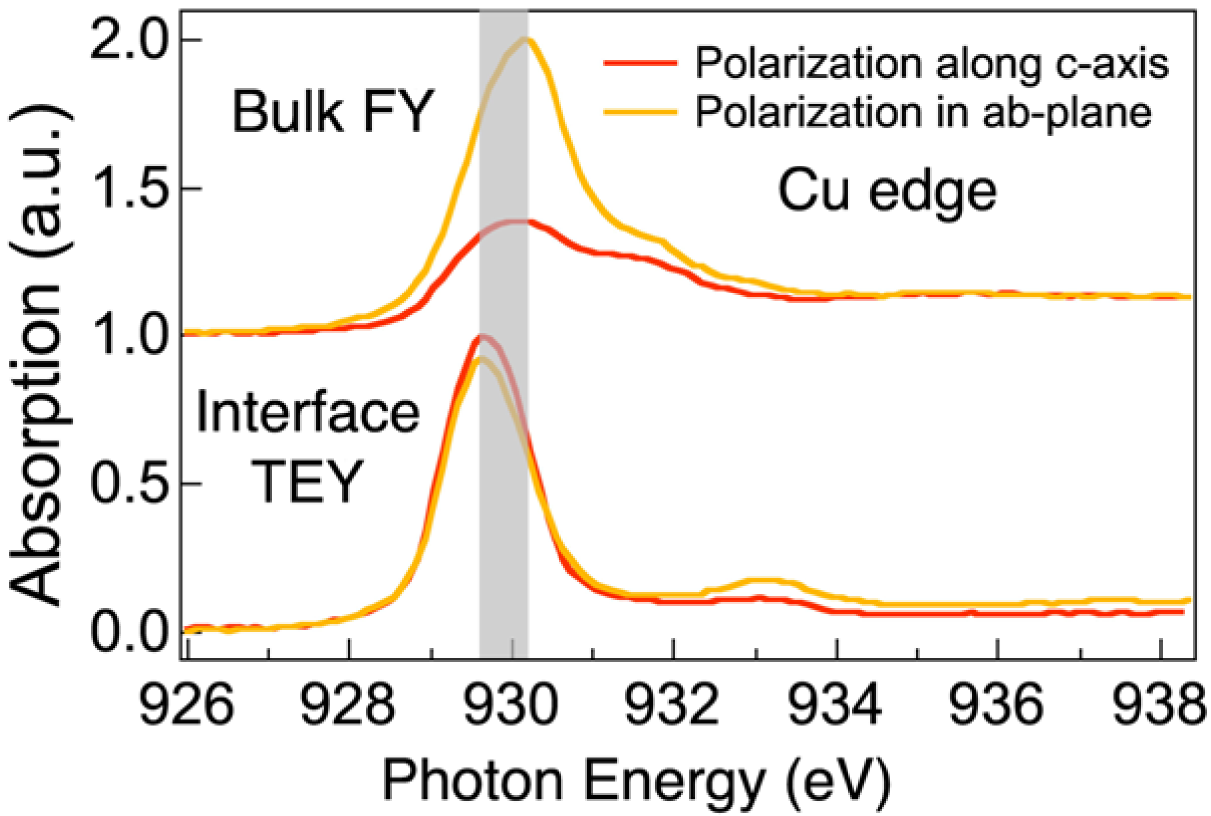

Chakhalian et al.
Science 2007

FY matches data on bulk YBCO

TEY **shifted** → ~ 0.2 electrons / Cu ion transferred across interface
not subject to Zhang-Rice singlet formation

almost isotropic → partial occupation of Cu $3z^2$-r^2 orbital

orbital reconstruction

Cluster calculations

possible origins

- different crystal fields at interface — unlikely
- covalent bonding ?

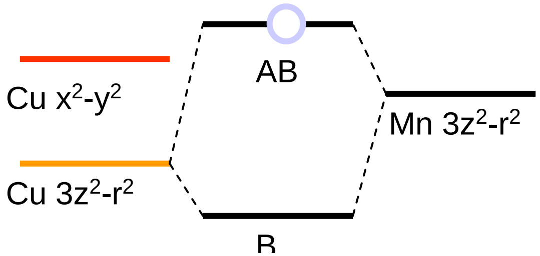

exact-diagonalization

calculations on small clusters

→ covalent bonding realistic

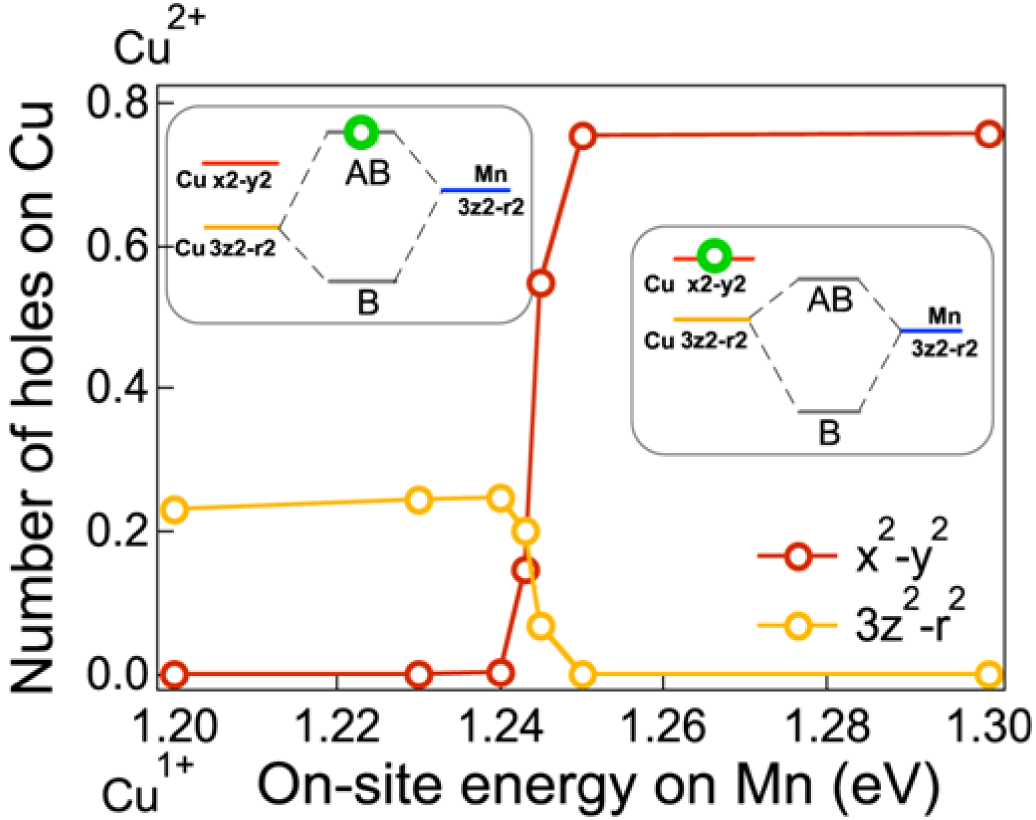

Exchange coupling across orbitally reconstructed interface

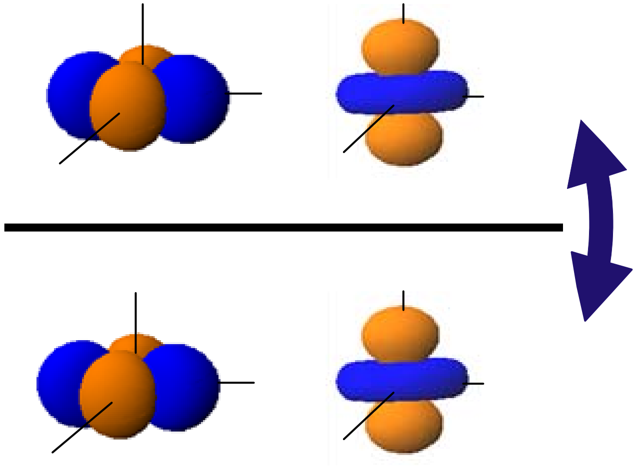

LCMO

J > 0

YBCO

Cu $3z^2$-r^2 orbital partially occupied

→ **strong antiferromagnetic exchange across interface**

→ **reduced in-plane antiferromagnetic correlations**

combination explains large ferromagnetic susceptibility,
suppression of metallicity and superconductivity of YBCO near interface

Oxide heterostructure research program

- understand and manipulate orbital and spin polarization at interfaces
- create dense correlated-electron systems with **controlled** interactions
- new quantum phases? ↔ FQHE in semiconductors
- lateral (nano)-structuring

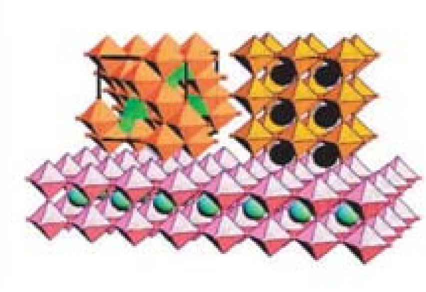

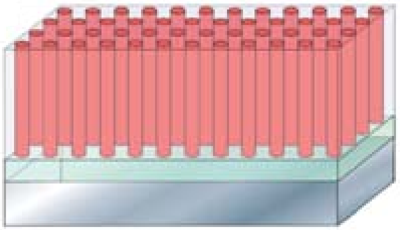

$CoFe_2O_4$ nanopillars in $BaTiO_3$ matrix
Zheng et al., Science 2004

La_2CuO_4 & $LaNiO_3$ electronic structure

La_2CuO_4

- spin-1/2
- 2D bond network
- orbitally non-degenerate
- Mott insulator

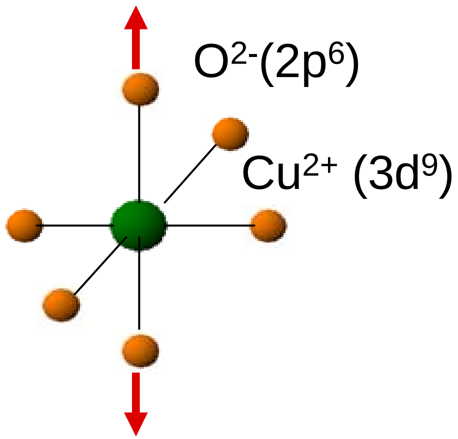

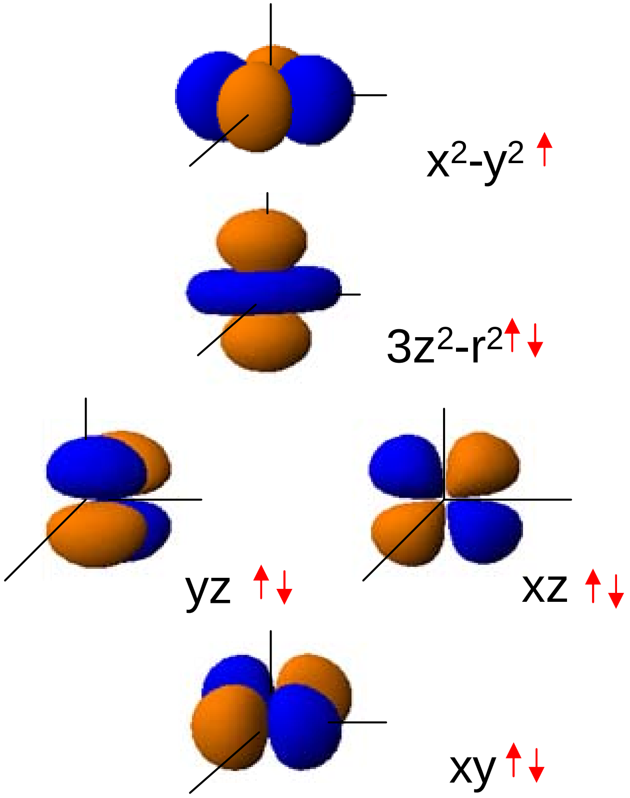

$LaNiO_3$

- spin-1/2
- 3D bond network
- orbitally degenerate
- metal

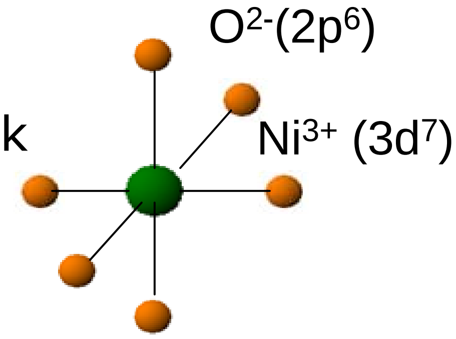

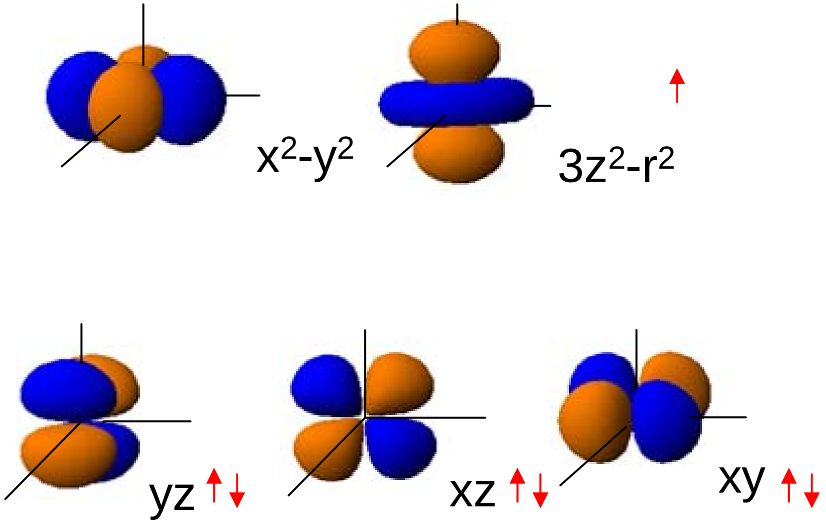

Strain-induced orbital polarization

X-ray linear dichroism in $La_{1-x}Sr_xMnO_3$ thin films

$SrTiO_3$ substrate: c/a=0.98

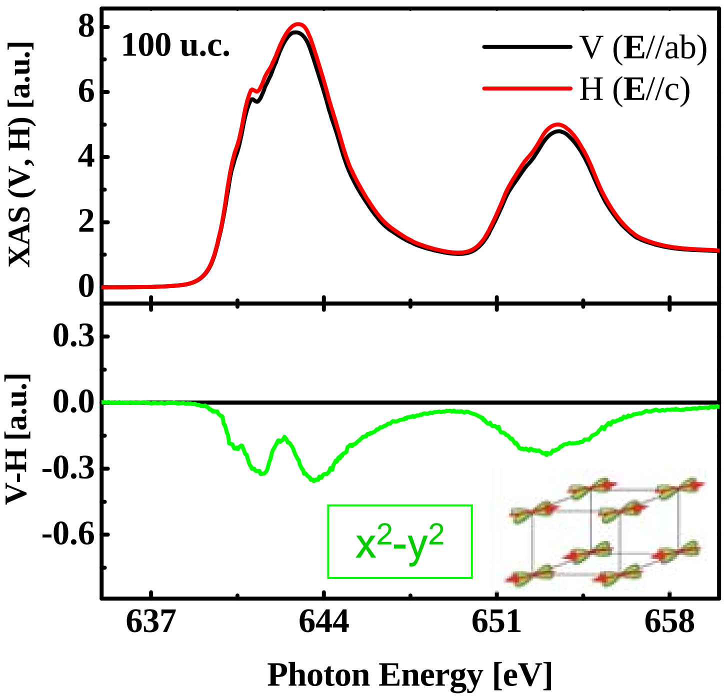

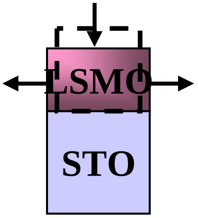

$LaAlO_3$ substrate: c/a=1.04

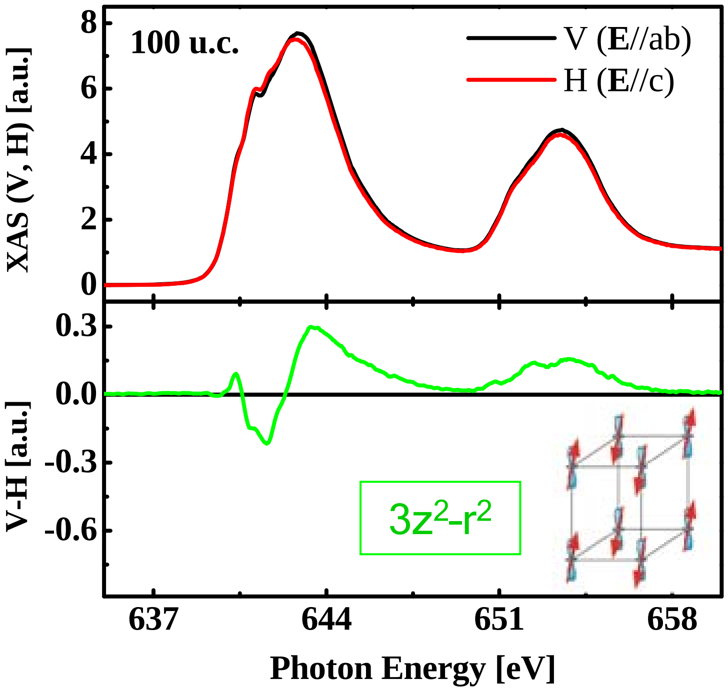

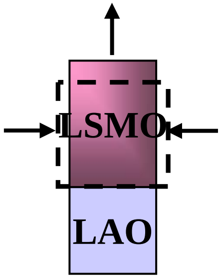

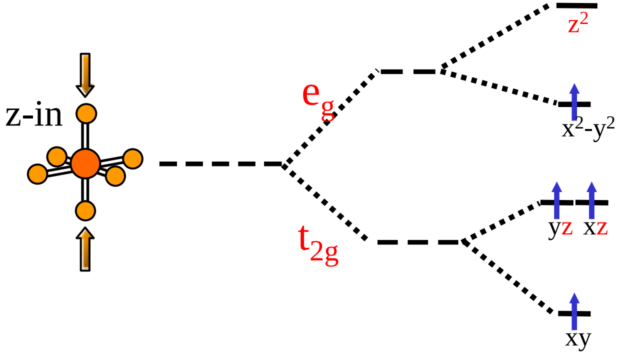

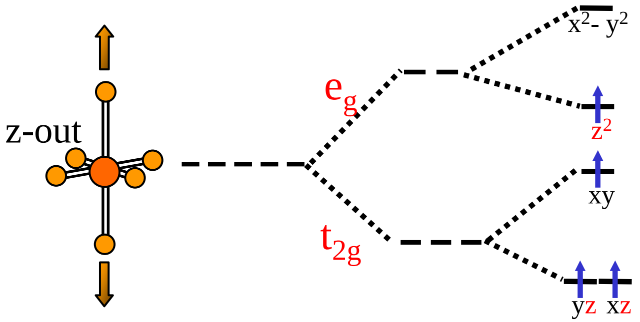

Aruta et al., Phys. Rev. B 2006

$LaNiO_3$-$LaMO_3$ superlattices

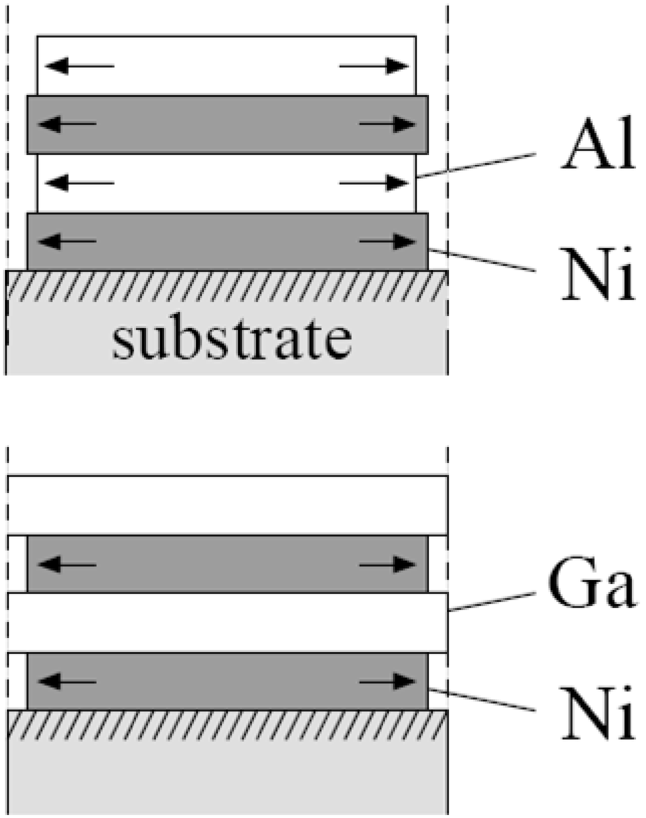

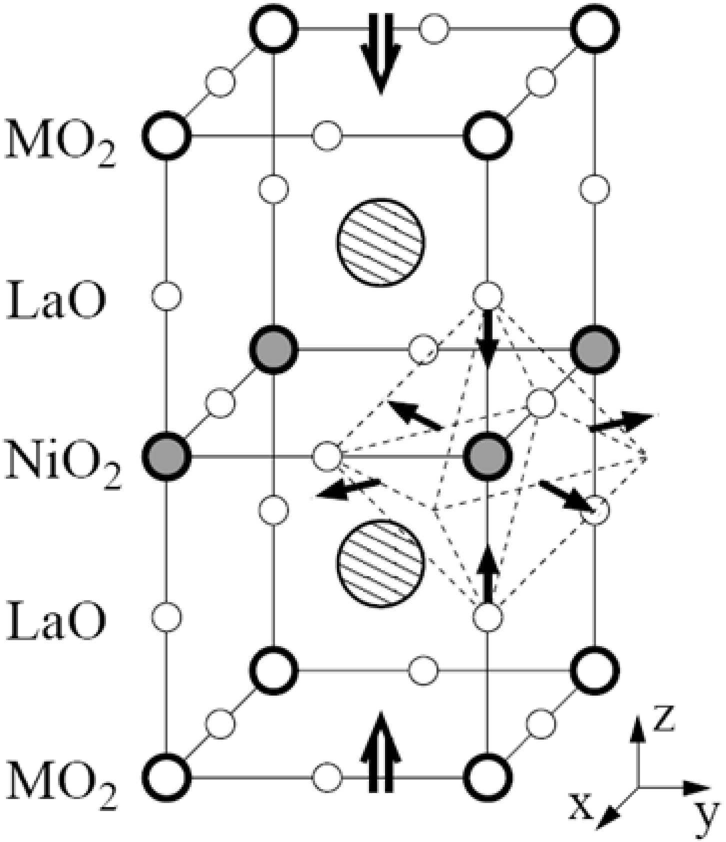

Chaloupka & Khaliullin, PRL 2008

- 2D electronic structure
- x^2-y^2 orbital favored

→ cuprate Hamiltonian?

LaNiO$_3$-LaMO$_3$ superconductivity?

mean-field superconducting transition temperature

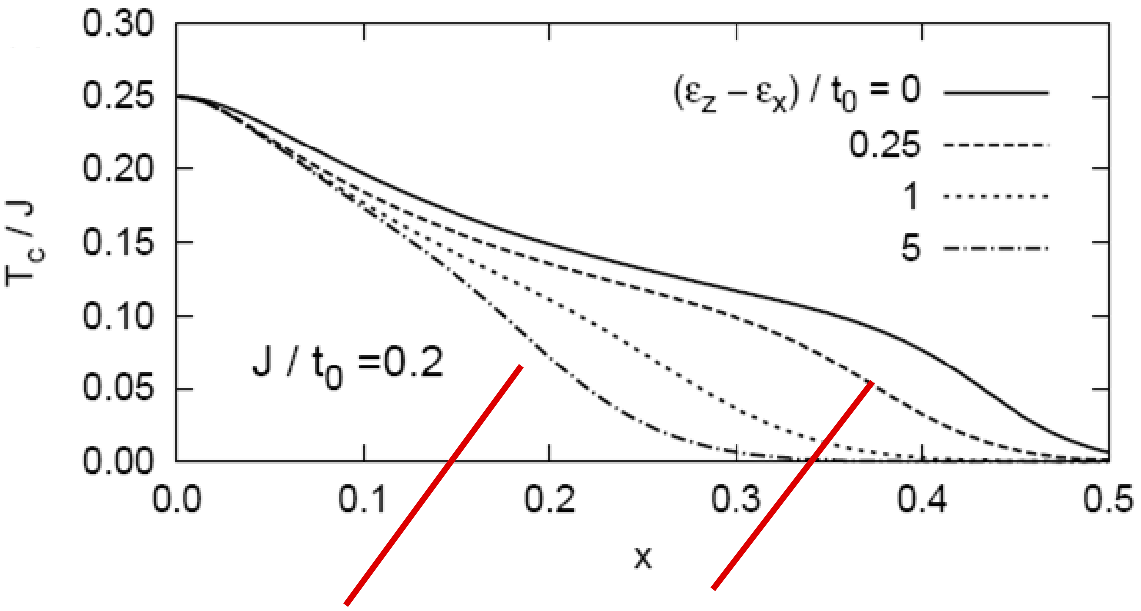

cuprates **LaNiO$_3$-LaMO$_3$**

Chaloupka & Khaliullin, PRL 2008

$LaNiO_3$-$LaAlO_3$ structure

TEM

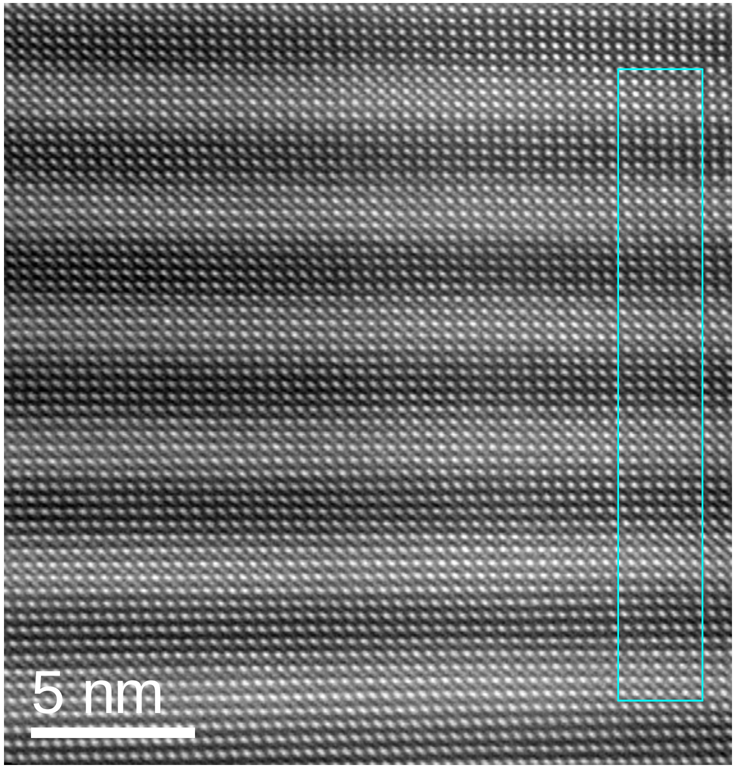

nonresonant x-ray reflectivity

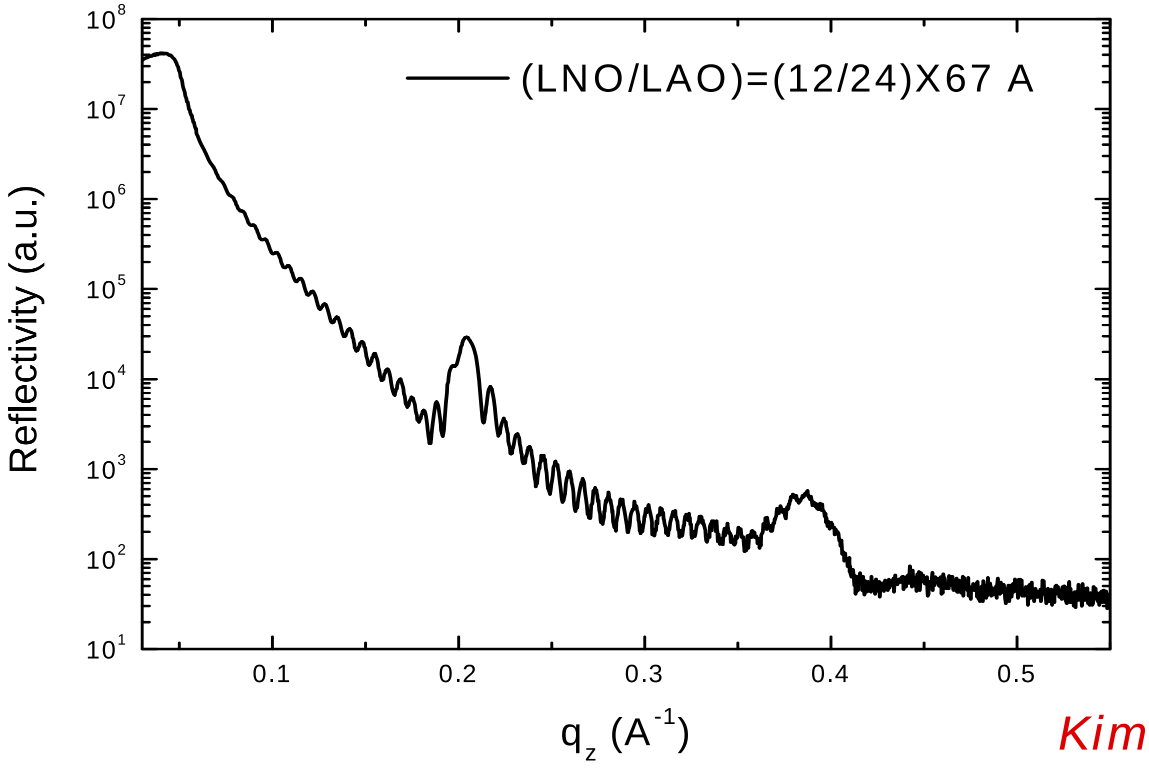

Kim

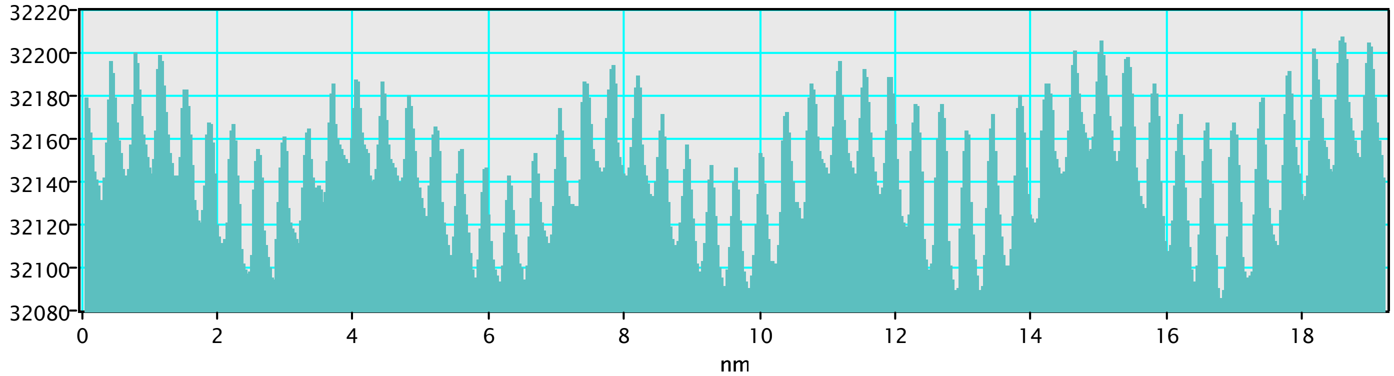

Zhang, Kaiser, van Aken

Max-Planck-Institut für Festkörperforschung

$LaNiO_3$-$LaAlO_3$ soft x-ray reflectivity

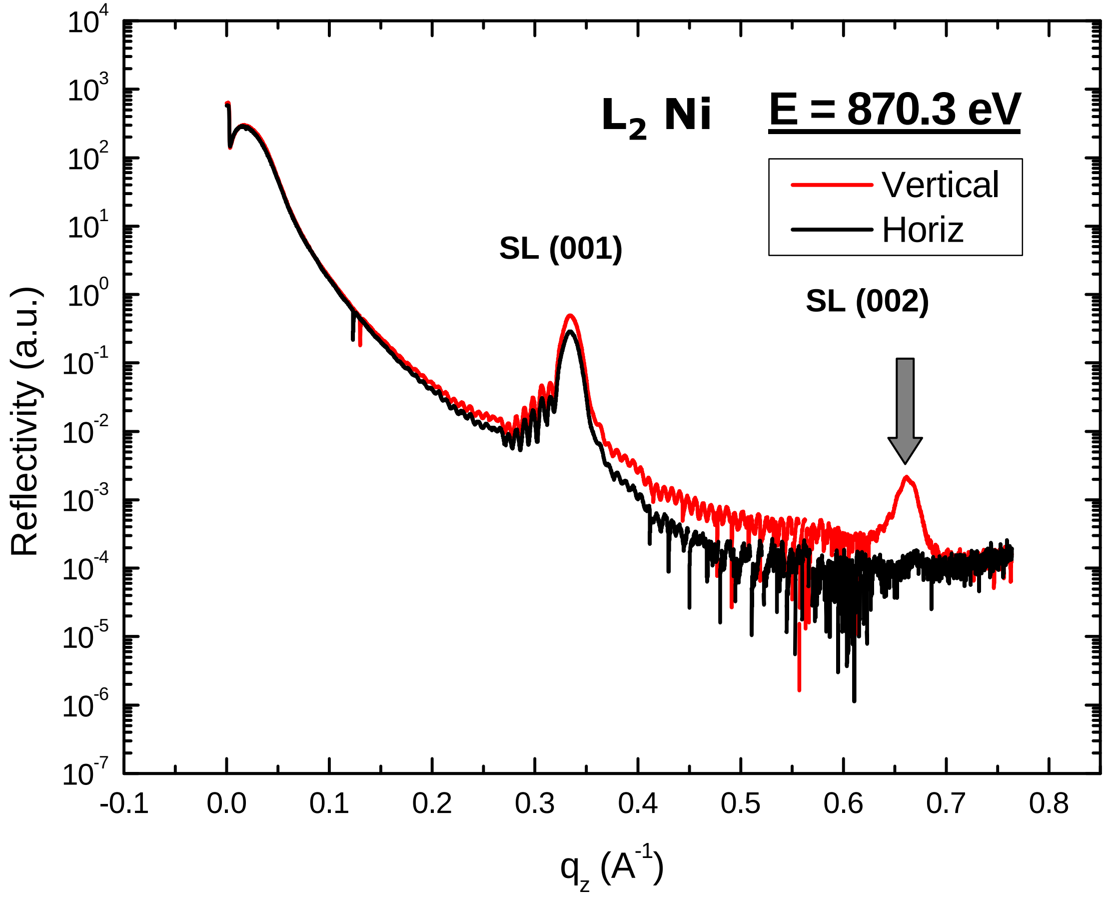

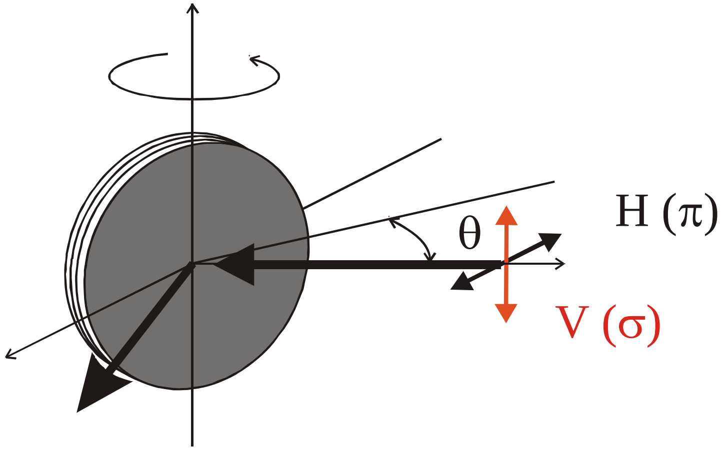

see also

Stahn et al., PRB 2005

Smadici et al., PRL 2007

"forbidden" superlattice peak

→ charge distribution of valence electrons ≠ atomic structure

→ signature of interface-induced charge order

$RNiO_3$ phase diagrams

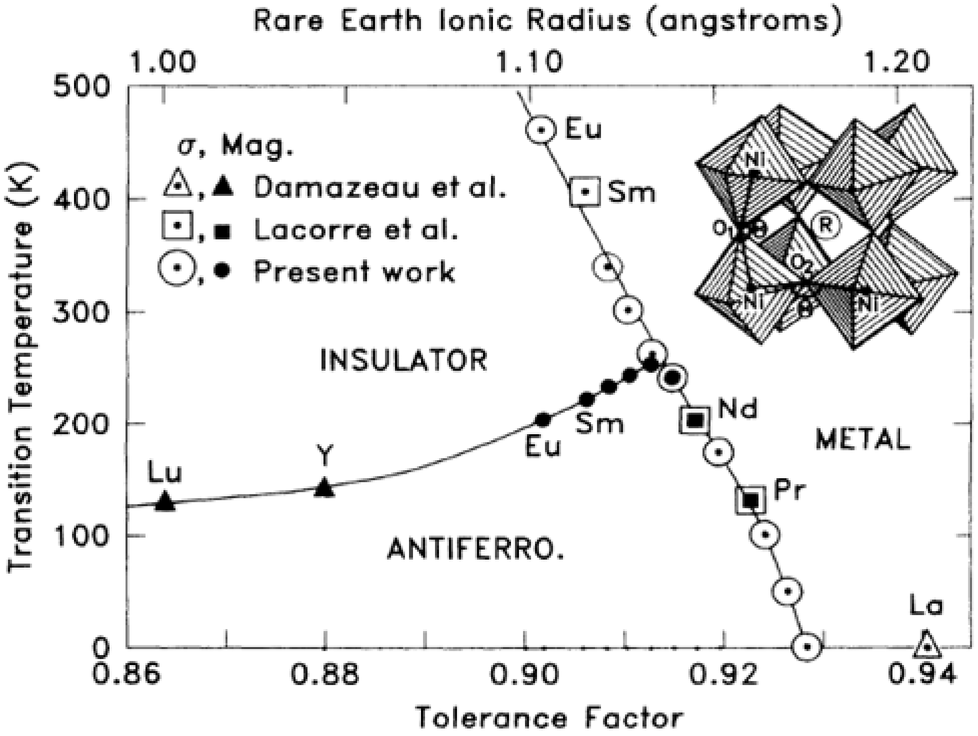

Torrance et al., PRB 1992

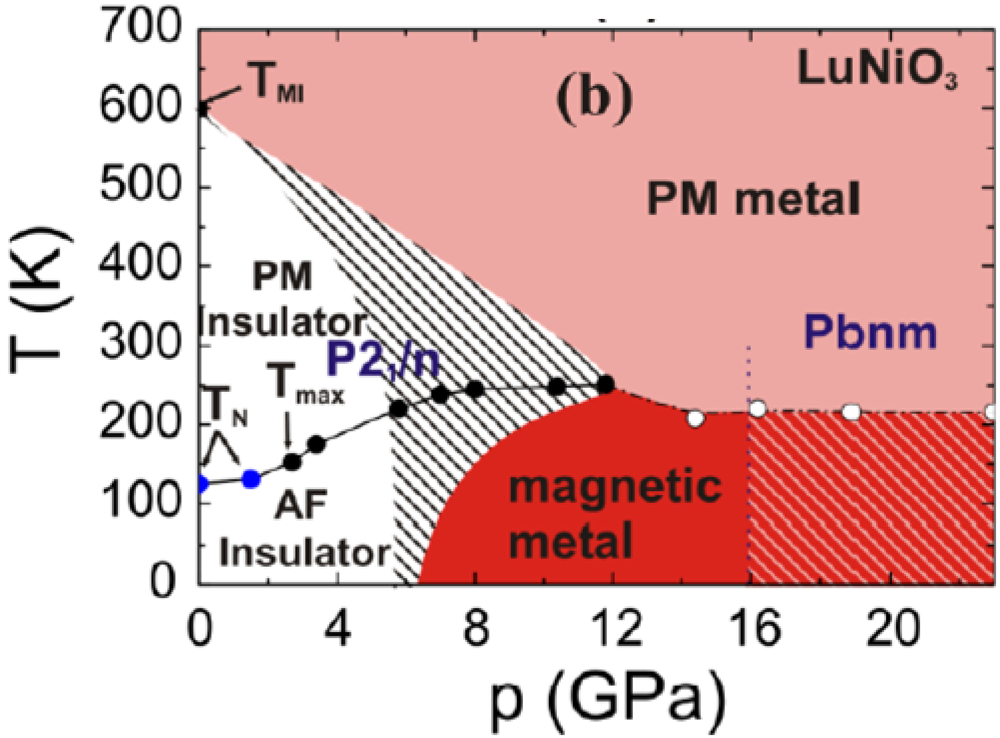

Mazin et al., PRL 2007

competing instabilities in bulk nickelates:

- antiferromagnetism
- charge order

Conclusions

YBCO-LCMO superlattices

- orbital and magnetic polarization at interface
- interface-induced antiferromagnetic insulating state (?)

$LaNiO_3$-$LaAlO_3$ superlattices

- interface-induced charge-ordering instability (not present in bulk)

Can high-temperature superconductivity be generated by suppressing competing instability?

Oxide heterostructure toolkit

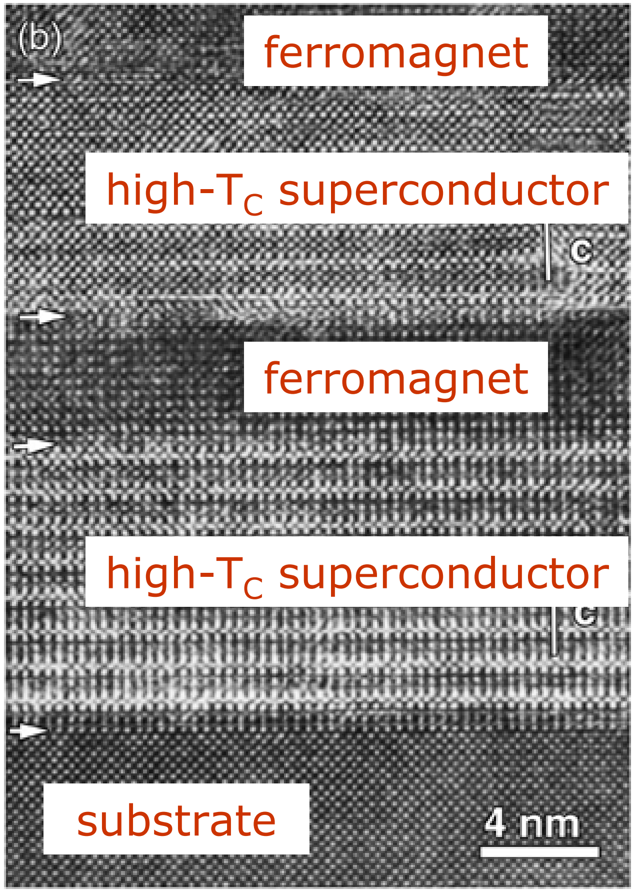

structure

TEM, XRD

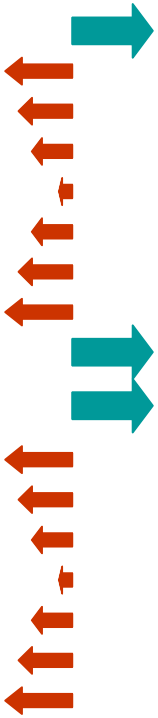

magnetization

neutrons, XMCD

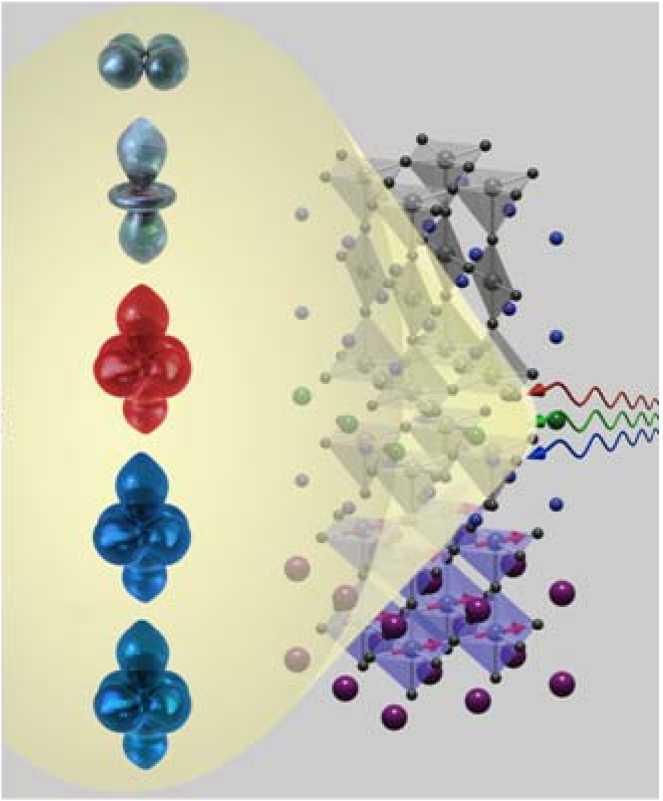

orbital occupation

XLD, RXS

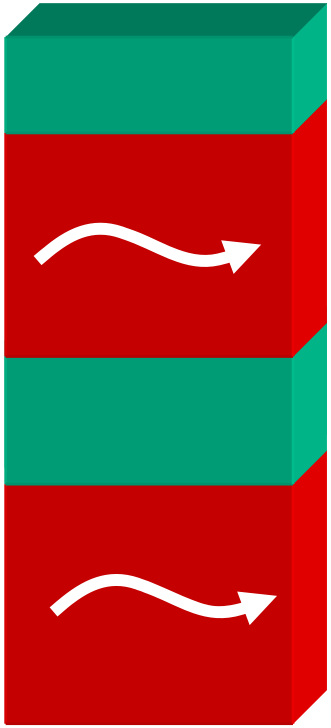

charge transport

FTIR